

ISSN: 2667-4203

ESKİŐEHİR TECHNICAL UNIVERSITY JOURNAL OF SCIENCE AND TECHNOLOGY
C– Life Sciences and Biotechnology

ESKİŐEHİR TEKNİK ÜNİVERSİTESİ BİLİM VE TEKNOLOJİ DERGİSİ
C – Yaşam Bilimleri ve Biyoteknoloji

Volume/Cilt **13** Number/Sayı **2** July / Temmuz - **2024**



ESKİŞEHİR TEKNİK ÜNİVERSİTESİ BİLİM VE TEKNOLOJİ DERGİSİ
C- YAŞAM BİLİMLERİ VE BİYOTEKNOLOJİ

Eskişehir Technical University Journal of Science and Technology
C -Life Sciences and Biotechnology

Estuscience – Life



Volume: 13 / Number: 2 / July - 2024

Eskişehir Technical University Journal of Science and Technology C – Life Sciences and Biotechnology (formerly Anadolu University Journal of Science and Technology C – Life Sciences and Biotechnology) is an **peer-reviewed** and **refereed international journal** by Eskişehir Technical University. Since 2010, it has been regularly published and distributed biannually and it has been published biannually and **electronically only since 2016**.

Manuscripts submitted for publication are analyzed in terms of scientific quality, ethics and research methods in terms of its compliance by the Editorial Board representatives of the relevant areas. Then, the abstracts of the appropriate articles are sent to two different referees with a well-known in scientific area. If the referees agree to review the article, full text in the framework of the privacy protocol is sent. In accordance with the decisions of referees, either directly or corrected article is published or rejected. Confidential reports of the referees in the journal archive will be retained for ten years. All post evaluation process is done electronically on the internet. Detailed instructions to authors are available in each issue of the journal.

Eskişehir Technical University holds the copyright of all published material that appear in Eskişehir Technical University Journal of Science and Technology C – Life Sciences and Biotechnology.

"Anadolu Üniversitesi Bilim ve Teknoloji Dergisi C- Yaşam Bilimleri ve Biyoteknoloji (Anadolu University Journal of Science and Technology C – Life Sciences and Biotechnology)" published within Anadolu University started to be published within Eskişehir Technical University which was established due to statute law 7141, in 2018. Hence, the name of the journal is changed to "Eskişehir Teknik Üniversitesi Bilim ve Teknoloji Dergisi C- Yaşam Bilimleri ve Biyoteknoloji (Eskişehir Technical University Journal of Science and Technology C – Life Sciences and Biotechnology)".

The Journal's Other Variant Title: **Estuscience-Life**; approved by ISSN National Centre for Türkiye on April 30, 2024.

Indexed by **ULAKBIM TR Dizin**

ISSN: 2667-4203



ESKİŞEHİR TEKNİK ÜNİVERSİTESİ BİLİM VE TEKNOLOJİ DERGİSİ
C- YAŞAM BİLİMLERİ VE BİYOTEKNOLOJİ

Eskişehir Technical University Journal of Science and Technology
C -Life Sciences and Biotechnology

Estuscience – Life



Volume: 13 / Number: 2 / July – 2024

Owner / Publisher: Prof. Dr. Adnan ÖZCAN for Eskişehir Technical University

EDITOR-IN-CHIEF

Prof. Dr. Semra KURAMA

Eskişehir Technical University, Institute of Graduate Programs, 26555 Eskişehir, TURKEY

Phone: +90 222 213 7470

e-mail: skurama@eskisehir.edu.tr

CO-EDITOR IN CHIEF

Assoc. Prof. Dr. Gülçin IŞIK

Eskişehir Technical University, Institute of Graduate Programs, 26555 - Eskişehir, TURKEY

Phone: +90 222-213 7472

e-mail: gulciny@eskisehir.edu.tr

CO-EDITOR IN CHIEF

Assit. Prof. Dr. Hüseyin Ersin EROL

Eskişehir Technical University, Institute of Graduate Programs, 26555 Eskişehir, TURKEY

Phone: +90 222-213 7473

e-mail: heerol@eskisehir.edu.tr

CONTACT INFORMATION

Eskişehir Technical University Journal of Science and Technology

Eskişehir Technical University, Institute of Graduate Programs, 26555 Eskişehir, TURKEY

Phone: +90 222 213 7485

e-mail : btcd@eskisehir.edu.tr



**ESKİŞEHİR TEKNİK ÜNİVERSİTESİ BİLİM VE TEKNOLOJİ DERGİSİ
C- YAŞAM BİLİMLERİ VE BİYOTEKNOLOJİ**

**Eskişehir Technical University Journal of Science and Technology
C -Life Sciences and Biotechnology**

Estuscience – Life



Volume: 13 / Number: 2 / July – 2024

OWNER / SAHİBİ

Adnan ÖZCAN, **The Rector of Eskişehir Technical University / Eskişehir Teknik Üniversitesi Rektörü**

EDITORIAL BOARD

Semra KURAMA, **Editor in Chief**

Gülçin IŞIK, **Co-Editor in Chief**

Hüseyin Ersin EROL, **Co-Editor in Chief**

LANGUAGE EDITORS - ENGLISH / İNGİLİZCE DİL EDITÖRLERİ

Hülya ALTUNTAŞ

SECTION EDITORS / ALAN EDITÖRLERİ

Ayşe AK (Kocaeli University, Turkey)
Dilek AK (Anadolu University, Turkey)
Ahmet AKSOY (Akdeniz University, Turkey)
Hülya ALTUNTAŞ (ESTU- Turkey)
Harun BÖCÜK (ESTU- Turkey)
Mediha CANBEK (Eskişehir Osmangazi University, Turkey)
Rasime DEMİREL (ESTU- Turkey)
Nesil ERTORUN (ESTU- Turkey)
Coşkun GÜÇLÜ (Eskişehir Osmangazi University, Turkey)
Gülçin IŞIK (ESTU- Turkey)
Gözde AYDOĞAN KILIÇ (ESTU- Turkey)
Yavuz Bülent KÖSE (Anadolu University, Turkey)
Emel SÖZEN (ESTU- Turkey)
İlkin YÜCEL ŞENGÜN (Ege University, Turkey)
Fatma Deniz SAYINER (Eskişehir Osmangazi University, Turkey)
Hakan ŞENTÜRK (Eskişehir Osmangazi University, Turkey)
Yusuf Ersoy YILDIRIM (Eskişehir Osmangazi University, Turkey)

Sekreterlik / Secretary

Typeset / Dizgi

Handan YİĞİT

ABOUT

Eskişehir Technical University Journal of Science and Technology C- Life Sciences and Biotechnology (formerly Anadolu University Journal of Science and Technology C - Life Sciences and Biotechnology) is an peer-reviewed and refereed international journal by Eskişehir Technical University. Since 2010, it has been regularly published and distributed biannually and it has been published biannually and electronically only since 2016.

The journal issues are published electronically in **JANUARY** and **JULY**.

- **The journal accepts TURKISH and ENGLISH manuscripts.**

AIM AND SCOPE

The journal publishes high quality original research papers, reviews and technical notes in the fields of life sciences: All aspects of biology such as taxonomy, physiology, biochemistry, ecology, environmental biology, biophysics, genetic, toxicology, biodiversity and biotechnology and, agricultural science, health sciences, biomedical sciences and pharmacy.

PEER REVIEW PROCESS

Manuscripts are first reviewed by the editorial board in terms of its its journal's style rules scientific content, ethics and methodological approach. If found appropriate, the manuscript is then send to at least two referees by editor. The decision in line with the referees may be an acceptance, a rejection or an invitation to revise and resubmit. Confidential review reports from the referees will be kept in archive. All submission process manage through the online submission systems.

OPEN ACCESS POLICY

This journal provides immediate open access to its content on the principle that making research freely available to the public supports a greater global exchange of knowledge.

Copyright notice and type of licence : **CC BY-NC-ND**.

The journal doesn't have Article Processing Charge (APC) or any submission charges.

ETHICAL RULES

You can reach the Ethical Rules in our journal in full detail from the link below:

<https://dergipark.org.tr/en/pub/estubtdc/policy>

Ethical Principles and Publication Policy

Policy & Ethics

Assessment and Publication

As a peer-reviewed journal, it is our goal to advance scientific knowledge and understanding. We have outlined a set of ethical principles that must be followed by all authors, reviewers, and editors.

All manuscripts submitted to our journals are pre-evaluated in terms of their relevance to the scope of the journal, language, compliance with writing instructions, suitability for science, and originality, by taking into account the current legal requirements regarding copyright

infringement and plagiarism. Manuscripts that are evaluated as insufficient or non-compliant with the instructions for authors may be rejected without peer review.

Editors and referees who are expert researchers in their fields assess scientific manuscripts submitted to our journals. A blind peer review policy is applied to the evaluation process. The Editor-in-Chief, if he/she sees necessary, may assign an Editor for the manuscript or may conduct the scientific assessment of the manuscript himself/herself. Editors may also assign referees for the scientific assessment of the manuscript and make their decisions based on reports by the referees. Articles are accepted for publication on the understanding that they have not been published and are not going to be considered for publication elsewhere. Authors should certify that neither the manuscript nor its main contents have already been published or submitted for publication in another journal.

The Journal; Implements the Publication Policy and Ethics guidelines to meet high-quality ethical standards for authors, editors and reviewers:

Duties of Editors-in-Chief and co-Editors

The crucial role of the journal Editor-in-Chief and co-Editors is to monitor and ensure the fairness, timeliness, thoroughness, and civility of the peer-review editorial process. The main responsibilities of Editors-in-Chief are as follows:

- Selecting manuscripts suitable for publication while rejecting unsuitable manuscripts,
- Ensuring a supply of high-quality manuscripts to the journal by identifying important,
- Increasing the journal's impact factor and maintaining the publishing schedule,
- Providing strategic input for the journal's development,

Duties of Editors

The main responsibilities of editors are as follows:

- An editor must evaluate the manuscript objectively for publication, judging each on its quality without considering the nationality, ethnicity, political beliefs, race, religion, gender, seniority, or institutional affiliation of the author(s). Editors should decline any assignment when there is a potential for conflict of interest.
- Editors must ensure the document(s) sent to the reviewers does not contain information of the author(s) and vice versa.
- Editors' decisions should be provided to the author(s) accompanied by the reviewers' comments and recommendations unless they contain offensive or libelous remarks.
- Editors should respect requests (if well reasoned and practicable) from author(s) that an individual should not review the submission.
- Editors and all staff members should guarantee the confidentiality of the submitted manuscript.
- Editors should have no conflict of interest with respect to articles they reject/accept. They must not have a conflict of interest with the author(s), funder(s), or reviewer(s) of the manuscript.
- Editors should strive to meet the needs of readers and authors and to constantly improve the journal.

Duties of Reviewers/Referees

The main responsibilities of reviewers/referees are as follows:

- Reviewers should keep all information regarding papers confidential and treat them as privileged information.
- Reviews should be conducted objectively, with no personal criticism of the author.
- Reviewers assist in the editorial decision process and as such should express their views clearly with supporting arguments.
- Reviewers should complete their reviews within a specified timeframe (maximum thirty-five (35) days). In the event that a reviewer feels it is not possible for him/her to complete the review of the manuscript within a stipulated time, then this information must be communicated to the editor so that the manuscript could be sent to another reviewer.
- Unpublished materials disclosed in a submitted manuscript must not be used in a reviewer's personal research without the written permission of the author. Information contained in an unpublished manuscript will remain confidential and must not be used by the reviewer for personal gain.
- Reviewers should not review manuscripts in which they have conflicts of interest resulting from competitive, collaborative, or other relationships or connections with any of the authors, companies, or institutions connected to the papers.
- Reviewers should identify similar work in published manuscripts that has not been cited by the author. Reviewers should also notify the Editors of significant similarities and/or overlaps between the manuscript and any other published or unpublished material.

Duties of Authors

The main responsibilities of authors are as follows:

- The author(s) should affirm that the material has not been previously published and that they have not transferred elsewhere any rights to the article.
- The author(s) should ensure the originality of the work and that they have properly cited others' work in accordance with the reference format.
- The author(s) should not engage in plagiarism or in self-plagiarism.
- On clinical and experimental humans and animals, which require an ethical committee decision for research in all branches of science;

All kinds of research carried out with qualitative or quantitative approaches that require data collection from the participants by using survey, interview, focus group work, observation, experiment, interview techniques,

Use of humans and animals (including material/data) for experimental or other scientific purposes,

- Clinical studies on humans,
- Studies on animals,
- Retrospective studies in accordance with the law on the protection of personal data, (Ethics committee approval should have been obtained for each individual application, and this approval should be stated and documented in the article.)

Information about the permission (board name, date, and number) should be included in the "Method" section of the article and also on the first/last page.

During manuscript upload, the "Ethics Committee Approval" file should be uploaded to the system in addition to the manuscript file.

In addition, in case reports, it is necessary to include information on the signing of the informed consent/ informed consent form in the manuscript.

- The author(s) should suggest no personal information that might make the identity of the patient recognizable in any form of description, photograph, or pedigree. When photographs of

the patient were essential and indispensable as scientific information, the author(s) have received consent in written form and have clearly stated as much.

- The author(s) should provide the editor with the data and details of the work if there are suspicions of data falsification or fabrication. Fraudulent data shall not be tolerated. Any manuscript with suspected fabricated or falsified data will not be accepted. A retraction will be made for any publication which is found to have included fabricated or falsified data.
- The author(s) should clarify everything that may cause a conflict of interests such as work, research expenses, consultant expenses, and intellectual property.
- The author(s) must follow the submission guidelines of the journal.
- The author(s) discover(s) a significant error and/or inaccuracy in the submitted manuscript at any time, then the error and/or inaccuracy must be reported to the editor.
- The author(s) should disclose in their manuscript any financial or other substantive conflicts of interest that might be construed to influence the results or interpretation of their manuscript. All sources of financial support should be disclosed under the heading of “Acknowledgment” or “Contribution”.
- The corresponding author(s) must ensure that all appropriate co-authors are not included in the manuscript, that author names are not added or removed and that the authors' address information is not changed after the review begins and that all co-authors see and approve the final version of the manuscript at every stage of the manuscript. All significant contributors should be listed as co-authors. Other individuals who have participated in significant aspects of the research work should be considered contributors and listed under “Author Contribution”.

Cancellations/Returns

Articles/manuscripts may be returned to the authors in order to increase the authenticity and/or reliability and to prevent ethical breaches, and even if articles have been accepted and/or published, they can be withdrawn from publication if necessary. The Editor-in-Chief of the journal has the right to return or withdraw an article/manuscript in the following situations:

- When the manuscript is not within the scope of the journal,
- When the scientific quality and/or content of the manuscript do not meet the standards of the journal and a referee review is not necessary,
- When there is proof of ruling out the findings obtained by the research, (When the article/manuscript is undergoing an assessment or publication process by another journal, congress, conference, etc.,)
- When the article/manuscript was not prepared in compliance with scientific publication ethics,
- When any other plagiarism is detected in the article/manuscript,
- When the authors do not perform the requested corrections within the requested time (maximum twenty-one (21) days),
- When the author does not submit the requested documents/materials/data etc. within the requested time,
- When the requested documents/materials/data etc. submitted by the author are missing for the second time,
- When the study includes outdated data,
- When the authors make changes that are not approved by the editor after the manuscript was submitted,
- When an author is added/removed, the order of the authors is changed, the corresponding author is altered, or the addresses of the authors are changed in the article that is in the evaluation process,
- When a statement is not submitted indicating that approval of the ethics committee permission was obtained for the following (including retrospective studies):

- When human rights or animal rights are violated,

ETHICAL ISSUES

Plagiarism

The use of someone else's ideas or words without a proper citation is considered plagiarism and will not be tolerated. Even if a citation is given, if quotation marks are not placed around words taken directly from other authors' work, the author is still guilty of plagiarism. Reuse of the author's own previously published words, with or without a citation, is regarded as self-plagiarism.

All manuscripts received are submitted to iThenticate®, which compares the content of the manuscript with a database of web pages and academic publications. Manuscripts are judged to be plagiarized or self-plagiarized, based on the iThenticate® report or any other source of information, will be rejected. Corrective actions are proposed when plagiarism and/or self-plagiarism is detected after publication. Editors should analyze the article and decide whether a corrected article or retraction needs to be published.

Open-access theses are considered as published works and they are included in the similarity checks.

iThenticate® report should have a maximum of 11% from a single source, and a maximum of 25% in total.

Conflicts of Interest

Eskişehir Technical University Journal of Science and Technology A - Applied Sciences and Engineering should be informed of any significant conflict of interest of editors, authors, or reviewers to determine whether any action would be appropriate (e.g. an author's statement of conflict of interest for a published work, or disqualifying a referee).

Financial

The authors and reviewers of the article should inform the journal about the financial information that will bring financial gain or loss to any organization from the publication of the article.

*Research funds; funds, consulting fees for a staff member; If you have an interest, such as patent interests, you may have a conflict of interest that needs to be declared.

Other areas of interest

The editor or reviewer may disclose a conflict of interest that, if known, would be embarrassing (for example, an academic affiliation or rivalry, a close relationship or dislike, or a person who may be affected by the publication of the article).

Conflict of interest statement

Please note that a conflict of interest statement is required for all submitted manuscripts. If there is no conflict of interest, please state "There are no conflicts of interest to declare" in your manuscript under the heading "Conflicts of Interest" as the last section before your Acknowledgments.

AUTHOR GUIDELINES

All manuscripts must be submitted electronically.

You will be guided stepwise through the creation and uploading of the various files. There are no page charges. Papers are accepted for publication on the understanding that they have not been published and are not going to be considered for publication elsewhere. Authors should certify that neither the manuscript nor its main contents have already been published or submitted for publication in another journal. We ask a signed copyright to start the evaluation process. After a manuscript has been submitted, it is not possible for authors to be added or removed or for the order of authors to be changed. If authors do so, their submission will be cancelled.

Manuscripts may be rejected without peer review by the editor-in-chief if they do not comply with the instructions to authors or if they are beyond the scope of the journal. After a manuscript has been accepted for publication, i.e. after referee-recommended revisions are complete, the author will not be permitted to make any changes that constitute departures from the manuscript that was accepted by the editor. Before publication, the galley proofs are always sent to the authors for corrections. Mistakes or omissions that occur due to some negligence on our part during final printing will be rectified in an errata section in a later issue.

This does not include those errors left uncorrected by the author in the galley proof. The use of someone else's ideas or words in their original form or slightly changed without a proper citation is considered plagiarism and will not be tolerated. Even if a citation is given, if quotation marks are not placed around words taken directly from another author's work, the author is still guilty of plagiarism. All manuscripts received are submitted to iThenticateR, a plagiarism checking system, which compares the content of the manuscript with a vast database of web pages and academic publications. In the received iThenticateR report; The similarity rate is expected to be below 25%. Articles higher than this rate will be rejected.

Uploading Articles to the Journal

Authors should prepare and upload 2 separate files while uploading articles to the journal. First, the Author names and institution information should be uploaded so that they can be seen, and then (using the additional file options) a separate file should be uploaded with the Author names and institution information completely closed. When uploading their files with closed author names, they will select the "Show to Referee" option, so that the file whose names are closed can be opened to the referees.

Preparation of Manuscript

Style and Format

Manuscripts should be **single column** by giving one-spaced with 2.5-cm margins on all sides of the page, in Times New Roman font (font size 11). Every page of the manuscript, including the title page, references, tables, etc., should be numbered. All copies of the manuscript should also have line numbers starting with 1 on each consecutive page.

Manuscripts must be upload as word document (*.doc, *.docx vb.). **Please avoid uploading texts in *.pdf format.**

Symbols, Units and Abbreviations

Standard abbreviations and units should be used; SI units are recommended. Abbreviations should be defined at first appearance, and their use in the title and abstract should be avoided. Generic names of chemicals should be used. Genus and species names should be typed in italic or, if this is not available, underlined.

Please refer to equations with capitalisation and unabbreviated (e.g., as given in Equation (1)).

Manuscript Content

Articles should be divided into logically ordered and numbered sections. Principal sections should be numbered consecutively with Arabic numerals (1. Introduction, 2. Formulation of problem, etc.) and subsections should be numbered 1.1., 1.2., etc. Do not number the Acknowledgements or References sections. The text of articles should be, if possible, divided

into the following sections: Introduction, Materials and Methods (or Experimental), Results, Discussion, and Conclusion.

Title and contact information

The first page should contain the full title in sentence case (e.g., Hybrid feature selection for text classification), the full names (last names fully capitalised) and affiliations (in English) of all authors (Department, Faculty, University, City, Country, E-mail), and the contact e-mail address for the clearly identified corresponding author. The first page should contain the full title, abstract and keywords (both English and Turkish).

Abstract

The abstract should provide clear information about the research and the results obtained, and should not exceed 300 words. The abstract should not contain citations and must be written in Times New Roman font with font size 9.

Keywords

Please provide 3 to 5 keywords which can be used for indexing purposes.

Introduction

The motivation or purpose of your research should appear in the “Introduction”, where you state the questions you sought to answer, and then provide some of the historical basis for those questions.

Methods

Provide sufficient information to allow someone to repeat your work. A clear description of your experimental design, sampling procedures, and statistical procedures is especially important in papers describing field studies, simulations, or experiments. If you list a product (e.g., animal food, analytical device), supply the name and location of the manufacturer. Give the model number for equipment used.

Results

Results should be stated concisely and without interpretation.

Discussion

Focus on the rigorously supported aspects of your study. Carefully differentiate the results of your study from data obtained from other sources. Interpret your results, relate them to the results of previous research, and discuss the implications of your results or interpretations.

Conclusion

This should state clearly the main conclusions of the research and give a clear explanation of their importance and relevance. Summary illustrations may be included.

Acknowledgments

Acknowledgments of people, grants, funds, etc. should be placed in a separate section before the reference list. The names of funding organizations should be written in full.

Conflict of Interest Statement

The authors are obliged to present the conflict of interest statement at the end of the article after the acknowledgments section.

CRediT Author Statement

Write the authors' contributions in detail using the specified CRediT notifications. Authors may have contributed in more than one role. The corresponding author is responsible for ensuring that descriptions are accurate and accepted by all authors.

CRediT Notifications	Explanation
Conceptualization	Ideas; formulation or evolution of overarching research goals and aims
Methodology	Development or design of methodology; creation of models
Software	Programming, software development; designing computer programs; implementation of the computer code and supporting algorithms; testing of existing code components
Validation	Verification, whether as a part of the activity or separate, of the overall replication/ reproducibility of results/experiments and other research outputs
Formal analysis	Application of statistical, mathematical, computational, or other formal techniques to analyse or synthesize study data
Investigation	Conducting a research and investigation process, specifically performing the experiments, or data/evidence collection
Resources	Provision of study materials, reagents, materials, patients, laboratory samples, animals, instrumentation, computing resources, or other analysis tools
Data Curation	Management activities to annotate (produce metadata), scrub data and maintain research data (including software code, where it is necessary for interpreting the data itself) for initial use and later reuse
Writing – Original Draft	Preparation, creation and/or presentation of the published work, specifically writing the initial draft (including substantive translation)
Writing – Review & Editing	Preparation, creation and/or presentation of the published work by those from the original research group, specifically critical review, commentary, or revision – including pre-or post-publication stages
Visualization	Preparation, creation and/or presentation of the published work, specifically visualization/ data presentation
Supervision	Oversight and leadership responsibility for the research activity planning and execution, including mentorship external to the core team

Project administration	Management and coordination responsibility for the research activity planning and execution
Funding acquisition	Acquisition of the financial support for the project leading to this publication

References

Writing Style; **AMA; References Writing format** should be used in the reference writing of our journal. If necessary, at this point, the reference writings of the articles published in our article can be examined.

Citations in the text should be identified by numbers in square brackets. The list of references at the end of the paper should be given in order of their first appearance in the text. All authors should be included in reference lists unless there are 10 or more, in which case only the first 10 should be given, followed by ‘et al.’. Do not use individual sets of square brackets for citation numbers that appear together, e.g., [2,3,5–9], not [2], [3], [5]–[9]. Do not include personal communications, unpublished data, websites, or other unpublished materials as references, although such material may be inserted (in parentheses) in the text. In the case of publications in languages other than English, the published English title should be provided if one exists, with an annotation such as “(article in Turkish with an abstract in English)”. If the publication was not published with an English title, cite the original title only; do not provide a self-translation. References should be formatted as follows (please note the punctuation and capitalisation):

Journal articles

Journal titles should be abbreviated according to ISI Web of Science abbreviations.

Guyon I, Elisseeff A. An introduction to variable and feature selection. *J Mach Learn Res* 2003; 3: 1157-1182.

Izadpanahi S, Ozcinar C, Anbarjafari G, Demirel H. Resolution enhancement of video sequences by using discrete wavelet transform and illumination compensation. *Turk J Elec Eng & Comp Sci* 2012; 20: 1268-1276.

Books

Haupt RL, Haupt SE. *Practical Genetic Algorithms*. 2nd ed. New York, NY, USA: Wiley, 2004.
Kennedy J, Eberhart R. *Swarm Intelligence*. San Diego, CA, USA: Academic Press, 2001.

Chapters in books

Poore JH, Lin L, Eschbach R, Bauer T. Automated statistical testing for embedded systems. In: Zander J, Schieferdecker I, Mosterman PJ, editors. *Model-Based Testing for Embedded Systems*. Boca Raton, FL, USA: CRC Press, 2012. pp. 111-146.

Conference proceedings

Li RTH, Chung SH. Digital boundary controller for single-phase grid-connected CSI. In: *IEEE 2008 Power Electronics Specialists Conference*; 15–19 June 2008; Rhodes, Greece. New York, NY, USA: IEEE. pp. 4562-4568.

Theses

Boynukalın Z. *Emotion analysis of Turkish texts by using machine learning methods*. MSc, Middle East Technical University, Ankara, Turkey, 2012.

Tables and Figures

All illustrations (photographs, drawings, graphs, etc.), not including tables, must be labelled “Figure.” Figures must be submitted in the manuscript.

All tables and figures must have a caption and/or legend and be numbered (e.g., Table 1, Figure 2), unless there is only one table or figure, in which case it should be labelled “Table” or “Figure” with no numbering. Captions must be written in sentence case (e.g., Macroscopic appearance of the samples.). The font used in the figures should be Times New Roman. If symbols such as \times , μ , η , or v are used, they should be added using the Symbols menu of Word.

All tables and figures must be numbered consecutively as they are referred to in the text. Please refer to tables and figures with capitalisation and unabbreviated (e.g., “As shown in Figure 2...”, and not “Fig. 2” or “figure 2”).

The resolution of images should not be less than 118 pixels/cm when width is set to 16 cm. Images must be scanned at 1200 dpi resolution and submitted in jpeg or tiff format. Graphs and diagrams must be drawn with a line weight between 0.5 and 1 point. Graphs and diagrams with a line weight of less than 0.5 point or more than 1 point are not accepted. Scanned or photocopied graphs and diagrams are not accepted.

Figures that are charts, diagrams, or drawings must be submitted in a modifiable format, i.e. our graphics personnel should be able to modify them. Therefore, if the program with which the figure is drawn has a “save as” option, it must be saved as *.ai or *.pdf. If the “save as” option does not include these extensions, the figure must be copied and pasted into a blank Microsoft Word document as an editable object. It must not be pasted as an image file (tiff, jpeg, or eps) unless it is a photograph.

Tables and figures, including caption, title, column heads, and footnotes, must not exceed 16 × 20 cm and should be no smaller than 8 cm in width. For all tables, please use Word’s “Create Table” feature, with no tabbed text or tables created with spaces and drawn lines. Please do not duplicate information that is already presented in the figures.

Article Corrections and Uploading to the System

Authors should upload the desired edits for their articles without destroying or changing the Template file of the article, by selecting and specifying the relevant edits as Colored, and also submit the Clean version of the article in 2 separate files (using the Additional file option if necessary). * In case of submitting a corrected article, a separate File in Reply to the Referees must be prepared and the "Reply to the Referees" option in the Add additional file option should be checked and uploaded. If a separate file is not prepared in response to the referees, the Author will definitely be asked to upload the relevant file again and the evaluation will be in the pending phase.

ESKİŞEHİR TECHNICAL UNIVERSITY JOURNAL OF SCIENCE AND TECHNOLOGY
C- Life Sciences and Biotechnology

ESKİŞEHİR TEKNİK ÜNİVERSİTESİ BİLİM VE TEKNOLOJİ DERGİSİ
C- Yaşam Bilimleri ve Biyoteknoloji

Estuscience - Life

Volume/ Cilt: 13 / Number/Sayı: 2 / July / Temmuz- 2024

CONTENTS / İÇİNDEKİLER

Sayfa / Page

ARAŞTIRMA MAKALESİ / RESEARCH ARTICLE

THE CLINICAL SIGNIFICANCE OF SOX9 GENE IN DIFFERENT CANCER TYPES: AN IN-SILICO ANALYSIS <i>E. S. Yavaş, S. H. Aktaş, G. Efendioğlu, D. F. Akın</i>	63
EARLY-STAGE DIABETES RISK PREDICTION USING MACHINE LEARNING TECHNIQUES BASED ON ENSEMBLE APPROACH <i>T. Palabaş</i>	74
THE PHARMACEUTICAL BOTANICAL STUDIES ON THE ENDEMIC <i>Asperula pestalozzae</i> Boiss. (RUBIACEAE) <i>K. Kayaş, A. Kaya</i>	86
THE EFFECTS OF DIFFERENT SONICATION METHODS ON ALPHA-SYNUCLEIN PRE-FORMED FIBRILS <i>H. Akyel, E. Bahador Zırh, S. Zırh, B. C. Tel</i>	100
ALLEVIATING SALT STRESS IN TOMATO PLANTS THROUGH HYDROGEN PEROXIDE PRIMING: DIFFERENTIATIONS OF ANTIOXIDANT ENZYME ACTIVITIES AND GENE EXPRESSION PATTERNS <i>M. Kar, G. Gökpınar, Ö. Doğan</i>	118
BIOCHAR-SUPPORTED IN VITRO CULTURES OF <i>Lavandula officinalis L.</i> <i>P. Nartop, S. Özdil Şener, S. B. Gök</i>	133



RESEARCH ARTICLE

THE CLINICAL SIGNIFICANCE OF SOX9 GENE IN DIFFERENT CANCER TYPES:
AN IN-SILICO ANALYSIS

Ethem Serhat YAVAS ¹, Sedef Hande AKTAS ^{1,2*}, Goksel EFENDİOĞLU ³, Dilara Fatma AKIN ⁴

¹ Eskişehir Osmangazi University, Graduate School of Natural and Applied Science, Department of Biotechnology and Biosafety, Eskişehir, Turkey

serhatyavas85@gmail.com - [0000-0002-9677-1605](https://orcid.org/0000-0002-9677-1605)

² Eskişehir Osmangazi University, Vocational School of Health Services, Eskişehir, Turkey

sedefhande@gmail.com - [0000-0002-1091-6974](https://orcid.org/0000-0002-1091-6974)

³ Eskişehir Osmangazi University, Graduate School of Natural and Applied Science, Department of Biotechnology and Biosafety, Eskişehir, Turkey

goksel.efendioglu1@gmail.com - [0000-0001-7903-6089](https://orcid.org/0000-0001-7903-6089)

⁴ Nigde Omer Halisdemir University, Faculty of Medicine, Department of Medical Biology, Nigde, Turkey

dilarafatmaakin@gmail.com - [0000-0002-0903-0017](https://orcid.org/0000-0002-0903-0017)

Abstract

One of the common problems in the pathogenesis of human cancer is characterized as the dysregulation of transcription factors. SOX9 is important as it is one of the critical transcription factors involved in various diseases, including cancer. In addition, SOX9 also acts as a proto-oncogene or tumor suppressor gene, depending on the cancer type. In this study, we aimed to reveal the mutation and expression status of the SOX9 transcription factor and the effect of this gene on the survival of patients with different cancer groups. The data sets for expression analysis and overall survival analysis were performed by the GEPIA database. Analysis of the mutation profile was performed by the cBio database. As a result, SOX9 gene expressions were significantly elevated in BLCA, CESC, CHOL, COAD, ESCA, GBM, KIRP, LGG, LIHC, LUSC, OV, PAAD, READ, SKCM, STAD, TGCT, THYM, UCEC and UCS in cancer tissues compared to that in normal tissues ($p < 0.05$). According to overall survival (OS) analysis; the SOX9 gene has a significant relationship with OS in ACC, CESC, KIRC, LGG, and THYM (ACC $p: 0.0079$, CESC $p: 0.038$, KIRC $p: 0.051$, LGG $p: 0.00055$, THYM $p: 0.031$). A total of 170 mutations in SOX9 were determined according to mutation analysis. Seventy-six of them were detected as driver mutations. The analysis shows that SOX9 expression status has a different effect in each cancer type, and although there is no significant mutation in the SOX9 gene in ACC cancer type, high expression of this gene is important for survival. Therefore, it is of great importance to analyze the epigenetic changes in the SOX9 gene in ACC cancer type. The analysis also indicates that the SOX9 gene is discriminatory for the survival of adrenocortical carcinoma, cervical squamous cell carcinoma and endocervical adenocarcinoma, renal clear cell carcinoma, brain low-grade glioma and thymoma cancer types.

Keywords

SOX9,
Transcription factor,
Tumorigenesis,
Mutation,
Gene expression

Time Scale of Article

Received : 20 June 2023
Accepted : 31 May 2024
Online date : 30 July 2024

Abbreviations

ACC: Adrenocortical carcinoma
BLCA: Bladder Urothelial Carcinom
BRCA: Breast invasive carcinoma
CESC: Cervical squamous cell carcinoma and endocervical adenocarcinoma
CHOL: Cholangio carcinoma
COAD: Colon adenocarcinoma
DLBC: Lymphoid Neoplasm Diffuse Large B-cell Lymphoma
ESCA: Esophageal carcinoma
GBM: Glioblastoma multiforme
HNSC: Head and Neck squamous cell carcinoma
KICH: Kidney Chromophobe
KIRC: Kidney renal clear cell carcinoma
KIRP: Kidney renal papillary cell carcinoma
LAML: Acute Myeloid Leukemia
LGG: Brain Lower Grade Glioma
LIHC: Liver hepatocellular carcinoma
LUAD: Lung adenocarcinoma
LUSC: Lung squamous cell carcinoma
MESO: Mesothelioma
OV: Ovarian serous cystadenocarcinoma
PAAD: Pancreatic adenocarcinoma
PCPG: Pheochromocytoma and Paraganglioma
PRAD: Prostate adenocarcinoma
READ: Rectum adenocarcinoma
SARC: Sarcoma
SKCM: Skin Cutaneous Melanoma
STAD: Stomach adenocarcinoma
TGCT: Testicular Germ Cell Tumors
THYM: Thyroid carcinoma (THCA), Thymoma
UCEC: Uterine Corpus Endometrial Carcinoma
UCS: Uterine Carcinosarcoma
UVM: Uveal Melanoma

1. INTRODUCTION

Dysregulation of transcription factors, which are critical in many important processes such as cell survival, proliferation, repair of DNA damage, tissue differentiation, homeostasis, metabolism, and apoptosis, constitutes one of the important problems in cancer development [1]. It has been stated that about 20% of oncogenes are identified as transcription factors (TF) [2]. Regulation of target gene transcription by TFs is performed via binding to specific DNA sequences in the promoter and/or enhancer region [3]. Therefore, direct and indirect mechanisms affecting TF activity were of significance such as point mutations, gene amplification or deletion, chromosomal translocations, expressional changes, and non-coding DNA mutations [4].

Transcription factors are divided into two groups; master TFs and differential TFs. The sex-determining region Y (SRY) – related HMG-box genes (SOX) genes, which are known as a developmental transcription factor, were examined in the differential TFs group. The SOX family consists of more than 20 members that mediate DNA binding by a highly conserved high mobility group (HMG) domain [5].

SOX transcription factors are known as regulators of developmental, physiological, and pathological events [6]. Considered within the SOX E family, the SOX9 gene plays a key role in chondrocyte differentiation and skeletal development and is one of the important transcription factors involved in various diseases, including cancer [1,6]. It is stated that the SOX9 gene is mutated in 2.76% of all cancers [7]. Significant associations were found between this gene and cancer of the breast, prostate, renal, thyroid, central nervous system (CNS), and gastrointestinal [6, 8-12]. Furthermore, SOX9 acts as a proto-oncogene or tumor suppressor gene depending on the type of cancer and certain conditions [13]. This makes SOX9 fascinating for cancer research. For instance, studies have shown that while SOX9 acts as an oncogene in lung, glioma, ovarian cancer, parathyroid cancer, hepatocellular carcinoma, breast cancer, pancreatic cancer, prostate cancer, gastric cancer, oral squamous cell carcinoma, esophageal squamous cancer, renal cancer, urothelial cancer, it acts as a tumor suppressor in colorectal cancer and cervical cancer. In the case of melanoma, it acts as both an oncogene and a tumor suppressor [13]. Besides, SOX proteins are stated as key players in cancer cell stemness, drug resistance, proliferation, invasion, and metastasis [13, 14-17]. SOX9 is considered also a biomarker in which its upregulation is correlated with undesirable prognosis [17, 18]. Especially in some types of cancer such as cervical cancer, SOX9 plays like a double-edged sword. It is therefore important to analyze this gene in different types of cancer.

In this study, we aimed to examine the expression, survival, and mutation analysis of SOX9 gene in a broad perspective of different cancer types. For this purpose, the GEPIA database was used to reveal the expression levels between normal and cancer tissues and the significance of this gene in overall survival. Additionally, the cBio database was used to analyze the mutation profiles.

2. MATERIALS AND METHODS

2.1. Database Analysis

The gene expression profiling interactive analysis was used to analyze the mRNA levels of the SOX9 gene in normal tissues, and its related cancer types. The impact of the SOX9 gene on cancer patients' overall survival in thirty-three cancer was carried out in the data set of The Cancer Genome Atlas (TCGA). The web interface is easy to use and data analysis is done through the "Expression DIY" and "Survival" tabs on the main page. In case of the gene name of interest and data sets are entered from the "Expression on Box Plot" tab, the system calculates using $\log_2(\text{transcripts per million}+1)$ for log scale and creates a plot for Match TCGA normal and GTEx data. For survival analysis, a plot is created after giving the gene symbol to the "Gene" tab and selecting the data set. In the calculation of the Hazard ratio, selecting a Cox PH Model and the group cut-off value as median, quartile or custom is optional. In our analysis, the hazard ratio was calculated based on the Cox PH Model, and the group cut-off value was chosen as the median.

2.2. Gene Expression Profiling Interactive Analysis

GEPIA (<http://gepia.cancer-pku.cn/>) is an online database containing expression profiles of 9736 tumor samples and 8587 healthy samples. This interactive bioinformatics tool was developed to provide customizable analysis such as differential expression analysis in tumor or normal tissues, profiling by cancer types or pathological stages, patient survival analysis, similar gene detection, correlation analysis, and dimensionality reduction analysis. In-silico analysis was performed with 9498 tumor samples and 5540 healthy samples for expression analysis and 9473 tumor samples for survival data. The targeted gene, SOX9, expression analysis was performed for 31 cancer types having convenient data from the GEPIA database.

2.3. Survival Analysis

The analysis was performed with available Overall Survival (OS) patient data from the GEPIA database. Overall survival analysis based on a Log-rank test with a 95% confidence interval was performed to generate survival plots. Survival analysis according to the low and high mRNA expression levels of the study genes was performed via the web interface.

2.4. cBio Cancer Genomics Portal (cBioPortal) Analysis

cBio Cancer Genomics Portal (<http://cbioportal.org>) is an open-access bioinformatics tool that provides mutation data, copy number changes, microarray, and RNA sequencing-based m-RNA expression changes, DNA methylation values, protein and phosphoprotein levels with data from “The Cancer Genome Atlas (TCGA)”. In all of the TCGA PanCancer Atlas studies; 32 projects were included in 10967 case studies. To comprehensively examine the mutations in the SOX9 gene, it was selected as the cancer type of interest from the web interface. For this purpose, comprehensive mutation profile analyses were performed using the features provided by the interface of the genes of interest using OncoPrint, Cancer Types Summary, and Mutation tools provided by cBioPortal.

2.5. Statistical Analysis

All statistical analyses were carried out on the GEPIA database. Kaplan-Meier analyses were conducted to estimate the OS rate of cancers. Low-high-expression groups were compared using the log-rank test. The p-values for the analyzes were calculated automatically by the database, and p-values below 0.05 were considered statistically significant.

3. RESULTS

3.1. Gene Expression Analysis of Selected Genes in GC

SOX9 gene expression was significantly high in BLCA, CESC, CHOL, COAD, ESCA, GBM, KIRP, LGG, LIHC, LUSC, OV, PAAD, READ, STAD, THYM, UCEC, UCS in cancer tissues compared to that in normal tissues ($p < 0.05$). Conversely, SOX9 gene expression was high in SKCM and TGCT in normal tissues compared to that in cancer tissues ($p < 0.05$) (Figure 1). Expression analysis of all cancer types were given in detail in Supplementary Figure 1.

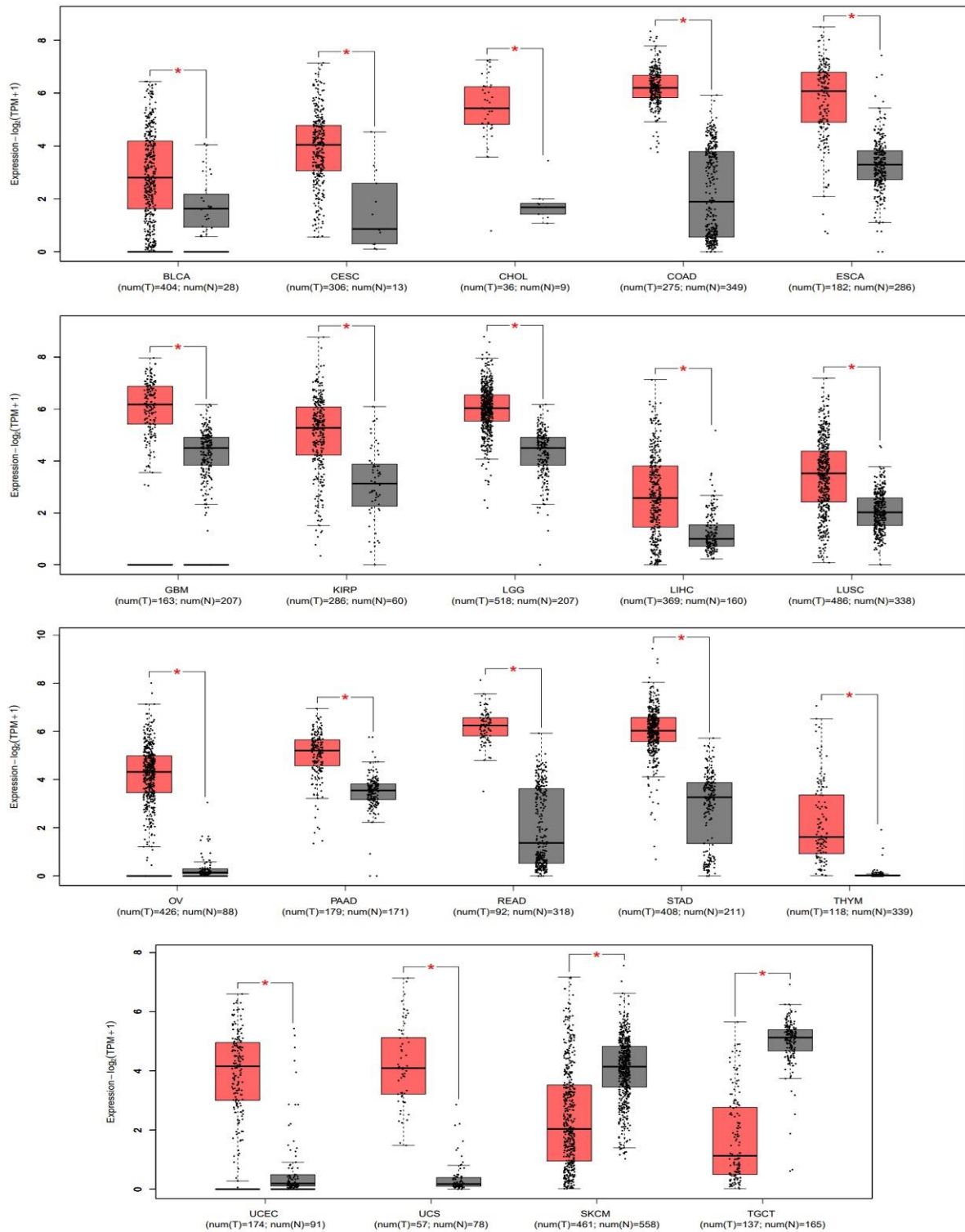


Figure 1. Comparative analysis of the tissue-specific differential expression of SOX9 gene using GEPIA (*indicates $p < 0.05$). Red bar indicates tumor, grey bar indicates normal tissue

3.2. Survival Analysis of Selected Genes in GC

The significance level of the SOX9 gene in 33 different cancer types on OS is as follows; ACC $p:0.0079$, BLCA $p:0.33$, BRCA $p:0.65$, CESC $p:0.038$, CHOL $p:0.78$, COAD $p:0.36$, DLBC $p:0.91$, ESCA $p:0.33$,

GBM p:0.23, HNSC p:0.11, KICH p:0.45, KIRC p:0.051, KIRP p:0.9, LAML p:0.13, LGG p:0.00055, LIHC p:0.23, LUAD p:0.079, LUSC p:0.19, MESO p:0.31, OV p:0.66, PAAD p:0.33, PCPG p:0.92, PRAD p:0.6, READ p:0.44, SARC p:0.37, SKCM p:0.17, STAD p:0.31, TGCT p:0.45, THCA p:0.55, THYM p:0.031, UCEC p:0.76, UCS p:0.32, UVM p:0.16. According to the survival graphs, it was found that the SOX9 gene has a significant relationship with OS in ACC, CESC, KIRC, LGG, and THYM (Figure 2). Survival graphs of all cancer types were given in detail in Supplementary Figure 2.

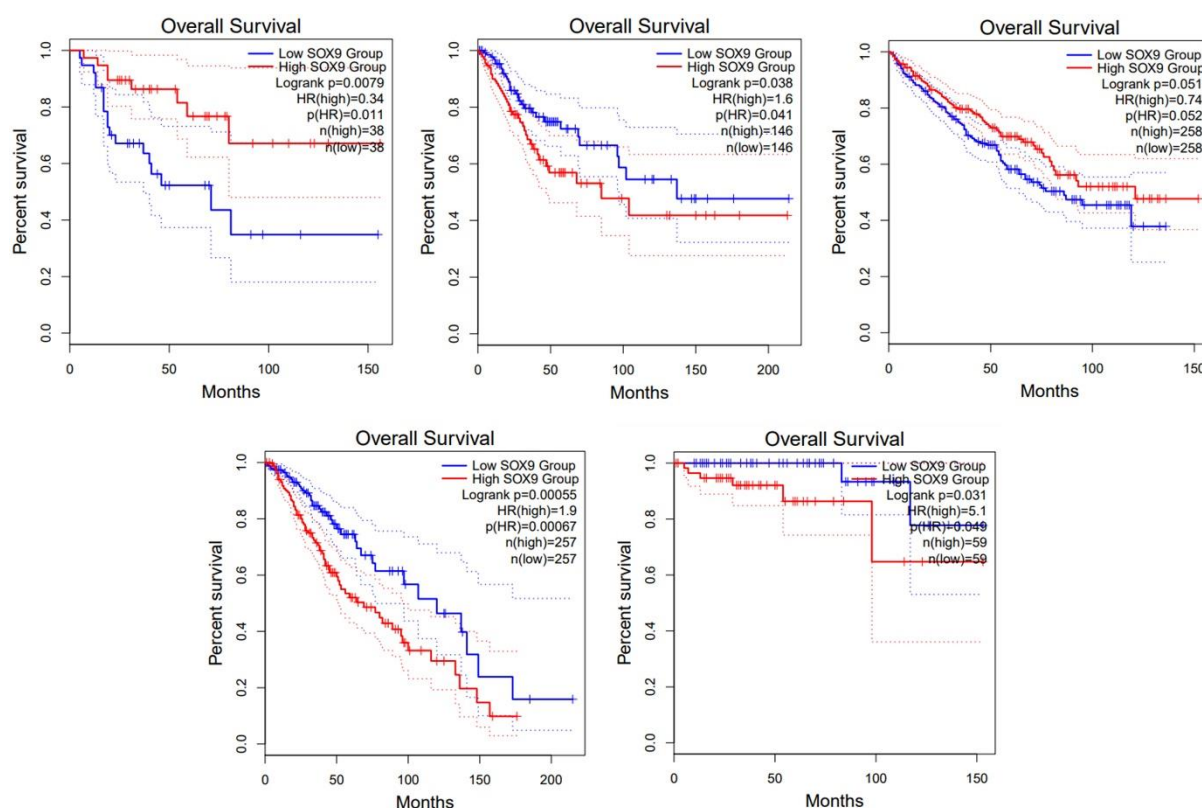


Figure 2. Overall survival analysis of the SOX9 gene in ACC, CESC, KIRC, LGG, THYM using GEPIA (*indicates $p < 0.05$).

3.3. Results of Comprehensive SOX9 Mutation Analysis

Genome sequencing data of patients were analyzed via the cBioPortal interface, aiming to identify genetic changes in the SOX9 gene in the TCGA pan-cancer Atlas cohort, which consisted of a total of 10967 patient samples. A total of 170 mutations (89 missense mutations, 69 nonsense, 9 frameshifts, 3 splice region) were determined in the SOX9 gene. The features of these mutations are thoroughly listed in Table 1. Seventy-six of these mutations were detected as driver mutations. Deep deletion and gene amplifications were also detected from the whole 32 TCGA PanCancer Atlas studies. At least one of the above-mentioned mutations was detected in 2.9% of the patient group (Figure 3A). The localization of the mutations detected on the domains of the proteins belonging to the SOX9 gene in TCGA PanCancer Atlas cohorts is shown in Figure 3B. Colorectal adenocarcinoma has the highest mutation rate in terms of carrying SOX9 genetic anomaly in 32 different cancer types (Figure 3C). SOX9 mutation was not detected in Acute Myeloid Leukemia (TCGA, PanCancer Atlas) Adrenocortical Carcinoma (TCGA, PanCancer Atlas) Cholangiocarcinoma (TCGA, PanCancer Atlas) Diffuse Large B-Cell Lymphoma (TCGA, PanCancer Atlas) Kidney Chromophobe (TCGA, PanCancer Atlas) and Testicular Germ Cell Tumors (TCGA, PanCancer Atlas).

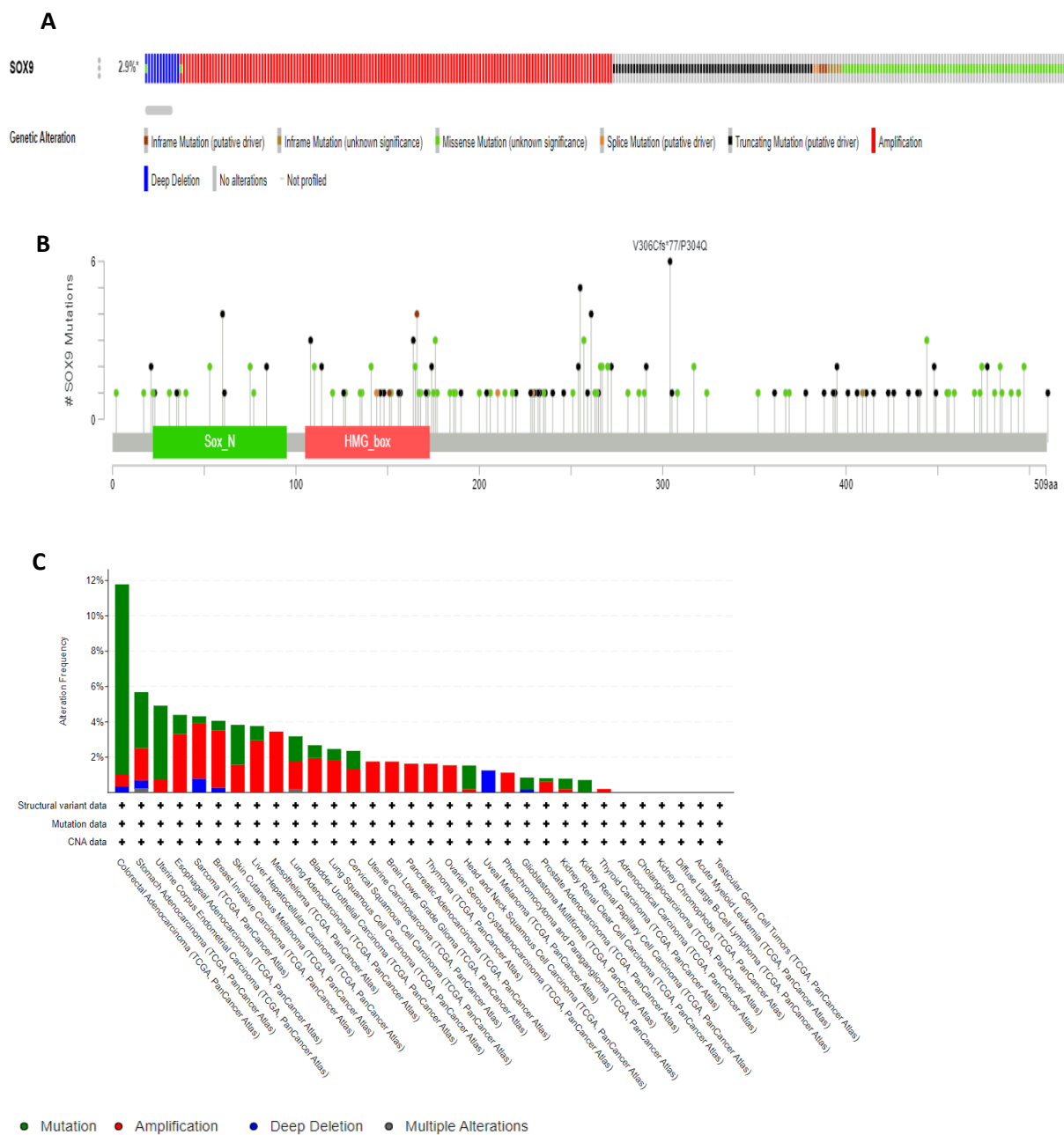


Figure 3. (A) Distribution of mutations in SOX9 gene in TCGA Pan Cancer cohorts from cBioPortal. Percentages of overall mutations for SOX9 gene is given on the left. (B) The lollipop graphic of domain architecture of the SOX9 protein and mutations detected in TCGA Pan Cancer Atlas cohorts. Human SOX9 is a polypeptide comprising 509 amino acids. SOX_N: Sox developmental protein N-terminal HMG_box: High-Mobility Group. (C) Distribution of SOX9 alterations across different cancer types and TCGA PanCancer studies.

4. DISCUSSION AND CONCLUSION

In the present analysis, SOX9 gene expression was found to have changed between cancer vs normal tissues in 61.29% (19 of 31) of investigated cancer types. SOX9 gene expression was significantly high in BLCA, CESC, CHOL, COAD, ESCA, GBM, KIRP, LGG, LIHC, LUSC, OV, PAAD, READ, STAD, THYM, UCEC, UCS in cancer tissues compared to that in normal tissues ($p < 0.05$). The expression of

the SOX9 gene in SKCM and TGCT cancer types was found high in normal tissues compared to cancer tissues. Especially in OV, THYM, UCEC, and UCS cancer types, it is noteworthy that SOX9 gene expression is very low in normal tissues. Therefore, increased SOX9 gene expression in these four cancer types; ovarian cancer, thymoma, endometrial cancer, and uterine carcinosarcoma may have diagnostic value. According to the survival graphs of our analysis of the SOX9 gene in 33 different cancer types, a significant relationship with OS in ACC, CESC, KIRC, LGG, and THYM (ACC p:0.0079, CESC p:0.038, KIRC p:0.051, LGG p:0.00055, THYM p:0.031) was found. However, the points to be considered in the interpretation of this analysis are as follows: as high SOX9 expression increases survival in ACC and KIRC cancer types, low SOX9 expression provides higher survival in CESC, LGG, and THYM cancer types. Therefore, the therapeutic use of SOX9 expected to be different in each type of cancer. Besides, literature expresses SOX9 as double-edged sword in cervical cancer since SOX9 possesses both tumor-suppressor and tumor-promoting role [19-21]. In addition, examining the results of the mutation analysis of the SOX9 gene of these cancer types (ACC, CESC, KIRC, LGG, THYM), which are important in terms of survival showed that the ACC cancer type does not have any mutation in the SOX9 gene. This is remarkable since there is no significance when normal tissue and cancerous tissue are compared for SOX9 gene expression in this cancer type, but in survival analysis, increased SOX9 gene expression indicates more survival. This suggests that epigenetic mechanisms may affect SOX9 expression in the ACC cancer type. In fact, in the review article by Ettaieb et al. examining the role of epigenetics in ACC diagnosis, prognosis and therapeutic strategies, CTNNB1 gene is referred as among the most altered genes by somatic mutations, DNA copy-number alterations and epigenetic silencing. It is also known that in ACC, the Wnt/ β -catenin (CTNNB1) is frequently activated with CTNNB1 mutations and this leads to poor prognosis [22]. The article, which also drew attention to epigenetic modifications in CTNNB1, allowed us to examine the relationship between CTNNB1 and SOX9. Therewith we performed an analysis for CTNNB1 and SOX9 interaction via STRING, a database of functional protein association networks, and found that CTNNB1 and SOX9 genes interacted (Supplementary Figure 3). As the radical surgical resection is the only curable option and the prognostic stratification is extremely important to individualize adjuvant therapies, it will be meaningful to examine in detail the epigenetic alterations and interaction between CTNNB1 and SOX9 in understanding the pathogenesis of ACC. Mutation analyses of four other cancer types in terms of SOX9 mutations were as follows; CESC and KIRC cancer types have missense mutation and gene amplification, LGG and THYM cancer types have gene amplification. According to the localization of the mutations, it was detected that all investigated mutations in our mutational analyses were found in the HMG domain. As the HMG box domain alone carries out DNA binding, DNA bending, protein interactions, and nuclear import or export functions, mutations in this domain are important. Another important inference can be related to the localization of the mutations on the HMG domain: HMG domain comprises two nuclear localization signal (NLS) sequences; one is located at the N-terminus and contributes to the nuclear translocation of SOX9 by binding to calmodulin (NLS1) and one is located at the C-terminus and interacts with importin b to form a complex (NLS2) and a leucine-rich nuclear export signal (NES) sequence. NES sequence, located between the two NLS sequences and mediate the nuclear export of SOX9 [23]. NLS1 sequence is present between 105-121, the NES sequence is present between 134-147 and the NLS2 sequence is present between 179-182 [24]. As it was stated that NLS sequences and the NES sequence can be activated by different pathways, it can be important to investigate the mutations found in these regions [23]. In the result of analysis P108S, N110T, N110S, W115Gfs*136, V114L, and R120C mutations are in the range of NLS1 sequence signal, L135F, K141E, K141N, and X144_splice mutations are in the range of NES sequence signal (Supplementary Table 1).

In conclusion, as it is clearly seen in the analysis we performed, SOX9 expression status has different effect in each cancer type. It is noteworthy that the ACC cancer type does not have a significant mutation in the SOX9 gene although the high expression of this gene makes a significant difference in terms of survival. Therefore, analyzing epigenetic changes in the SOX9 gene in the ACC cancer type is of great importance. The analysis also points out that the SOX9 gene is distinctive for the survival of

adrenocortical carcinoma, cervical squamous cell carcinoma and endocervical adenocarcinoma, kidney renal clear cell carcinoma, brain lower grade glioma, and thymoma cancer types.

ACKNOWLEDGEMENTS

The data used in our study are obtained from the public database the TCGA Research Network: <https://www.cancer.gov/tcga>. We thank the TCGA and GEPIA databases for the availability of the data.

CONFLICT OF INTEREST

The authors stated that there are no conflicts of interest regarding the publication of this article.

CRedit AUTHOR STATEMENT

Ethem Serhat Yavas: Investigation, Formal analysis, Writing, Visualization. **Sedef Hande Aktas:** Original draft, Writing, Supervision, Visualization, Conceptualization. **Göksel Efendioğlu:** Investigation, Formal analysis, Writing. **Dilara Fatma Akın:** Writing, Visualization, Conceptualization.

REFERENCES

- [1] Kumar P, Mistri TK. Transcription factors in SOX family: Potent regulators for cancer initiation and development in the human body. *Semin Cancer Biol* 2020; 67: 105–113.
- [2] Lambert M, Jambon S, Depauw S, David-Cordonnier MH. Targeting Transcription Factors for Cancer Treatment. *Molecules* 2018; 23: 1479.
- [3] Hawkins LJ, Al-attar R, Storey KB. Transcriptional regulation of metabolism in disease: From transcription factors to epigenetics. *PeerJ* 2018; 6: e5062.
- [4] Bushweller JH. Targeting transcription factors in cancer—From undruggable to reality. *Nat Rev Cancer* 2019; 19: 611–624.
- [5] Grimm D, Bauer J, Wise P, Krüger M, Simonsen U, Wehland M, Infanger M, Corydon TJ. The role of SOX family members in solid tumours and metastasis. *Semin Cancer Biol* 2020; 67:122–153. Academic Press.
- [6] Grimm D, Bauer J, Wise P, Krüger M, Simonsen U, Wehland M, Infanger M, Corydon, TJ. The role of SOX family members in solid tumours and metastasis. *Semin. Cancer Biol* 2020; 67: 122–153.
- [7] McDowall S, Argentaro A, Ranganathan S, Weller P, Mertin S, Mansour S, Tolmie J, Harley V. Functional and Structural Studies of Wild Type SOX9 and Mutations Causing Campomelic Dysplasia. *J. Biol. Chem* 1999; 274: 24023–24030.
- [8] Cheng PF, Shakhova O, Widmer DS, Eichhoff OM, Zingg D, Frommel SC, Belloni B, Raaijmakers MI, Goldinger SM, Santoro R. et al. Methylation-dependent SOX9 expression mediates invasion in human melanoma cells and is a negative prognostic factor in advanced melanoma. *Genome Biol* 2015; 16: 42.

- [9] Richtig G, Aigelsreiter A, Schwarzenbacher D, Röss AL, Adiprasito JB, Stiegelbauer V, Hoefler G, Schauer S, Kiesslich T, Kornprat P, Winder T, Eisner F, Gerger A, Stoeger H, Stauber R, Lackner C, Pichler M. SOX9 is a proliferation and stem cell factor in hepatocellular carcinoma and possess widespread prognostic significance in different cancer types. *PLoS one* 2017; 12: e0187814.
- [10] Yang X, Liang R, Liu C, Liu JA, Cheung MPL, Liu X, Man OY, Guan XY, Lung HL, Cheung M. SOX9 is a dose-dependent metastatic fate determinant in melanoma. *J. Exp. Clin. Cancer Res* 2019; 38: 17.
- [11] Sumita Y, Yamazaki M, Maruyama S, Abé T, Cheng J, Takagi R, Tanuma J. Cytoplasmic expression of SOX9 as a poor prognostic factor for oral squamous cell carcinoma. *Oncol. Rep* 2018; 40: 2487-2496.
- [12] Liu C, Liu L, Chen X, Cheng J, Zhang H, Shen J, Shan J, Xu Y, Yang Z, Lai M, Qian C. Sox9 regulates self-renewal and tumorigenicity by promoting symmetrical cell division of cancer stem cells in hepatocellular carcinoma: Hepatobiliary Malignancies. *Hepatology* 2016; 64: 117–129.
- [13] Panda M, Tripathi SK, Biswal BK. SOX9: An emerging driving factor from cancer progression to drug resistance. *Biochim Biophys Acta Rev Cancer* 2021; 1875: 188517.
- [14] Zhang S, Che D, Yang F, Chi C, Meng H, Shen J, Qi L, Liu F, Lv L, Li Y et al. Tumor-associated macrophages promote tumor metastasis via the TGF- β /SOX9 axis in non-small cell lung cancer. *Oncotarget* 2017; 8: 99801–99815.
- [15] Huang JQ, Wei FK, Xu XL, Ye SX, Song JW, Ding PK, Zhu J, Li HF, Luo XP, Gong H, SOX9 drives the epithelial–mesenchymal transition in non-small-cell lung cancer through the Wnt/ β -catenin pathway. *J. Transl. Med* 2019; 17: 143.
- [19] Xiao S, Li Y, Pan Q, Ye M, He S, Tian Q & Xue M. MiR-34c/SOX9 axis regulates the chemoresistance of ovarian cancer cell to cisplatin-based chemotherapy. *J. Cell. Biochem* 2019; 120: 2940–2953.
- [16] Xiao S, Li Y, Pan Q, Ye M, He S, Tian Q & Xue M. MiR-34c/SOX9 axis regulates the chemoresistance of ovarian cancer cell to cisplatin-based chemotherapy. *J. Cell. Biochem* 2019; 120: 2940–2953.
- [17] Higashihara T, Yoshitomi H, Nakata Y, Kagawa S, Takano S, Shimizu H, Kato A, Furukawa K, Ohtsuka M, Miyazaki M. Sex Determining Region Y Box 9 Induces Chemoresistance in Pancreatic Cancer Cells by Induction of Putative Cancer Stem Cell Characteristics and Its High Expression Predicts Poor Prognosis. *Pancreas* 2017; 46: 1296–1304.
- [18] Zhu H, Tang J, Tang M, Cai H. Upregulation of SOX9 in osteosarcoma and its association with tumor progression and patients' prognosis. *Diagn. Pathol* 2013; 8: 183.
- [19] Wu JH, Liang XA, Wu YM, Li FS, Dai YM. Identification of DNA methylation of SOX9 in cervical cancer using methylated-CpG island recovery assay. *Oncol rep* 2013; 29:125-32.
- [20] Zhao J, Li H, Yuan M. EGR1 promotes stemness and predicts a poor outcome of uterine cervical cancer by inducing SOX9 expression. *Genes Genom* 2021; 43:459-70.

- [21] Wang HY, Lian P, Zheng PS. SOX9, a potential tumor suppressor in cervical cancer, transactivates p21WAF1/CIP1 and suppresses cervical tumor growth. *Oncotarget* 2015; 6:20711.
- [22] Ettaieb M, Kerkhofs T, van Engeland M, Haak H. Past, present and future of epigenetics in adrenocortical carcinoma. *Cancers* 2020; 12: 1218.
- [23] Chen H, He Y, Wen X, Shao S, Liu Y & Wang J. SOX9: Advances in Gynecological Malignancies. *Front. Oncol* 2021; 11: 768264.
- [24] Belo J, Krishnamurthy M, Oakie A & Wang R. The Role of SOX9 Transcription Factor in Pancreatic and Duodenal Development. *Stem Cells Dev* 2013; 22: 2935–2943.




RESEARCH ARTICLE

EARLY-STAGE DIABETES RISK PREDICTION USING MACHINE LEARNING
TECHNIQUES BASED ON ENSEMBLE APPROACH

Tuğba PALABAŞ^{1,*}

¹ Biomedical Engineering, Faculty of Engineering, Zonguldak Bulent Ecevit University, Zonguldak, Turkey

tugba.palabas@gmail.com -  [0000-0002-6985-6494](https://orcid.org/0000-0002-6985-6494)

Abstract

Diabetes Mellitus which is considered as one of the deadliest is a common, chronic disease. It also causes the emergence of many diseases, especially neuropathy, nephropathy, and retinopathy. In this context, initiating a rapid treatment process is very important by accurately evaluating the symptoms and making an early diagnosis of the disease. This study aims to provide an effective model that can determine the risk of diabetes at an early stage with the best accuracy. For this purpose, classification algorithms frequently used in diabetes risk prediction are supported by ensemble approaches. Firstly, the performance of Naive Bayes (NB), Trees-J48, k Nearest Neighbor (kNN), and Sequential Minimal Optimization (SMO) classifiers are analyzed separately by using a dataset of 520 samples collected with direct questionnaires from Sylhet Diabetes Hospital patients in Sylhet, Bangladesh. Then, the effects of Adaboost, Bagging and Random Sub-Space (RSS) algorithms on classifier success are investigated and it is shown that the J48 classifier based on Adaboost approach has the best accuracy. Finally, the Wrapper Subset Eval (WSE) feature extraction algorithm is applied to reduce the estimation cost and increase classification success. Thus, the best accuracy (99%) is achieved using reduced data set with proposed classifier method.

Keywords

Diabetes,
Classification,
Ensemble Approach,
Feature Extraction

Time Scale of Article

Received :29 June 2023
Accepted : 17 July 2024
Online date :30 July 2024

1. INTRODUCTION

The body uses carbohydrates, proteins and fats within foods as an energy source. While these nutrients, which are broken down into small particles to be absorbed, are digesting, a simple sugar called glucose is released. Glucose is an important nutrient source for all organs, especially the mammalian brain. Thus, glucose must be taken into the cell to be used the energy. It is the insulin hormone located behind the stomach and released from the pancreatic gland, which allows glucose to enter the cell and be stored as glycogen [1-2]. Diabetes Mellitus is a disease caused by excessively high levels of glucose as a result of the pancreas not producing enough insulin for the body, or the insulin produced by the pancreas not being used effectively by the body [3]. Thus, the glucose that passes from food into the blood cannot be used and the sugar level in the blood increases. This situation causes damage to many tissues and organs in the long term. Moreover, it triggers many diseases such as heart diseases, kidney problems and blindness.

According to the 2021 International Diabetes Federation (IDF) data, around 537 million adults aged 20-79 years live with diabetes worldwide in 2021 and this number is expected to increase to 643 in 2030 and 784 million in 2045. According to the Federation's report, one in 11 adults has diabetes and one in every two adults is unaware they have diabetes [4-5]. Early diagnosis of the disease is extremely

*Corresponding Author: tugba.palabas@gmail.com

important to prevent or slow the progress of advanced complications by allowing rapid intervention [6]. However, diagnosis is a very complex stage as it requires the evaluation of many factors together [7-9]. Machine learning algorithms, such as Naive Bayes (NB), Decision Trees (DT), k Nearest Neighbor (kNN) and Support Vector Machine (SVM) are frequently performed in healthcare systems to predict various disorders such as Diabetes Mellitus and they provide a great contribution to progress of the diagnosis process rapidly and accurately [10]. In addition, automatic taking of the patient's history and computer-aided decision-making provides a significant benefit in the physician's ability to initiate an effective and rapid treatment process, as possible problems are detected in early.

Many studies have been performed about early diagnosis by using data mining and statistical analysis methods that consider the general complaints of the patient and the prominent symptoms of the disease. For instance, Khafaga et al. [11] analyzes the diabetes dataset with NB, Logistic Regression (LR), and Random Forest (RF) Algorithms. Authors obtain the best accuracy using RF method on this dataset after applying 10-Fold Cross Validation and Percentage Split evaluation techniques. Similarly, Islam et al. [12] proposed a methodology using three ensemble techniques, AdaBoost, Bagging, and RF for estimation of the early diabetes risk. To test the success of the classification algorithms, the same diabetes dataset in the UCI machine learning repository is used and it is shown that RF algorithm provides maximal accuracy, precision, recall, and F-measure. Then Laila et al. [10] present an integrative approach that combines classification algorithms with association rules to improve prediction accuracy. Namely, they present a method by using Local Outlier Factor, Balanced Bagging Classifier, and association rules for early-stage prediction of diabetes. As a result, they obtain the prediction accuracy (97.36%). Pima Indians Diabetes dataset is another dataset which is widely used in much research. [Sisodia D and Sisodia DS [13] compare the performance of NB, SVM and DT classifiers in early diagnosis of diabetes according to various parameters such as Recall, F-Measure, Accuracy and ROC using this dataset in the UCI database. It is shown that the NB method achieves the highest correct classification success (76.30%). Naz and Ahuja [14] present a study comparing data mining classification techniques as Artificial Neural Network (ANN), NB, DT and Deep Learning (DL) and the accuracy is obtained by these functional classifiers within the range of 90–98%. Peker et al. [15] present a study by using diabetes data obtained from Köycegiz and Dalaman State Hospitals of Mugla in Turkey and comparing different algorithms as RF, Feed Forward Neural Network (FFNN), DT, kNN and SVM.

In this study, firstly, Early-Stage Diabetes Risk Prediction dataset in the UCI machine learning repository is analyzed with NB, Trees-J48, kNN and sequential minimal optimization (SMO) algorithm. Then, the effects of ensemble algorithms on the performance of these classifier are examined in detail by using three different methods (Adaboost [16], Bagging [17], Random Sub-Spaces (RSS) [18]). The success of classifiers and the effect of ensemble algorithms on classification performance are compared for 4 different criteria (Accuracy, Kappa, Root Mean Squared Error (RMSE) and Area Under of Curve (AUC)). In addition, to reduce the cost in the collection of data related to the detection of diabetes risk and increase the detection speed, the importance ratios of the features are determined by using the Wrapper Subset Eval (WSE) algorithm When the attributes are removed from the data set according to these rates, classification success is increased. Thus, the features are reduced in the preprocessing step, allowing the training and testing steps to be executed faster. A higher success is achieved in a shorter time.

2. MATERIAL AND METHOD

"The first sentence of Section 2 should be changed as "The Early-Stage Diabetes Risk Prediction dataset" in "UC Irvine Machine Learning Repository database" is analyzed in this study. This dataset has been collected using direct questionnaires from the patients of Sylhet Diabetes Hospital of Sylhet province in Bangladesh and approved by a consultant. It contains the sign and symptom data of newly diabetic or would be diabetic patient [19]. The content of the training data consists of 520 examples of 17 attributes shown in Table 1.

All results are obtained through with the “Waikato Environment for Knowledge Analysis (WEKA)” machine learning software.

Table 1. For the Early-Stage Diabetes Risk Prediction dataset, the attributes, which indicative the risk factors, and value type of attributes.

	Attribute	Value Type
1	Age (Age)	Numeric
2	Gender (Male/Female)	Nominal
3	Polyuria (Yes/No)	Nominal
4	Polydipsia (Yes/No)	Nominal
5	Sudden weight loss (Yes/No)	Nominal
6	Weakness (Yes/No)	Nominal
7	Polyphagia (Yes/No)	Nominal
8	Genital thrush (Yes/No)	Nominal
9	Visual blurring (Yes/No)	Nominal
10	Itching (Yes/No)	Nominal
11	Irritability (Yes/No)	Nominal
12	Delayed healing (Yes/No)	Nominal
13	Partial paresis (Yes/No)	Nominal
14	Muscle stiffness (Yes/No)	Nominal
15	Alopecia (Yes/No)	Nominal
16	Obesity (Yes/No)	Nominal
17	Class (Positive/Negative)	Nominal

2.1. Feature Extraction

First, 17 risk factors expressed in Table 1 are considered as features. A feature vector with 520x17 is obtained by using 520 positive (class1) and negative (class2) records with diabetes or symptoms in the 20-65 age range. The performance of classifiers and the effects of ensemble algorithms on classification success are investigated by using this vector. Then, feature extraction is performed using WSE–Greedy Stepwise (GS) algorithm among 17 features and the importance ratio of the features is determined as shown in Table 2. The performance criteria are evaluated again for the same methods ignoring 6th, 13th, 16th risk factors.

2.2. Classification

In this study, 4 classification algorithms, namely NB, Trees-J48, kNN, and SMO are used, and the classification performances of these algorithms are evaluated and presented comparatively. To improve the success of classification, Adaboost, Bagging, RSS algorithms, which are ensemble learning methods, are used together with the classifiers.

2.2.1. Naïve Bayes

Naive Bayes classifier that is a statistical classification method based on Bayes theorem finds the class to which the samples belong, assuming that the attributes are independent of each other. To do so, it determines the conditional probability $P(A|B)$ of event A for given event B. Namely, the case $P(C_i|Y)$ for the class C_i that maximizes the probability is calculated as below [20]:

$$P(C_i|Y) = \frac{P(Y|C_i)P(C_i)}{P(Y)} \quad (1)$$

$P(C_i|Y)$ is the posterior probability of C_i given Y. $P(Y|C_i)$ is the conditional probability of Y given C_i . $P(C_i)$ is the prior probability of i_{th} C class. $P(Y)$ is the prior probability for Y [21].

2.2.2. Trees-J48

In decision tree methods, the training set is recursively divided into subsets from root to leaves considering certain criteria. The leaf level of the tree represents the class labels. The most important problem in decision trees is that determining the root node and the order of branching to the leaves. For this purpose, the entropy measurement shown in Eq.2 is frequently used. Accordingly, the division criterion from root node to leaves is determined by calculating the entropy-dependent information gain [22-24].

$$H(X) = - \sum_{i=1}^n (p_i) \log_2(p_i) \tag{2}$$

Here, X is an attribute, p_i is each element with i_{th} position of each X element. A small entropy value indicates that the uncertainty and indecision about the result is small. So, a class or attribute has a small entropy is selected for another step [25].

2.2.3. k-Nearest Neighbor (kNN)

The kNN classifier is an instance-based method. Accordingly, the distance (d) of the relevant sample to j_{th} sample in the training set is calculated to determine the class of i_{th} x sample in p-dimensional space. The class has the most samples, which has the smallest d value among the k samples, is determined as the target class. The Euclidean Distance method shown in Eq.3 is frequently used in distance measurement [26-27].

$$d(i, j) = \sqrt{|x_{i1} - x_{j1}|^2 + |x_{i2} - x_{j2}|^2 + \dots + |x_{ip} - x_{jp}|^2} \tag{3}$$

3. RESULTS

In the study, for the purpose of predicting the risk of early diabetes, the values recorded for 520 samples are examined in terms of 17 features that may be associated with the disease. In the dataset, positive and negative case of diabetes or symptoms are labeled as 'class1' and 'class2'.

Table 2. Evaluation of classification success of NB, J48, kNN and SMO algorithms and comparison of performance criteria of classifiers based on ensemble approaches.

Ens	Classifier	Accuracy (%)	Kappa	RMSE	AUC
None	NB	88	0.742	0.316	0.95
	J48	95	0.887	0.222	0.96
	kNN	98	0.951	0.149	0.98
	SMO	93	0.854	0.263	0.92
Adaboost	NB	88	0.745	0.296	0.96
	J48	98	0.963	0.129	0.99
	kNN	98	0.951	0.149	0.98
	SMO	93	0.849	0.229	0.98
Bagging	NB	87	0.738	0.316	0.95
	J48	97	0.927	0.171	0.99
	kNN	97	0.939	0.152	0.99
	SMO	93	0.841	0.244	0.96
RSS	NB	88	0.738	0.311	0.94
	J48	96	0.907	0.196	0.99
	kNN	98	0.959	0.158	0.99
	SMO	89	0.754	0.279	0.96

In classification step, NB, J48, kNN and SMO classifier performances are investigated using k (15) fold cross-validation method. In this context, accuracy rate, kappa coefficient, RMSE and AUC performance

measures are obtained. Then, the effect of ensemble algorithms (Ens), Adaboost, Bagging, RSS, to the success of classifier is evaluated separately using these performance parameters as shown in Table 2.

Here, accuracy represents the rate at which the class of each sample is correctly labeled and is calculated as in Equation 4.

$$Accuracy = \frac{tp+tn}{tp+tn+fp+fn} \quad (4)$$

In the equation, f_p , f_n , t_p , and t_n are the number of false positives, false negatives, true positives and true negatives, respectively.

When ensemble algorithms are not used, the best estimates of diabetes risk are obtained using kNN (97.69%). However, the accuracy rate for J48 increases significantly when classification performances are supported by ensemble algorithms. In particular, the J48 classification based on the Adaboost algorithm provides the maximum accuracy rate among all methods.

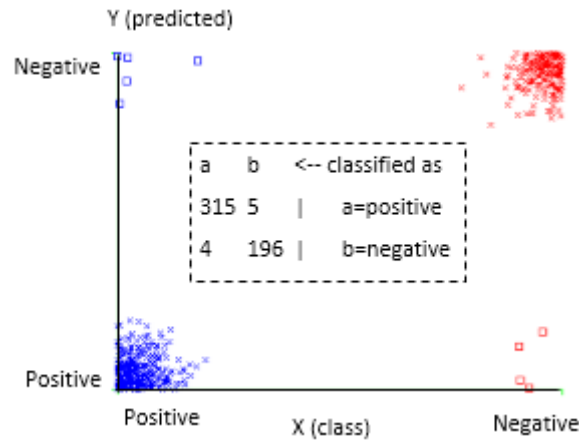


Figure 1. Confusion matrix and distribution of correctly and incorrectly classified samples explaining the classification accuracy of J48 algorithm based on Adaboost ensemble approach.

As shown in Figure 1, the classes of 315 positive and 196 negative samples are correctly labeled. On the other hand, only 5 positive and 4 negative samples are labeled in incorrect class. As a result, 98.26 % correct classification success is achieved.

Similarly, the highest value of the Kappa coefficient (κ) is also obtained by the J48 classifier based on the Adaboost approach. Kappa coefficient is mainly used to calculate the classification accuracy. To calculate κ value, two different probabilities, $Pr(a)$ and $Pr(e)$, are used as follows [29].

$$\kappa = \frac{Pr(a)+Pr(e)}{1-Pr(e)} \quad (5)$$

Here, $Pr(a)$ is the actual observed agreement, while $Pr(e)$ is the probability of this fit occurring by chance. "1" indicates a perfect fit, and "0" indicates a poor fit.

Third performance criteria RMSE is calculated using the square root of mean squares error (MSE). It measures the mean size of errors and deals with deviations from the true value. So, the lower of RMSE is the better prediction and "0" indicates a perfect fit [30]. As seen in the Table 2, all ensemble algorithms decrease the RMSE value of the J48 classifier and Adaboost has ensured that the best RMSE is obtained. Lastly, AUC criteria are examined for all classification algorithms in the table. AUC is the area of the two-dimensional measure under the ROC (Receiver Operating Characteristic) curve and its value ranges

are [0, 1]. Accordingly, if a model prediction is 100% wrong, AUC is "0"; a model predictions are 100% accurate, AUC is "1" [31-33].

More specifically, in ROC curve, the true positive rate (sensitivity is calculated by Eq. 6) is plotted as a function of the false positive rate (specificity is calculated by Eq. 7) for different cut-off points [34-36].

$$Sensitivity = \frac{tp}{tp+fn} \tag{6}$$

$$Specificity = \frac{tn}{tn+fp} \tag{7}$$

Thus, each point on the curve correspond to a sensitivity/specificity pair. If 100% sensitivity and specificity value is obtained, the ROC curve, which is very close to the upper left corner (the area under the curve is larger), shows a perfect separation without overlapping in the two distributions [37].

Accordingly, Figure 2 (a-b-c-d) shows the ROC curves for NB, J48, kNN and SMO classifiers, respectively. As can be seen from these figures, the most obvious distinction between the classes and the left-justified graph is provided in panel (c) by the kNN method. Then, the best success is achieved with J48 in (b), NB in (a), and SMO in (d), respectively.

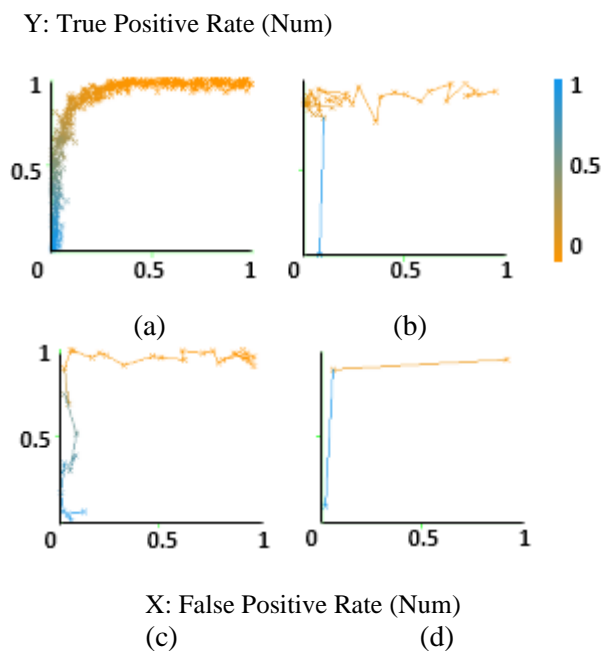


Figure 2. ROC curves include sensitivity/specificity pair representation which expresses the classification success of four different classification methods (a) NB, (b) J48, (c) kNN, (d) SMO.

In Figure 3, classifier performances based on Adaboost algorithm are evaluated. Here, the distinction between classes can be seen quite clearly in panel (b). In addition, the curve leans almost entirely to the left. In (c) and (d), the kNN and SMO methods have similar distribution and steepness. In (a), NB is the graph where the curve is furthest to the left side.

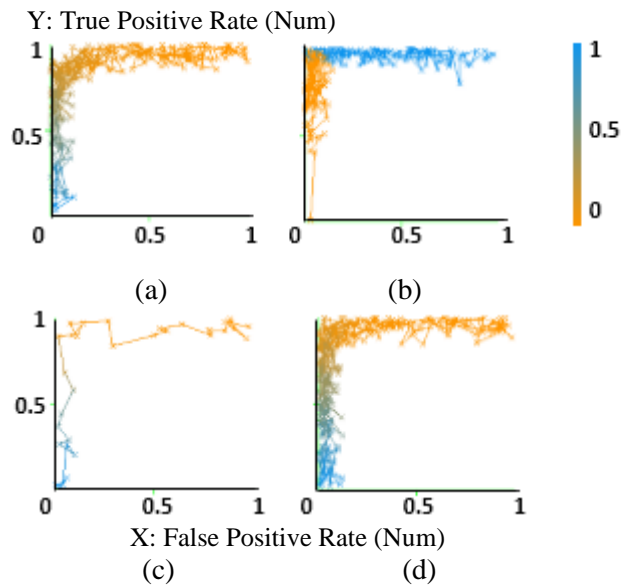


Figure 3. ROC curves of classifiers based on Adaboost ensemble algorithms (a) NB, (b) J48, (c) kNN, (d) SMO.

In Figure 4, the classifier performances based on the Bagging algorithm show that in panel (b) and (c), J48 and kNN classifier achieve the highest performance with left-justified ROC curves and a similar separation between classes. Then, SMO in (d) and NB in (a) with the worst performance are shown.

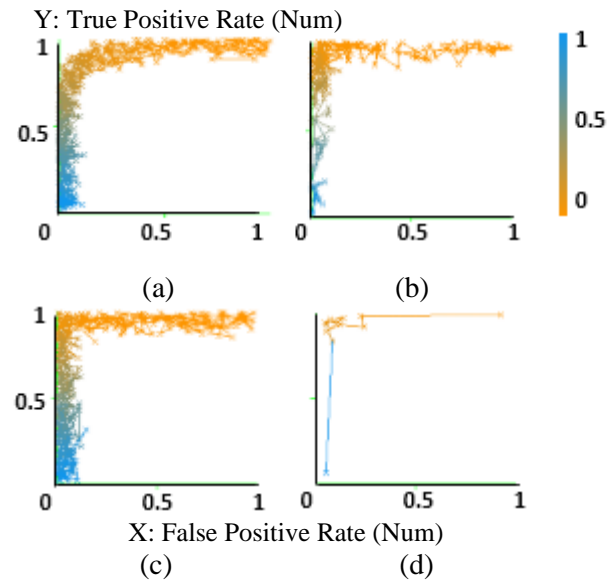


Figure 4. ROC curves of classifiers based on Bagging ensemble algorithms (a) NB, (b) J48, (c) kNN, (d) SMO.

The ROC curves obtained by the RSS algorithm in Figure 5 are quite like the Bagging algorithm, so the performance order is obtained as (b)=(c)>(d)>(a).

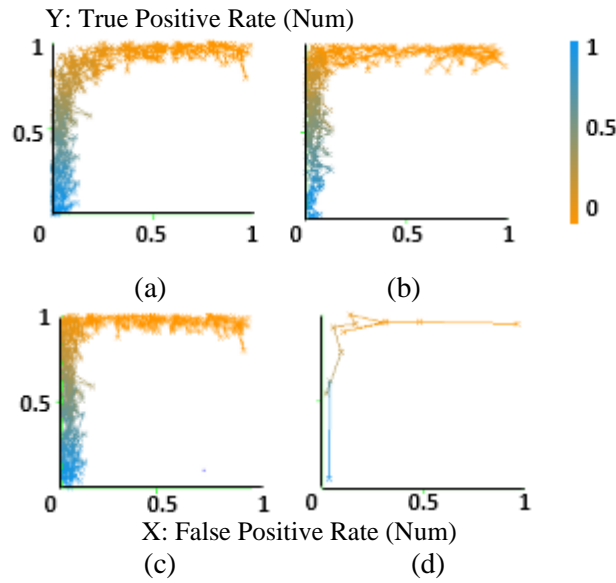


Figure 5. ROC curves of classifiers based on Bagging ensemble algorithms (a) NB, (b) J48, (c) kNN, (d) SMO.

As a result, both the AUC values obtained in Table 2 and the ROC curves shown in Figure 2-3-4-5 indicate that ensemble algorithms increase the classifier performance. In other words, as seen in the table, the performance of classifiers based on ensemble algorithms in general resulted in AUC values close to “1”. J48 classifier provides the maximum AUC value for all ensemble algorithms. On the other hand, ROC curves very close to the upper left corner are obtained with a perfectly discriminating distribution as seen in panels (b) of the four figures presented. In addition, it becomes very difficult to perform the machine learning task or gain insight into the data in the case of very large datasets. Because the complexity of the model and the time required to train the model also increase by the reason of increasing data size. Moreover, inaccurate, or less reliable results may be obtained. In this context, feature selection algorithms provide to obtain a better classification performance in a shorter time by removing some features that are unrelated or less important to the dependent variable from the data set.

Table 3. The significant rates of attributes which are obtained with the WSE algorithm.

	Attribute	Significant Rate (%)
1	Age (Age)	100
2	Gender (Male/Female)	100
3	Polyuria (Yes/No)	100
4	Polydipsia (Yes/No)	100
5	Sudden weight loss (Yes/No)	67
6	Weakness (Yes/No)	20
7	Polyphagia (Yes/No)	40
8	Genital thrush (Yes/No)	47
9	Visual blurring (Yes/No)	40
10	Itching (Yes/No)	53
11	Irritability (Yes/No)	47
12	Delayed healing (Yes/No)	100
13	Partial paresis (Yes/No)	13
14	Muscle stiffness (Yes/No)	40
15	Alopecia (Yes/No)	87
16	Obesity (Yes/No)	0

For instance, when "wrapper feature selection algorithm (Wrapper Subset Eval-WSE) following the greedy search approach based on bi-directional elimination (Stepwise Selection)" is used, it is

determined that "obesity" as an uncorrelated feature (0%) in the original data set consisting of 17 attributes belonging to each individual. In addition, "weakness" and "partial paresis" are less correlated features (20% and 13%) as seen in Table 3. When these features are removed from the dataset and the same algorithms are run again, the effect of WSE on the correct classification performance is clearly seen.

Table 4. The effect of WSE algorithm to classifiers 'performance criteria.

Ens	Classifier	Accuracy (%)	Kappa	RMSE	AUC
Adaboost	NB	89	0.775	0.288	0.96
	J48	99	0.967	0.120	1.00
	kNN	98	0.947	0.255	0.98
	SMO	92	0.834	0.228	0.98

As can be seen in Table 4, an overall increase in performance measures is observed for the NB, J48 and kNN classifiers. More specifically, the accuracy of J48 classifier increases to 99% by using Adaboost ensemble algorithm with 15-fold cross validation. In addition, improvement is observed in other performance criteria as well.

Table 5. The comparison of the studies' performance on Early-stage diabetes risk prediction dataset published by UCI.

Method	input number	Techniques	Accuracy
[11]	12	kNN	97.36%
[12]	16	RF+10-Fold Cross Validation+ Percentage Split Evaluation	99.00%
[38]	16	Adaboost and Bagging+NBTree	98.65%
[39]	16	Multi-Layer Perceptron+Improved Crow Search Algorithm	
		*one hidden layer	97.69%
		*two hidden layer	96.92%
proposed	13	WSE+Adaboost +J48	99.00%

In [11], 97.36% classification success is achieved by using the kNN classifier with 12 input features. To increase the success in [12], the RF classifier is supported by the Percentage Split Evaluation method and 99% accurate classification is provided with 16 inputs. In [38], 98.65% success is obtained by using 16 inputs with Adaboost, Bagging, NBTree algorithms. [39] uses Multi-Layer Perceptron and Improved Crow Search Algorithm. The method has 97.69% and 96.92% success for one and two hidden layers for 16 inputs. On the other hand, the proposed method, not only saves time and memory as it uses less input, but also achieves a very high success rate of 99%.

4. DISCUSSION

Diabetes Mellitus, which is at the forefront of the diseases of the age, is a type of disease that is very common all over the world. Moreover, long-term high blood sugar due to diabetes can cause permanent damage to the whole body, especially the cardiovascular system, kidneys, or eyes. For this reason, early diagnosis of the disease and initiation of the treatment process are also vital for the prevention of other diseases. In this paper, it is aimed that a prediction system is modeled for detection of early-stage diabetes. To do so, firstly, the performances of NB, J48, kNN, SMO classifiers are compared for four

performance criteria which are Accuracy, Kappa, RMSE, AUC. 98% accuracy rate is achieved with the kNN algorithm. Then, classifier performances are examined separately based on Adaboost, Bagging and RSS ensemble approximations. The results show that the highest classification success of 98% is obtained when the J48 classifier is used together with the Adaboost algorithm. The other performance criteria Kappa, RMSE and AUC values are 0.963, 0.129 and 0.99, respectively. Finally, the WSE feature extraction algorithm is applied to the data set and the irrelevant or least relevant "obesity" (0%), "weakness" (20%) and "partial paresis" (13%) attributes are removed from the diabetes dataset. Thus, the classification success of the J48 algorithm based on the Adaboost ensemble approach increases to 99% when 13 inputs are used. In addition, Kappa, RMSE and AUC values are 0.967, 0.120 and 1.00, respectively.

Thus, it has been shown that the Adaboost ensemble algorithm can contribute to obtaining effective results in the training of different artificial intelligence models to be defined in diabetes risk prediction in the future.

CONFLICT OF INTEREST

The author(s) stated that there are no conflicts of interest regarding the publication of this article.

CRedit AUTHOR STATEMENT

Tuğba Palabaş: Investigation, Formal and computational analysis, Writing - original draft, Visualization, Conceptualization, Supervision.

REFERENCES

- [1] Alberts B, Johnson A, Lewis J, Raff M, Roberts K, Walter P. How cells obtain energy from food. In *Molecular Biology of the Cell*. 4th edition. Garland Science, 2002.
- [2] Mergenthaler P, Lindauer U, Dienel GA, Meisel A. Sugar for the brain: the role of glucose in physiological and pathological brain function. *Trends in neurosciences*, 36(10), 587-597, 2013.
- [3] Brutsaert EF. *Diabetes mellitus (DM)*. Merck Manual, 2020.
- [4] International Diabet Federation, "IDF Diabetes Atlas". <https://diabetesatlas.org/>(16.05.2023).
- [5] Sağlık Bakanlığı, "Kronik Hastalıklar". <https://www.saglik.gov.tr/yazdir?2DE933CD45A7AD200096270A9E25E935> (16.05.2023).
- [6] Marshall SM, Flyvbjerg A. Prevention and early detection of vascular complications of diabetes. *Bmj*, 333(7566), 475-480, 2006.
- [7] Sümbül H, Yüzer AH. Development of diagnostic device for COPD: a MEMS based approach. *Int J Comput Sci Network Secur*. 2017;17 (7):196–203.
- [8] Sümbül H, Yüzer AH. Estimating the value of the volume from acceleration on the diaphragm movements during breathing. *J Eng Sci Technol*. 2018;13(5):1205–1221.

- [9] Sümbül H, Yüzer AH. Measuring of diaphragm movements by using iMEMS acceleration sensor. In 2015 9th International Conference on Electrical and Electronics Engineering (ELECO) EEE; 2015: 166–170.
- [10] Laila UE, Mahboob K, Khan AW, Khan F, Taekeun W. An ensemble approach to predict early-stage diabetes risk using machine learning: An empirical study. *Sensors* 2022; 22(14), p 5247.
- [11] Khafaga DS, Alharbi AH, Mohamed I, Hosny KM. An Integrated Classification and Association Rule Technique for Early-Stage Diabetes Risk Prediction. In *Healthcare* 2022; 10(10), p 2070.
- [12] Islam MM, Ferdousi R, Rahman S, Bushra HY. Likelihood prediction of diabetes at early stage using data mining techniques. In *Computer vision and machine intelligence in medical image analysis* (pp. 113-125). Springer, Singapore, 2020.
- [13] Sisodia D, Sisodia DS. Prediction of diabetes using classification algorithms. *Procedia computer science* 2018; 132, p 1578-1585.
- [14] Naz H, Ahuja S. Deep learning approach for diabetes prediction using PIMA Indian dataset. *Journal of Diabetes & Metabolic Disorders* 2020; 19, p 391-403.
- [15] Peker M, Özkaraca O, Şaşar A. Use of orange data mining toolbox for data analysis in clinical decision making: The diagnosis of diabetes disease. In *Expert System Techniques in Biomedical Science Practice* 2018; p 143-167.
- [16] Kalaycı TE. Comparison of machine learning techniques for classification of phishing web sites. *Pamukkale Üniversitesi Mühendislik Bilimleri Dergisi* 2018; 24(5), p 870-878.
- [17] Aytuğ O, Korukoğlu S. A review of literature on the use of machine learning. *Pamukkale Üniversitesi Mühendislik Bilimleri Dergisi* 2016; 22(2), p 111-122.
- [18] Özdemir A, Aytuğ O, Ergene VÇ. Machine learning and ensemble learning based method using online employee assessments to identify and analyze job satisfaction factors. *Avrupa Bilim ve Teknoloji Dergisi* 2022; 40, p 19-28.
- [19] UCI Machine Learning Repository, “Early-stage diabetes risk prediction dataset”. <https://archive.ics.uci.edu/ml/datasets/Early+stage+diabetes+risk+prediction+dataset> (16.05.2023).
- [20] Tsymbal A, Puuronen S, Patterson DW. Ensemble feature selection with the simple Bayesian classification. *Information fusion* 2003; 4(2), p 87-100.
- [21] Banchhor C, Srinivasu N. Integrating Cuckoo search-Grey wolf optimization and Correlative Naive Bayes classifier with Map Reduce model for big data classification. *Data & Knowledge Engineering* 2020; 127, p 101788.
- [22] Altaş D, Gülpınar V. A Comparison of Classification Performances Of The Decision Trees and The Artificial Neural Networks: European Union, *Trakya Üniversitesi Sosyal Bilimler Dergisi* 2012; 14(1) p 1-22.
- [23] Kavzoğlu T, Çölkesen İ. Classification of Satellite Images Using Decision Trees: Kocaeli Case. *Harita Teknolojileri Elektronik Dergisi* 2010; 2(1), p 36-45.

- [24] Sangeorzan L. Effectiveness analysis of ZeroR and J48 classifiers using WEKA toolkit. *Bulletin of the Transilvania University of Brasov. Series III: Mathematics and Computer Science* 2019; p 481-486.
- [25] Chen CH. A novel multi-criteria decision-making model for building material supplier selection based on entropy-AHP weighted TOPSIS. *Entropy* 2020; 22(2), p 259.
- [26] Hemmatian F, Sohrabi MK. A survey on classification techniques for opinion mining and sentiment analysis. *Artificial intelligence review* 2019; 52(3), p 1495-1545.
- [27] Alharbi Y, Alferaidi A, Yadav K, Dhiman G, Kautish S. Denial-of-service attack detection over IPv6 network based on KNN algorithm. *Wireless Communications and Mobile Computing* 2021; p 1-6.
- [28] Platt JC. Fast training of support vector machines using sequential minimal optimization, advances in kernel methods. *Support vector learning* 1999; p 185-208.
- [29] McHugh ML. Interrater reliability: the kappa statistic. *Biochemia medica* 2012; 22(3), p 276-282.
- [30] Alghamdi A S, Polat K, Alghoson A, Alshdadi AA, Abd El-Latif AA. A novel blood pressure estimation method based on the classification of oscillometric waveforms using machine-learning methods. *Applied Acoustics* 2020; 164, p 107279.
- [31] Pepe MS, Cai T, Longton G. Combining predictors for classification using the area under the receiver operating characteristic curve. *Biometrics* 2006; 62(1), p 221-229.
- [32] Hajian-Tilaki K. Receiver operating characteristic (ROC) curve analysis for medical diagnostic test evaluation. *Caspian journal of internal medicine* 2013; 4(2), p 627.
- [33] Kemalbay G, Alkış BN. Prediction of stock index movement direction with multiple logistic regression and k-nearest neighbors algorithm. *Pamukkale Üniversitesi Mühendislik Bilimleri Dergisi* 2020; 27(4), p 556-569.
- [34] Janssens ACJ, Martens FK. Reflection on modern methods: Revisiting the area under the ROC Curve. *International journal of epidemiology* 2020; 49(4), p 1397-1403.
- [35] Ruisánchez I, Jiménez-Carvelo AM, Callao MP. ROC curves for the optimization of one-class model parameters. A case study: Authenticating extra virgin olive oil from a Catalan protected designation of origin. *Talanta* 2021; 222, p 121564.
- [36] Cihan P, Kalipsiz O, Gökçe E. Computer-aided diagnosis in neonatal lambs. *Pamukkale Üniversitesi Mühendislik Bilimleri Dergisi* 2020; 26(2), p 385-391.
- [37] Zweig MH, Campbell G. Receiver-operating characteristic (ROC) plots: a fundamental evaluation tool in clinical medicine. *Clinical chemistry* 1993; 39(4), p 561-577.
- [38] Taser PY. Application of bagging and boosting approaches using decision tree-based algorithms in diabetes risk prediction. *Proceedings* 2021; 74(1), p 6.
- [39] Wijayaningrum VN, Saragih TH, Putriwijaya NN. Optimal multi-layer perceptron parameters for early stage diabetes risk prediction. In *IOP Conference Series: Materials Science and Engineering* 2021; 1073(1), p 012070.



RESEARCH ARTICLE

THE PHARMACEUTICAL BOTANICAL STUDIES ON THE ENDEMIC *Asperula pestalozzae*
Boiss. (RUBIACEAE)

Kader KAYIŞ^{1,*}, Ayla KAYA²

¹ Department of Pharmaceutical Botany, Faculty of Pharmacy, Anadolu University, Eskişehir, Turkey
kaderkavis@anadolu.edu.tr - [0000-0002-6060-5613](https://orcid.org/0000-0002-6060-5613)

² Department of Pharmaceutical Botany, Faculty of Pharmacy, Anadolu University, Eskişehir, Turkey
avkaya@anadolu.edu.tr - [0000-0002-7598-7132](https://orcid.org/0000-0002-7598-7132)

Abstract

In this study, endemic *Asperula pestalozzae* Boiss. (Rubiaceae) was investigated in aspects of pharmaceutical botany. The morphological, anatomical, micromorphological, palynological, and chemical (antioxidant activity and total amount of phenolic substance) characteristics were reported in detail for the first time. Expanded descriptions and images of *A. pestalozzae* were given. The anatomical description was presented in detail and supported by photographs. The stem is usually angular or orbicular shaped and the leaf is monofacial. Its trichome and pollen micromorphology were examined with a scanning electron microscope (SEM). The pollen grains of *A. pestalozzae* are monad, radial symmetry, isopolar, and hexacolpate (sometimes heptacolpate). DPPH and ABTS radicals were used to determine antioxidant activity. The DPPH 50% inhibition concentration (IC₅₀) value was found to be 0.0011±0.0002 mg/mL for standard gallic acid and 0.134±0.017 mg/mL for *A. pestalozzae* extract. 0.1 mg/mL extract calculated 0.022±0.36 mM TEAC activity; 1.437±0.51 mM TEAC activity was determined in 10 mg/mL extract. The total amount of phenolic substances was calculated as 53 mg gallic acid equivalent (GAE).

Keywords

Anatomy,
Antioxidant activity,
Asperula,
Morphology,
Palynology

Time Scale of Article

Received : 28 October 2023
Accepted : 19 February 2024
Online date : 30 July 2024

1. INTRODUCTION

The Rubiaceae family includes approximately 620 genera and 13,000 species in the world [1]. It is a cosmopolitan family and fourth family in terms of the number of species [2, 3]. There are 13 genera and 234 taxa in Türkiye [4]. The species of this family have been used in dyeing since ancient times; for example, *Rubia tinctorum* L. [5]. Some species, such as coffee, have economic value. Pharmaceutical raw materials are obtained from some genera, such as *Uncaria* Schreber, *Cinchona* L., and *Coffea* L., and are used for treatment purposes. [6].

Asperula, one of the important genera in this family, has many therapeutic properties. In Turkish folk medicine, some *Asperula* species have been used as tonic, antidiarrheal and diuretic [7]. The species representing the genus *Asperula* is *Asperula arvensis*. Thanks to polyphenol acids, iridoids, tannins, and flavones, it is used as a blood and lymph system cleaner and for skin diseases and cancer treatments [8]. The main ingredients in the dry extract of *A. odorata* L. utilized in Ukrainian traditional medicine are chlorogenic acid and cynaroside. The plant's dry extract has twice the antihypoxic impact of the medication that was used as a reference. This plant also has a sedative effect [9].

The genus *Asperula* represents 183 species and 230 taxa in the world [8]. In Türkiye, there are 58 taxa belonging to the genus, and almost half of them are endemic [10]. *Asperula* is an annual or perennial

*Corresponding Author: kaderkavis@anadolu.edu.tr

herb, a low shrub, with 4-6 or multiple circumscribed leaves. Stipules are rarely reduced, and flowers are in loose panicles or spikes. The calyx is missing. The corolla is composed of (3-)4-5 parts. The corolla lobes are shorter than the tube [11]. The inflorescence is mostly used to define this genus. *Asperula cynanchica* L. has an enzyme on the tips of flowering branches that are used to ferment milk, and this enzyme is used in yogurt production. Thus, its traditional name is “yoğurt otu” in Türkiye [8]. However, one of the common names is “yapışkan otu”. In current sources, it is referred to as “belumotu” [10]. *Asperula pestalozzae* Boiss. is an endemic species that is in the *Cynanchicae* section of the genus *Asperula*. It grows on rocky slopes, steppes, limestone, sandstone, calcareous soil, and clayey areas at altitudes of 300 to 2300 m, an euxine element, and it spreads in areas around the Black Sea and Central Anatolia. The Turkish name of the plant is “has belumotu” [10, 11].

There are some floristic [12, 13], anatomical [5, 14], karyological [14, 15], chemical [16- 21], and biological activity studies [7, 21- 23] on *Asperula* species in the literature. Morphological, anatomical, and pollen structures, as well as the antioxidant activity of *A. pestalozzae* have not previously been studied. Therefore, the present study aims to give a detailed account of the internal and external morphological properties and pollen characteristics of *A. pestalozzae*, which is endemic to Türkiye. It also determined whether it had antioxidant effects in terms of chemicals.

2. MATERIALS AND METHODS

2.1. Plant Material

During the flowering and fruiting period (May–July, 2020), *Asperula pestalozzae* was collected from the Bozüyük district of Bilecik province (30°0'49.485" E-39°54' 48.482"N). For plant identification, P.H. Davis's [11] "Flora of Turkey and the Aegean Islands" was used. Some of the dried plants in the press were numbered and turned into herbarium samples. They were placed in the Anadolu University Faculty of Pharmacy Herbarium (ESSE No. 15610).

2.2. Morphological, Anatomical Studies

Herbarium specimens and fresh specimens were used for defining morphological findings. Morphological features were described in detail. General appearance, stem structure and hairs, leaf structure and hairs, flower state, corolla structure, longitudinally opened corolla, anther, ovary, fruit, bract, and bracteole shapes were drawn in detail. A WILD TYP 181300 stereo microscope and drawing tube were used for the drawings in Figure 1. In morphological terminology, Baytop (1998)'s English-Turkish Botanical Manual [24] was used.

The micromorphology of the stem, leaf, corolla, and ovary surfaces was viewed with a scanning electron microscope in the Anadolu University Plant, Medicine, and Scientific Research Center (BIBAM). Stems and leaves were preserved in 70% alcohol, and they were used for anatomical studies. Transverse sections were taken from the stem, and superficial sections were taken from both the transverse and lower upper parts of the leaves. All cells in preparations were exposed to chloralhydrate to render them transparent. Then they were stained with Sartur reagent. The preparations were photographed with an Olympus BX51T brand trinocular microscope and described. For anatomical descriptions, the terminology proposed by Metcalfe & Chalk (1950) [25] was followed.

2.3. Palynological Study

For palynological findings, pollen from dry corolla samples was placed on double-sided tape. The samples were coated with gold (SBC-900 Single Target Plasma (Gold) Sputtering Thin Film Coating) and examined with a table-top scanning electron microscope (TM3030 Plus Tabletop Microscope, HITACHI). The polar axis and equatorial axis lengths of the pollen were measured, and the shape of the

pollen was determined by dividing the polar axis value (P) by the equatorial axis value (E). The terminology for data proposed by Walker and Doyle (1975) [26] was followed.

2.4. Extraction

The aerial parts of the plants that dried at room temperature were turned into coarse powder. Then 100 mL of 70% ethanol was added to 20 g of powdered plant. It was shaken for 24 hours (ORBITAL, shaker) At the end of the period, the mixture was filtered, and 100 mL of ethanol was added to the filtrate. The process was repeated three times and terminated [18, 27]. The filtrates were collected in an Erlenmeyer flask, and the ethanol in their contents evaporated for 30 minutes at 41 °C under pressure. The water in the structure of the samples was crystallized in a deep freeze. A lyophilizer was used to remove the ice water.

2.5. Total Content of Phenolic Substances and Antioxidant Activity Tests

The total amount of phenolic substances was determined with the Folin-Ciocalteu method. This test is based on the color reaction, and a blue-colored complex formation is observed in the reaction [28]. A solution with a concentration of 10 mg/mL was prepared by dissolving 20 mg of plant extract in 2 mL of methanol. Solutions at different concentrations (0.1 mg/mL, 0.35 mg/mL, 0.5 mg/mL, 0.7 mg/mL, and 1 mg/mL) were prepared from the standard gallic acid. 20 µL of the solutions were placed in the microplate wells, and 1560 µL of distilled water and 100 µL of Folin-Ciocalteu reagent were added. After waiting for a while, the reaction was started by adding 300 µL of 20% sodium carbonate (Na₂CO₃). After 2 hours in the dark at room temperature, the absorbance values were measured at 760 nm [29, 30] (ELISA Microplate Reader, Biotek Synergy HTX).

The extract's antioxidant activity was assessed by the DPPH• scavenging effect and ABTS• scavenging effect assays. A serial dilution was made from the plant sample dissolved in MeOH (methanol) for the determination of the DPPH scavenging effect. Radical scavenging activity was calculated using the 50% inhibition concentration equation [28]. A plant sample (10 mg/mL concentration) dissolved in 200 µL MeOH was transferred to the well of a 96-well microtitration plate. 100 µL of MeOH was added to the other wells. 100 µL of the sample was taken from the first well, and 10 serial dilutions were made, respectively. 100 µL of DPPH• solution was added, and the mixture was left in the dark for 30 minutes. It was measured at 517 nm with a spectrophotometer [31].

In the ABTS scavenging effect test, it was mixed with 7 milliMolar ABTS•⁺ and 2.5 mM sodium persulfate (Na₂S₂O₈). The mixture was kept in the dark for 12-16 hours, and blue-green radical formation was achieved. Solutions at concentrations of 0.1 mg/mL and 10 mg/mL were obtained from the plant extract. Then, different concentrations (2.5 mM, 2 mM, 1.5 mM, 1 mM, 0.5 mM, and 0.1 mM) were prepared from 3 mM Trolox to be used as a standard. Gallic acid with concentrations of 0.1 mg/mL and 1 mg/mL was used as the positive control. 10 µL of the prepared samples were placed in the microplate wells, respectively, and 990 µL of ABTS•⁺ was added. After 30 minutes, its absorbance was measured at 734 nm [32].

3. RESULTS

3.1. Morphological Features

A. pestalozzae is perennial, semi-shrub (Figure 1 I-a), stems ascending to erect, basally densely leafy (Figure 1 II-a), flowering and vegetative branches. Flowering stems are 18-63 cm, quadrangular or slightly rounded on the undersides, puberulent-hispid haired on the underside (Figure 1 II-b), and glabrous on the top.

Leaves are 4, verticillasters (Figure 1 III-a), linear or filiform (Figure 1 III-b), strongly revolute (Figure 1 III-c), base leaves are 5-20 x 0.2-1 mm, upper leaf is 5.8-16 x 0.3-0.8 mm, apex aristate, arista 0.2-0.7

mm and hyaline, straight-sided, base truncate; generally dense hispid hairy, erect or slightly tilted back, glabrous or few hairy (Figure 1 III-d).

The inflorescence is cymose at the tip of the branch consisting of paniculate (Figure 1 II-c), simple or branched, clusters 3–15; inflorescence stalk 5–35 mm.

Bract is lanceolate-ovate, 2-4.3 x 0.5-1.3 mm, bottom with flaps, margin straight, glabrous, aristate, arista 0.2-0.7 mm, hyaline, straight or slightly curved (Figure 1 IV-d,e,f).

Bracteole is oblong-lanceolate, 1.5-3.3 x 0.4-1 mm, margin straight, aristate, hyaline and 0.2-0.5 mm (Figure 1 IV-g,h).

Calyx none.

Corolla is gamopetalous, funnel (Figure 1 III-e,f), 2.2-3.3 mm; tube 1-2.2 mm, equal to or 2 times longer than lobes, lobes 1-1.2 x 2-3 mm, ovate-oblong, apex acute, lobes pinkish-white tube pink (Figure 1 I-b), dense hispid-tooth hairy, few or glabrous on lobes.

Stamen is 4, epipetalous, alternate with lobes (Figure 1 III-g), anther is dorsifixed, linear, 1-1.2 mm (Figure 1 IV-a) brown, filament adhered to the corolla.

The ovary is 1 x 0.5 mm, dark brown, densely papillate (Figure 1 IV-b); style 0.5-1.6 mm, bipartite equally branched, pinkish-purplish, stigma 2 and round.

Mericaip is ovate-oblong, 1.2-2 x 1 mm, green at first, dark brown in maturity (Figure 1 I-c), and densely warty (Figure 1 IV-c).

Flowering Time: July- August

Habitat: Rocky slopes and steppes, limestone, sandstone, marl, and clay areas

Altitude: 300-2300 m

Endemic

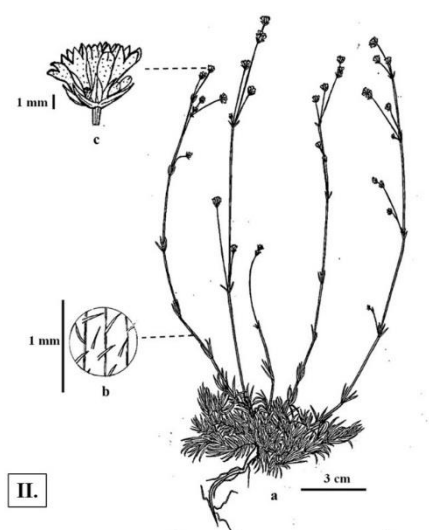


Figure 1 continues..

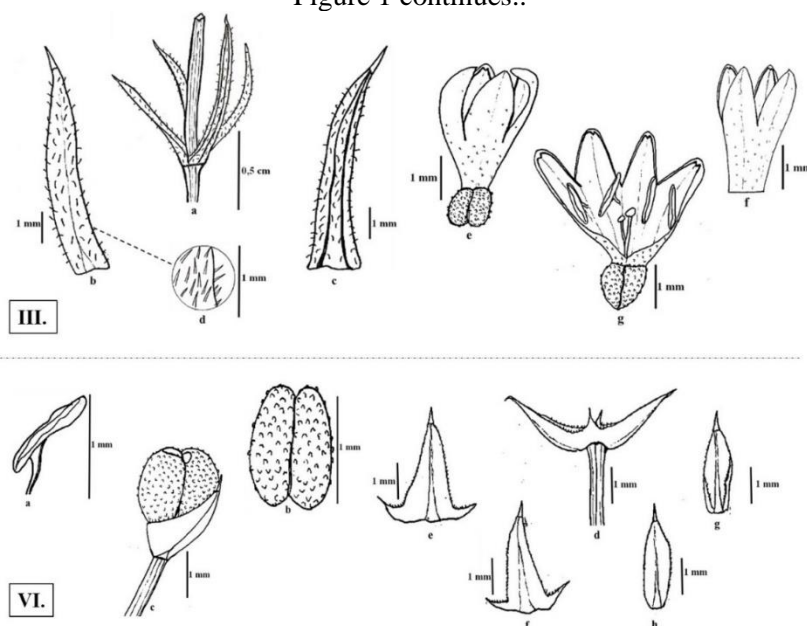


Figure 1. Morphological photographs and drawings **I-a)** General view of the plant **b)** flowers –**c)** fruits **II-a)** plant general drawing **-b)** stem hairs **-c)** flower status **III-a)** the arrangement of the leaves **-b)** the upper surface of the leaf **-c)** the lower surface of the leaf **-d)** hairs **-e)** corolla with ovaries **-f)** corolla without ovaries **-g)** inner surface of corolla **IV-a)** anther **-b)** ovary **-c)** mericarps (fruit) **-d)** bracts surrounding the flower **-e)** inner surface of the bract **-f)** outer surface of the bract **-g)** inner surface of the bracteole **-h)** outer surface of the bracteole

3.2. Trichome Morphology

The hairs on the organs of the plant and their characteristics are summarized in Table 1. The hairs are denser on the lower part of the stem.

Table 1. Hair characteristics and density in vegetative and generative organs

The Organs	Characteristics	Density	
Stem	88.3 µm-196 µm Hispid, Unicellular	Upper	±
		Lower	++
Leaf	55.2- 298 µm Hispid, Unicellular	Upper Surface	+
		Lower Surface	+
Corolla	32.9 µm-91.3 µm Dense hispid-Tooth hairy	Tube	++
		Lob	± or -
Ovary surface	Round and convex papillary	All surface	++

(-) none, (±) rare, (+) intense, (++) instenser

Trichomes are simple, unicellular, usually short-conical, erect or oblique, hispid, 88.3 µm- 196 µm, and with dense cuticle blisters (Figure 2a). Trichomes are dense on both surfaces of the leaf. They are unicellular, long, with dense cuticle ridges, oblique or slightly tilted back, hispid, 55.2- 298 µm (Figure 2b).

The outer surface of the corolla appears as wavy lines formed by epidermal folds. The part from the bottom of the corolla lobes to the ovary is covered with dense hispid and tooth hairs (Figure 2c). Trichomes are 32.9 µm- 91.3 µm long and above with cuticle blisters. The ovary is 1 x 0.5 mm in size and contains dense papillae, the surface of which is generally rounded. Large and small convex papillae have straight, or curved lines formed by epidermal folds (Figure 2d).

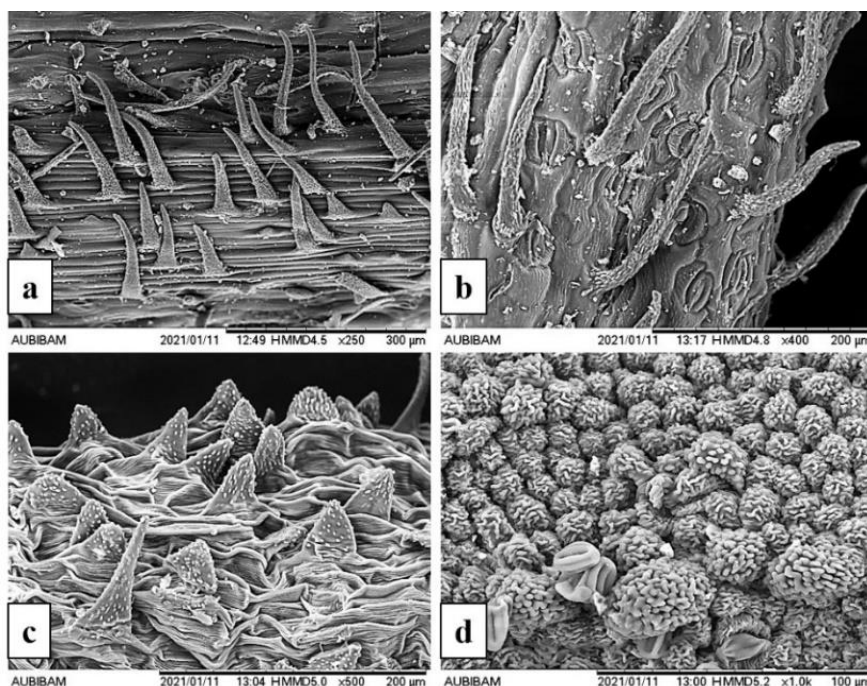


Figure 2. SEM images of hairs **a)**hispid hairs on stem **b)**hispid hairs on leaf **c)** tooth hairs on corolla **d)** papillae on ovary

3.3. Anatomical Features

3.3.1. Stem anatomy

The stem is usually angular or orbicular in transverse sections from the middle part of the stem (Figure 3a). The epidermis is composed of a single layer of almost square, compactly arranged cells. The upper surface is covered with a relatively thick cuticle and is covered with trichomes. Trichomes are simple, one-celled, short, or long (Figure 3b). Collenchyma tissue is located under the epidermis at the corners and is 5-10 layered (Figure 3c). The parenchymatic tissue is 3-5 layers and ring-shaped. It contains intense ergastic substances. The endoderma is single-layered and prominent. These cells are large transverse, and rectangular shaped. Vascular bundles surround the stem. Phloem is 3–5 layered and consists of irregular cells. Cambium is 1-2 layered or inconspicuous. Xylem comprises the regular trachea and tracheid cells. Rays are 1-2 layered. Those cells underlying the xylem are narrower. Pith is composed of large, orbicular, or polygonal parenchymatic cells, often with abundant intercellular spaces or cavities formed by the rupture of cell walls (Figure 3d).



Figure 3. Anatomical structures of stem cross-sections **a)** cross-section general view of the body(100µm) **b)** hairs (cross-section) (50µm) **c)** stem corner detail(25µm) **d)** tracheal elements and center(25µm) (cu: cuticle, co: collenchyma, cp: cortex parenchyma, e: epidermis, en: endodermis, h: hair, p: pith, pa: pith arm, ph: phloem, xy: xylem)

3.3.2. Leaf anatomy

The general view in the cross-section is transverse oval-rectangular (Figure 4a). The backward-curved leaves are slightly indented on the lower surface. The upper and lower epidermis consist of uniseriate oval and rectangular cells in transverse sections. The upper walls of the epidermis are thicker than the lower and lateral walls. Both epidermis surfaces are covered with an almost thick cuticle. The cells of the upper epidermis are larger than those of the lower. In superficial sections, the upper and lower epidermis cells are long and rectangular in shape and with many simple passages; the lower epidermis is longer and more wavy-walled than the upper epidermis. Trichomes are simple, unicellular, and conical-long (Figure 4b). The stoma (amphistomatic) located on both sides of the epidermis is of the parasitic type (Figure 4 c, d). The stomata are more common on the upper surface of the leaf than on the lower face. The leaf is monofacial. Under the upper epidermis in the mesophyll layer, there are 2 seriate of long, cylindrical, palisade parenchyma, and it continues up to the lower epidermis as uniseriate on the sides. In the lower epidermis, 3-4 seriates of longitudinally cylindrical or oval, loosely arranged sponge parenchyma are located above the palisade parenchyma. Under the midrib, a large layer of collenchyma is distinguished. The vascular bundles are of the collateral type and occur in a narrow area, surrounded by a bundle sheath and 3-5 small vascular bundles to the left and right of the central bundle.

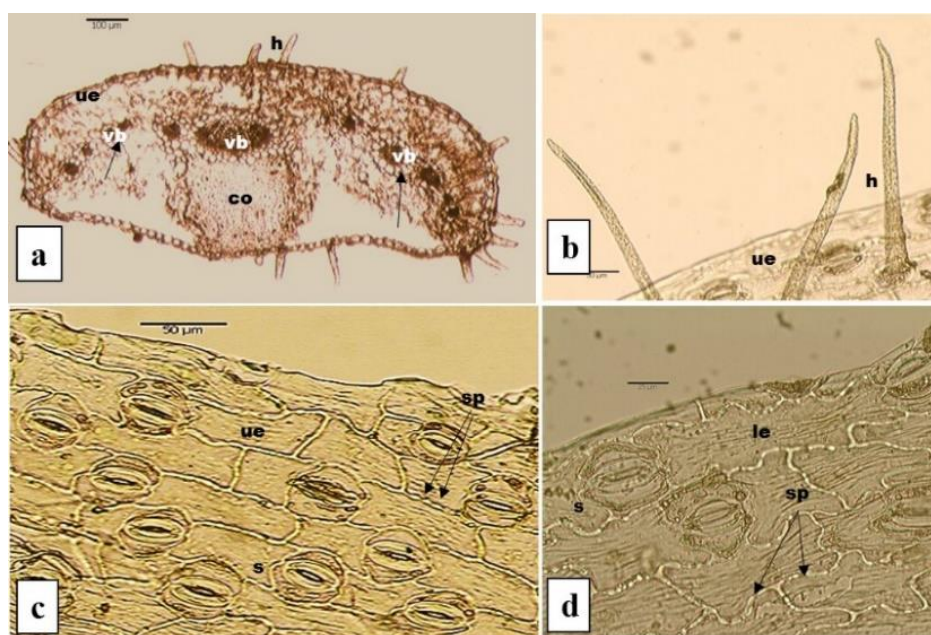


Figure 4. Leaf anatomical images **a)** leaf cross-section overview (100µm) **b)** hairs in leaf upper superficial section (50µm) **c)** upper superficial section(50µm) **d)** underside superficial section (25µm) (co: collenchyma, h: hair, s: stoma, sp: simple pass, le: lower epidermis, ue: upper epidermis, vb: vascular bundle)

3.4. Pollen Characteristics

The pollen grains of *A. pestalozzae* are monad, radial symmetry, isopolar, and hexacolpate (sometimes heptacolpate). The polar axis (P) is 16.9-20.6 µm, and the equatorial axis (E) is 10.9-14.3 µm. The P/E ratio is 1.44-1.55 µm. The shape of the pollen grains is euprolate. Equatorial images of pollen grains are elliptical (Figure 5a), whereas polar images are almost circular (Figure 5b). Colpus length is 12.5 µm-15.8 µm, and colpus width is less than 1µm. Skulptur (ornamentation) is scabrate-perforate (Figure 5c).

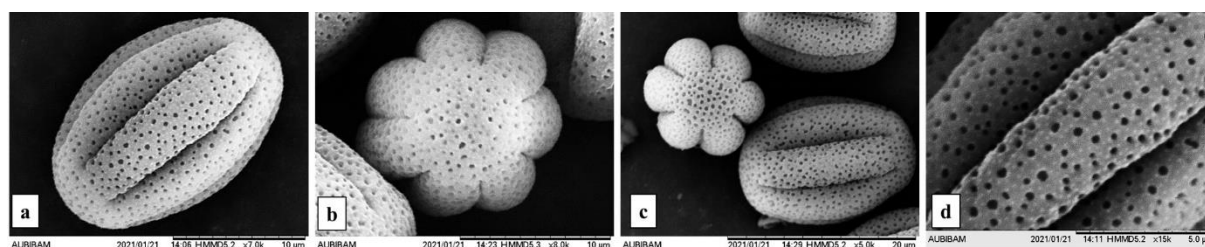


Figure 5. SEM microphotographs **a)** equatorial view **b)** polar view **c)** hexacolpate pollen **d)** close view of pollen surface

3.5. Total Content of Phenolic Substances and Antioxidant Activity Tests

The total amount of phenolic substances was found to be equivalent to 53 mg of gallic acid (GAE) in 1 g of *A. pestalozzae* extract. It was observed that the color complex of the extract was darker. The antioxidant properties of the methanol extract tested with the scavenging effect of the 1,1-diphenyl-2-picrylhydrazil radical (DPPH^{•+}) and the scavenging effect of the 2,2'-azino-bis-3-ethylbenzothiazoline-6-sulfonic acid radical cation (ABTS^{•+}). The results of antioxidant tests are shown in Table 2 and Table 3.

Table 2. Results of DPPH antioxidant test

Antioxidant Capacity Test	Extract	IC ₅₀ value (mg/mL)
DPPH test	<i>A. pestalozzae</i> (10 mg/mL)	0,134±0.017
	Gallic acid (1 mg/mL)	0,0011±0.0002

Table 3. Results of ABTS antioxidant test

Antioxidant Capacity Test	Extract	mM TEAC (mg/mL)
ABTS test	<i>A. pestalozzae</i> (0,1 mg/mL)	0,022±0.36
	<i>A. pestalozzae</i> (10 mg/mL)	1,437±0.51
	Gallic acid (0,1 mg/mL)	1,436±0.45
	Gallic acid (1 mg/mL)	2,630±0.07

4. DISCUSSION

In this study, the morphology, anatomy, palynology and antioxidant activity of the endemic *A. pestalozzae* in Türkiye was investigated for the first time and the results are discussed below.

Morphological results have been compared to the Flora of Turkey in Table 4, and some differences were observed. While the plant height was 13-60 cm in the Flora of Turkey, it was 18-63 cm in our study. While the four-cornered stem is compatible with our results, a slightly rounded shape was observed in the lower parts. The leaf width was found to be larger (0.2-1 mm) than the flora (0.3-0.75 mm), and the hyaline tip was found to be smaller. In the flora, the bract was 2-4 mm; in our results, it was 2-4.3 x 0.5-1.3 mm. The corolla size (2.2-3.3 mm) was almost the same as the flora. The color of the corolla was pinkish-white in the lobes and pink in the tube. In our study, the mericarps were smaller, and they were dense with warts. These differences are thought to be caused by geographical and climatic-edaphic factors. Also, leaf number, leaf margin and base, flower number, inflorescence stem, bract tip, bracteole, corolla lobe length, stamen, anther, filament, ovary length and color, stylus, stigma, and fruit shape characters were determined for the first time by our study. All morphological images were drawn, and the deficiencies were resolved in the flora.

Table 4. Comparison of our morphological findings with the Flora of Turkey

Characters		Our Results	Flora of Turkey
Plant Height		18-63 cm	(13-)20-60 cm
Stem	Shape	Ascending to erect, angular or slightly rounded on the undersides	Ascending to erect, quadrangular
	Hairs	Puberulent-hispid on the underside; glabrous on the top	Puberulent or scabrid-hispid in lower parts; glabrous or few hairy
Leaf	Size	Base leaf 5-20 x 0.2-1 mm, upper leaf 5.8-16 x 0.3-0.8 mm	4-15(-25) x 0.3-0.75 mm
	Number	4 and verticillastrum	-
	Arista	0.2-0.7 mm	0.7 mm
	Margin	Straight	-
	Base	Truncate	-
	Hairs	Dense hispid, erect or slightly tilted back, glabrous or few hairy	Scabrid to hispid or glabrous; slightly tilted
Inflorescence	Number of flowers	Cluster 3-15	-
	Stalk length	5-35 mm	-
Bract	Size	2-4.3 x 0.5-1.3 mm	2-4 mm
	Margin	Straight	Straight or denticulate
	Tip	0.2-0.7 mm, aristate, hyaline	-
Bracteole	Size	1.5-3.3 x 0.4-1 mm	-
	Shape	Oblong-lanceolate	-
	Margin	Straight	-
	Apex	Aristate	-
	Tip	0.2-0.5 mm, hyaline	-

Table 4. Comparison of our morphological findings with the Flora of Turkey (Continues)

Corolla	Size	2.2-3.3 mm	2-3 mm
	Color	Lobes pinkish-white, tube pink	Pale pink
	Tube size	1-2.2 mm, equal to or 2 times longer than lobes	2 times longer or shorter than ovate-oblong
	Lob size	1-1.2 x 2-3 mm	-
	Hairs	Dense hispid-tooth hairy, few or glabrous on lobes	Hispid, sometimes glabrous
Stamen	Number	4	-
	Shape	Dorsifixed	-
	Position	Alternating with lobes	-
Anther	Length	1-1.2 mm	-
	Shape	Linear	-
	Color	Brown	-
Filament	Length	< 1mm	-
Ovary	Size	1 x 0.5 mm	-
	Color	Dark brown	-
Style	Length	0.5-1.6 mm	-
	Shape	Bipartite equally branched	-
	Color	Pinkish-purplish	-
Stigma	Shape	Round	-
	Number	2	-
Mericarp	Size	1.2-2 x 1 mm	2 mm
	Shape	Ovate-oblong	-
	Color	Dark brown	Dark brown
	Surface	Densely warty	Warty

“The features shown with lines in the table were determined for the first time.”

The anatomical views of the stem and leaf were presented and supported by the photographs. There were collenchymatic corner projections, prominent endoderma, absence of pericycles, presence of raphide crystals, and long unicellular trichomes in the stems. The leaf was monofacial, and parasitic stomata on both epidermal surfaces of the leaves were observed. According to Metcalfe and Chalk (1950), the stems of the genus have a polygonal shape with collenchymatic corner projections, and no fungal structure is observed. The endoderma is well developed; however, the sclerenchymatic pericycle is not observed. The xylem is narrow and cylindrical, and the tracheal elements are small in diameter. A centric (*Asperula*) or homogeneous (*Borreria* G.F.W. Mey.) structure can be seen in some members of the family, which generally have a dorsiventral leaf structure. The hairs are long, unicellular, and sometimes curled at the ends in species of *Asperula* and some genera. Stomas are also located on the lower and upper sides of *Asperula* and some species of genera. They are of the rubiaceus (parasitic) type. Epidermal cells have smooth or wavy walls. Family members contain crystals and are extremely important in species identification. In *Asperula* stems the crystals consist only of raphides [25]. The stem and leaf anatomical features of the Rubiaceae family and the *Asperula* genus described by Metcalfe and Chalk, are usually compatible with our study results. Our findings coincide with those of Gücel (2015) [14]. The cell groups in the stem and leaf anatomy were similar.

The characteristics of the pollen, which have been mentioned by many authors, have taxonomic significance for Rubiaceae species. The pollen shapes of *A. serotina* (Boiss. Et Heldr.) Ehrend. and *A. purpurea* subsp. *apiculata* (SM.) Ehrend. have been recorded as spheroidal, the structure of the sexine was perforate, and the ornamentation was microechinate [33]. The pollen of *A. cankiriense* B.Şahin & Sağıroğlu was subprolate (P/E= 1.22), the number of colpus was 6-7, the colpus width was more than 1 µm, and its ornamentation was microechinate-perforate [34]. The pollen shape of *A. comosa* Schönb.-Tem was oblate-spheroidal; the pollen grain of *A. anatolica* was defined as spheroidal [1]. The pollen type of the endemic *A. daphneola* O. Schwarz was stefanocolpate, and the pollen shape (P/E=1.06) was spheroidal [14]. The pollen forms of some taxa were prolate-spheroidal and oblate-spheroidal; it has

been reported that the ornamentation was scabrate and perforate. The pollen shapes were different from our findings. Additionally, the pollen ornamentation in our study was scabrate-perforate. Our results showed similar ornamentation to previous research [8]. In previous research, the number of colpus in *Asperula* species has been given as usually 6-8, rarely 9 [1, 8, 14, 33, 34]. In our results, it was 7-8, compatible with other studies.

Some *Asperula* species have antioxidant activity. Minareci et al. (2011) investigated the antioxidant activities of five endemic *Asperula* species. The highest antioxidant activity value belongs to *A. pseudochlorantha* var. *pseudochlorantha* and is 1.88 mg/mL. The lowest antioxidant activity value belongs to *A. serotina* and is 1.22 mg/mL. In this study, it was determined that *Asperula* taxa showed different levels of antioxidant activity [16]. This result supports the antioxidant activity feature in our study. In another study, Halimi and Nasrabadi (2015) used the species *Asperula oppositifolia*. The antioxidant activity of methanol extracts of the aerial parts of the plant was tested. A high inhibitory effect was observed at high concentrations [17]. As a result of this study, it was stated that the *Asperula* taxon showed antioxidant activity. This situation is similar to ours. Loizzo et al. (2008) examined the *Asperula glomerata* species from the Rubiaceae family among plants with medicinal uses. The amount of total phenolic compounds was determined by the Folin–Ciocalteu method. The total phenolic component amount of *A. glomerata* extract was found to be 81.5 ± 0.13 mg/g [23]. It seems that the total phenolic substance amount in *A. glomerata* extract is higher than the result of our extracts.

At the same time, flavonoids and iridoids were determined in taxa whose components were examined [18- 21]. Kırmızıbekmez et al., (2014) worked with the aboveground parts of the *Asperula lilaciflora* species. They identified a new iridoid with a new flavonol glycoside. The name of the flavonol glycoside is lilacifluoracid; they reported iridoid as asperulogenin [20].

In all studies, different *Asperula* species have antioxidant properties. The fact that *Asperula pestalozzae* species also exhibit antioxidant activity suggests that they may contain flavonoid and iridoid structures in their phenolic components. For this reason, the subject of our future study will be the detection of flavonoid, iridoid, and other phenolic components.

5. CONCLUSION

The anatomical, morphological, micromorphological, palynological, and chemical properties of the endemic *A. pestalozzae* were compared to Flora of Turkey and other studies in detail for the first time in this study. Working on it for the first time increases its original value. Also, it shows that it is a pioneering work that contributes to further research.

When we looked at the results of all our studies, it was determined that our data matched the literature information, but some differences were determined. Our plant has shown antioxidant properties as a result of chemical studies. So, it could be used as a new source of antioxidant agents. The determination of its components is considered the subject of our future study.

CONFLICT OF INTEREST

The authors stated that there are no conflicts of interest regarding the publication of this article.

CRedit AUTHOR STATEMENT

Kader Kayış: Investigation, Resources, Writing – original draft, Visualization. **Ayla Kaya:** Resources, Writing – Review & Editing, Supervision, Project administration.

REFERENCES

- [1] Öztürk M. *Asperula anatolica* (Rubiaceae), a new species from south-east Anatolia, Turkey. Turkish Journal of Botany 2013; 37 (1): 46-54.
- [2] Soza VL, Olmstead RG. Molecular systematics of tribe Rubieae (Rubiaceae): evolution of major clades, development of leaf-like whorls, and biogeography. Taxon 2010; 59 (3): 755–771.
- [3] Ehrendorfer F, Barfuss MHJ, Manen JF, Schneeweiss GM. Phylogeny, character evolution and spatiotemporal diversification of the species rich and world-wide distributed tribe Rubieae (Rubiaceae). PLOS ONE 2018; 13 (12): 1-26.
- [4] Minareci E. The revision of the section *Thliptithisa* (Griseb.) Ehrend. of the genus *Asperula* L. (Rubiaceae) spreading in Turkey. PhD, Celal Bayar University, Manisa, Turkey, 2007.
- [5] Özgen U, Coşkun M. Morphological and anatomical studies on *Asperula taurina* L. subsp. *caucasica* (Pobed.) Ehrend. (Rubiaceae). Ankara Üniversitesi Eczacılık Fakültesi Dergisi 1999; 28 (2): 71-83.
- [6] Martins D, Nunez CV. Secondary metabolites from Rubiaceae species. Molecules 2015; 20 (7): 13422-13495.
- [7] Özgen U, Şener SÖ, Badem M, Seçinti H, Hatipoğlu SD, Gören AC, Kazaz C, Palaska E. Evaluation of HPLC, phytochemical, anticholinesterase and antioxidant profiles of the aerial parts of *Asperula taurina* subsp. *caucasica*. Ankara Üniversitesi Eczacılık Fakültesi Dergisi 2018; 42 (1): 1-13.
- [8] Akdeniz S. Pollen morphology of some taxa belonging to the genera *Asperula* L., *Galium* L. (Rubiaceae) distributed in Turkey. MSc, Bitlis Eren University, Bitlis, Turkey, 2019.
- [9] Iurchenko NS, Ilyina TV, Kovaleva AM, Toryanik EL, Kulish IA. The antihypoxic and sedative activity of the dry extract from *Asperula odorata* L. Pharmacognosy Communications 2015; 5 (4): 233-236.
- [10] Web Address of BİZİM BİTKİLER: <https://www.bizimbitkiler.org.tr> (accessed: 04.02.2024)
- [11] Davis PH. Flora of Turkey and the East Aegean Islands. Volume 7: Edinburgh University Press, Edinburgh, 1982, pp.722-767.
- [12] Sezer O, Öztürk D, Ocak A, Koyuncu O. Flora of Phrygian Valley (Mountain Phrygia/Turkey). Biological Diversity and Conservation 2017; 10 (3), 163-183.
- [13] Erdem CB The flora and ethnobotany of Abbaslık village (Bilecik). MSc, Hacettepe University, Ankara, Turkey, 2018.
- [14] Gücel S. Morphology, anatomy and cytology of critically endangered endemic *Asperula daphneola* from, West Anatolia, Turkey. Journal of Environmental Biology 2015; 36 (1): 129-132.
- [15] Minareci E, Yıldız K. Karyotype characterization of Turkish taxa of the genus *Asperula* L.-section *Thliptithisa* (Rubiaceae). Indian Society of Genetics & Plant Breeding 2011; 71 (1), 49-54.

- [16] Minareci E, Ergönül B, Kayalar H, Kalyoncu F. Chemical compositions and antioxidant activities of five endemic *Asperula* taxa. Archives of Biological Sciences 2011; 63 (3): 537-543.
- [17] Halimi M, Nasrabadi M. Essential oil composition and antioxidant activity of aerial parts of *Asperula oppositifolia* collected from Darkesh, Iran. Journal of Medicinal Plants Research 2015; 9 (46): 1118-1122.
- [18] Güvenalp Z, Demirezer LÖ. Flavonol glycosides from *Asperula arvensis* L. Turkish Journal of Chemistry 2005; 29 (2): 163-169.
- [19] Özgen U, Kazaz C, Seçen H, Coşkun M. Phytochemical studies on the underground parts of *Asperula taurina* subsp. *caucasica*. Turkish Journal of Chemistry 2006; 30 (1): 15-20.
- [20] Kırmızıbekmez H, Bardakçı H, Masullo M, Kamburoğlu Ö, Eryılmaz G, Akaydın G, Yeşilada E, Piacente S. Flavonol glycosides and iridoids from *Asperula lilaciflora*. Helvetica Chimica Acta 2014; 97 (11): 1571-1576.
- [21] Kırmızıbekmez H, Tiftik K, Kusz N, Orban-Gyapai O, Zomborszki ZP, Hohmann J. Three new iridoid glycosides from the aerial parts of *Asperula involucreta*. Chemistry & Biodiversity 2017; 14 (3): 1-7.
- [22] Kalyoncu F, Minareci E, Minareci O. Antimicrobial activity of five endemic *Asperula* species from Turkey. Iranian Journal of Pharmaceutical Research 2009; 8 (4): 263-268.
- [23] Loizzo MR, Saab AM, Tundisa R, Menichinia F, Bonesia M, Piccola V, Statti GA, De Cindio B, Houghton PJ, Menichinia F. In vitro inhibitory activities of plants used in Lebanon traditional medicine against angiotensin converting enzyme (ACE) and digestive enzymes related to diabetes. Journal of Ethnopharmacology 2008; 119 (1): 109-116.
- [24] Baytop A. English-Turkish Botanical Manual, İstanbul University Press, İstanbul, 1998, pp.359-375.
- [25] Metcalfe CR, Chalk L. Anatomy of the Dicotyledons, Vol 2: Oxford University Press, London, 1950, pp.759-776.
- [26] Walker JW, Doyle JA. The bases of angiosperm phylogeny: polynology. Annals of the Missouri Botanical Garden 1975, 62, pp.664-723.
- [27] Zhao M, Ito Y, Tu P. Isolation of a novel flavanone 6-glucoside from the flowers of *Carthamus tinctorium* (Honghua) by high-speed counter-current chromatography. Journal of Chromatography A 2005; 1090: 193–196.
- [28] Büyüktuncel E. Main spectrophotometric methods for the determination of total phenolic content and antioxidant capacity. Marmara Pharmaceutical Journal 2013; 17: 93-103.
- [29] Kosar M, Göger F, Can Baser KH. In vitro antioxidant properties and phenolic composition of *Salvia virgata* Jacq. from Turkey. J. Agric. Food Chem. 2008; 56 (7): 2369-2374.
- [30] Singleton VL, Orthofer R, Lamuela-Raventós RM (1999). Analysis of total phenols and other oxidation substrates and antioxidants by means of folin-ciocalteu reagent. Meth. Enzymol. 1999; 299: 152-178.

- [31] Kumarasamy Y, Byres M, Cox PJ, Jaspars M, Nahar L, Sarker SD. Screening seeds of some Scottish plants for free radical scavenging activity. *Phytother. Res.* 2007; 21 (7): 615-621.
- [32] Re R, Pellegrini N, Proteggente A, Pannala A, Yang M, Rice-Evans C. Antioxidant activity applying an improved ABTS radical cation decolorization assay. *Free Radic. Biol.* 1999; 26 (9-10): 1231-123.
- [33] Minareci E, Yıldız K. *Asperula pseudochlorantha* var. *antalyensis* comb. et stat. nov. (Rubiaceae). *Annales Botanici Fennici* 2010; 47: 121-128.
- [34] Şahin B, Sağırođlu M, Bařer B. A new *Asperula* L. (Rubiaceae) species from gypsum steppes of Çankırı province in Turkey. *Turkish Journal of Botany* 2021; 45 (2): 243-252.



RESEARCH ARTICLE

THE EFFECTS OF DIFFERENT SONICATION METHODS ON ALPHA-SYNUCLEIN PRE-FORMED FIBRILS

Hilal AKYEL ^{1,2*}, Elham BAHADOR ZIRH ³, Selim ZIRH ⁴, Banu Cahide TEL ¹

¹ Pharmacology Department, Faculty of Pharmacy, Hacettepe University, Ankara, Turkey

hilalakyl34@gmail.com - [0000-0003-2841-6668](https://orcid.org/0000-0003-2841-6668)

² Pharmacology Department, Faculty of Pharmacy, Baskent University, Ankara, Turkey

elhambahador1969@gmail.com - [0000-0002-6921-2365](https://orcid.org/0000-0002-6921-2365)

³ Histology and Embryology Department, Faculty of Medicine, TOBB Economy and Technology University, Ankara, Turkey

dr.szirh@gmail.com - [0000-0002-7962-6078](https://orcid.org/0000-0002-7962-6078)

⁴ Histology and Embryology Department, Faculty of Medicine, Erzincan Binali Yıldırım University, Erzincan, Turkey

banutel@hacettepe.edu.tr - [0000-0001-5453-1294](https://orcid.org/0000-0001-5453-1294)

Abstract

Alpha-synuclein (α -syn) aggregation is associated with neuronal death and the pathological hallmark of Parkinson's disease (PD). The α -syn preformed fibril model (α -syn-PFFs), reflects α -syn aggregation and is currently used in PD studies. To pass through the cell membrane, long fibrils should be fragmented by sonication. In our study, the effects of temperature, pulse modifications and/or device type on the sonication of α -syn-PFFs were investigated. Sonication was performed ultrasonic bath and in laminar-flow cabinet with probe sonicator. Dilutions were made from 5 μ g/ μ l α -syn-PFFs stock in sterile-filtered dH₂O to a final concentration and volume of 0.1 μ g/ μ l and 200 μ l, respectively. Sonication was performed in an ultrasonic bath containing water at 10°C for 1 hour. All probe sonications were performed at 30% amplitude for 1 minute and 20 repetitions. The effect of temperature on sonication has been evaluated by performing sonication at room temperature (RT), in ice and in ice surrounded by dry ice. Also, the effects of pulse duration on sonication were evaluated using pulse durations of 1second(sec) on/1sec off, 3sec on/3sec off and 5sec on/5sec off. Furthermore, by waiting one minute between each sonication cycle, the heat released by the probe was prevented from affecting the fibrillar structure. The particle size was measured in triplicate by dynamic light scattering method. For transmission electron microscopy, formvar/carbon-coated grids were run through ddH₂O-sonicated fibril-uranyl acetate solutions and kept dry until examined. Due to the variation in breakage of long α -syn fibrils, the effect of different parameters on sonication was investigated. In comparison of pulse durations, 5sec on/5sec off application produced shorter fibrils. Comparing the temperature interventions, lowering the temperature decreased the fibril size at 1sec on/1sec off settings but increased it at 3sec on/3sec off and 5sec on/5sec off. However, the shortest fibrils were obtained by sonication for 5sec on/5sec off at RT.

Keywords

Sonication,
Alpha-synuclein,
Pre-formed fibril,
Particle size,
Transmission electron microscopy

Time Scale of Article

Received: 09 Kasım 2023
Accepted: 29 April 2024
Online date: 30 July 2024

1. INTRODUCTION

Parkinson's Disease (PD) is a neurodegenerative disorder caused by a progressive loss of dopaminergic neurons in the substantia nigra pars compacta (SNpc). Over the age of 65, it affects 1-2% of the population [1]. In addition to the motor symptoms of PD, non-motor symptoms accompany the disease in both

*Corresponding Author: hilalakyl34@gmail.com

premotor and late stages [2]. The presence of alpha-synuclein (α -syn) aggregates in Lewy bodies and neurites, which are specific markers of the disease, indicates its importance in the pathogenesis of PD [3].

α -syn is a protein that contains 140 amino acids and is found in an alpha-helical structure. The protein is mainly located at the presynaptic terminals of neurons, where it plays a crucial role in maintaining synaptic vesicular homeostasis and synaptic transmission [4,5]. Physiologically, α -syn exists as an unfolded monomer, tetramer [6], and multimer bound to lipid membranes (Figure 1) [7]. In pathological conditions, posttranslational modifications such as ubiquitination, phosphorylation and misfolding result in the formation of insoluble α -syn aggregates in the beta-sheet conformation [8]. Upon accumulation, aggregates form in the soma, axons, and dendrites, forming Lewy bodies and Lewy neurites, respectively. Fibrillar α -syn is one of the main components of Lewy bodies/neurites [9].

The aggregation of a monomeric α -syn is a multi-step process that begins with a nucleation reaction in which monomeric α -syn is converted into oligomers of varying sizes (dimers, trimers, low molecular weight, high molecular weight). The oligomers are then converted into protofibrils, which in turn give rise to the insoluble fibrils (Figure 1) [10-12].

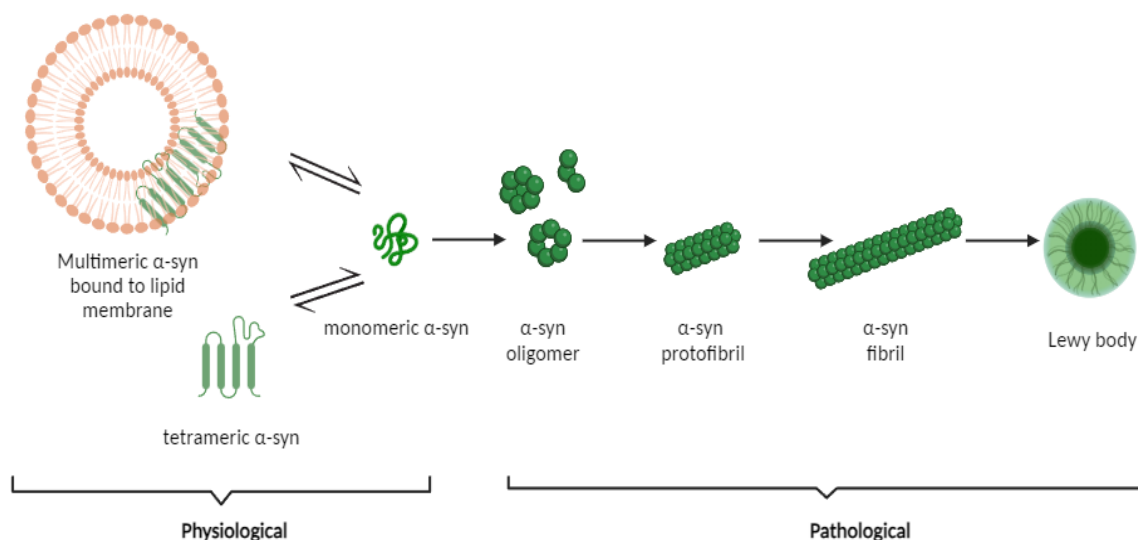


Figure 1. A process of forming α -syn fibrils. In physiological conditions, monomeric α -syn exists in equilibrium with multimeric structure bound to the lipid membrane and tetrameric structure. The formation of α -syn fibrils occurs in a nucleation reaction that transforms the soluble monomer into a beta-structured, stable, and insoluble fibril (designed with BioRender) [10].

The α -syn pre-formed fibril (α -syn-PFF) model is currently being used in PD research to recapitulate the Lewy pathology. In this model, exogenous α -syn fibrils trigger endogenous α -syn [13, 14] phosphorylating it at pS129, causing insoluble α -syn aggregates to form within the cell [15-21]. Therefore, the α -syn-PFF, which can mimic the pathogenesis of the disease in terms of α -syn aggregation and Lewy pathology, has gained increasing importance [22, 23].

In order for α -syn fibrils to be taken into the cell from the pathology *in vitro* or *in vivo*, fibrils should have a size between 50-100 nanometers (nm) or shorter in length. Long fibrils are therefore broken into short fragments using a probe sonicator or ultrasonic bath sonicator, which generates energy with vibration and sound waves, respectively [24, 25]. After sonication, a heterogeneous mixture of monomers, oligomers, and short fibrils is obtained [26-28]. Validation of sonication parameters is required to produce reliable *in vitro* and/or *in vivo* fibril models [24, 25]. Thus, it is necessary to investigate multiple sonication parameters [24, 25, 29]. Accordingly, sonication studies have shown that pulse duration, temperature of the experimental environment, sonication repetitions, and sonication device type vary.

In our study, we compared the effects of pulse duration, temperature, and sonication device type on 20 repeated sonications of α -syn-PFFs produced in the same series. After sonication, samples were analyzed using transmission electron microscopy (TEM). In addition, the hydrodynamic diameter-particle size was determined by dynamic light scattering (DLS).

2. MATERIALS AND METHODS

2.1. MATERIALS

Table 1: Experimental materials and equipments.

Equipment/Material Name	Company	Catalog Number
Human alpha-synuclein preformed fibrils	Produced in Ryan Lab and purchased from this lab	
Steril conical centrifuge tubes, 15 ml	Greiner Bio-One, Cellstar®	
Steril microcentrifuge tube, 1.5 ml	Greiner Bio-One, Cellstar®	
Parafilm	Parafilm M	PM-996
Stopper	Made in our laboratory	
Uranyl acetate	Eletron Microscopy Sciences	22400
Sterile-filtered deionized and distilled water		
Lockable tweezer		
Formvar/Carbon coated electron microscopy copper grids	Ted Pella Inc.	1801
Electron Microscopy Grids Box	Ted Pella Inc.	
Quartz cuvette		
Centrifuge Device	Hitachi	Himac CT6E
Probe sonicator	Sonics Vibra-Cell™	VCX 750
Probe	Sonics Vibra-Cell™ (microtip)	630-0422
Ultrasonic bath sonicator	Branson	CPX5800H
Transmission electron microscope	FEI Tecnai™ G2 Spirit BioTwin model	
Device of Dynamic Light Scattering	Malvern Instruments, UK	Zetasizer Nano-ZS

2.2. METHODS

2.2.1. Sonication of α -syn-PFFs

Human α -syn fibrils was produced in Assoc Prof. Scott Ryan's laboratory (Ryan Lab, University of Guelph, Canada) as described [30] and purchased from this laboratory at a concentration of 5 $\mu\text{g}/\mu\text{l}$ in a volume of 200 μl . α -syn fibrils were aliquoted until sonication and stored at -80°C in a volume of 4 μl . Sonication was carried out using a probe sonicator (Sonics Vibra-Cell™, VCX 750) and an ultrasonic bath sonicator (Branson-CPX5800H). After the α -syn fibrils were dissolved at room temperature, they were diluted with sterile-filtered deionized water to a final concentration of 0.1 $\mu\text{g}/\text{ml}$ and a volume of 200 μl . Sterile centrifuge tubes (15 ml) were used for probe sonication and sterile microcentrifuge tubes for ultrasonic bath sonication.

2.2.1.1. Probe Sonication

Sonication was carried out in a laminar flow cabinet to avoid exposure to fibrils that may become aerosolized during sonication and to maintain sterility. A probe with a diameter of 3 mm was placed on a stabilizer in a laminar flow cabinet (Figure 2. a1, a2, a3). The probe was sterilized with 70% ethanol. Then, it was cleaned with distilled water and wiped dry. For 15 minutes, it was sterilized with UV light. The sterile centrifuge tube containing the fibrils (15 ml) is placed in tube holder during sonication at

room temperature. During sonications in ice and in ice surrounded by dry ice, the centrifuge tube was fixed with a white foam holder with a hole in the middle to prevent it from slipping. In the centrifuge tube containing 200 µl of diluted fibrils, a stopper was placed with an opening in the middle through which the probe can pass without touching the stopper. Due to the probe size, centrifuge tubes had to be used, even though the amount of sonicated liquid was much less. Therefore, a stopper was used to reduce the loss of liquid adhering to the wall or evaporating. The stopper was wrapped with parafilm to collect the liquid splashed on its surface by centrifugation.

The probe tip was inserted into the tube through the gap in the middle of the stopper. Sonication was performed by placing the probe tip in the center of a 200 µl solution to prevent volume loss. In order to avoid energy loss, the probe should not contact the walls of the tube or the stopper.

Sonation parameters are as follows:

- a. The amplitude was set at 30%.
- b. The total time was set at 00:01:00.
- c. The pulse duration was set as 1 second (sec) on/1 sec off, 3 sec on/3 sec off, and 5 sec on/5 sec off, as shown in Table 2.
- d. As shown in Table 2, the ambient temperature was adjusted to room temperature, ice, and ice surrounded by dry ice for each on/off period.
- e. As shown in Table 2, there are 20 repetitions of sonication. The interval between repetitions should be one minute.

Upon completion of the sonication, the probe was removed from the solution and the tube was briefly centrifuged for 1 sec at 2000 rpm to collect the splashing liquid on the walls of tube. The sonicated samples were then placed in a sterile 1.5 ml microcentrifuge tube for imaging with TEM. The hydrodynamic diameter/particle size of the sample was measured by the DLS method by dilution of 2 µl of the sample with sterile-filtered deionized water to a final volume of 1000 µl (dilution ratio: 1:500). After each experiment, all surface of the laminar flow cabinet and probe tip was cleaned first with 1% sodium dodecyl sulfate (SDS) and then with 70% ethanol. The device was then sterilized for 15 minutes using ultraviolet light.

2.2.1.2. Ultrasonic Bath Sonication

The bath tank was filled with distilled water to the level indicated on the tank. Temperature of the water was set at 10°C. The fibrils in the 1.5 ml sterile microcentrifuge tube are fixed on the water surface with the holder so that the entire 200 µl volume is submerged in water. Sonication is performed for 1 hour. For TEM imaging, all 1.5 ml of a sterile microcentrifuge tube are used. In order to measure hydrodynamic diameter/particle size with DLS, 2 µl of the sample is diluted with sterile-filtered deionized water to a final volume of 1000 µl (dilution ratio: 1:500) [31].

Table 2: Protocols for sonication by probe and ultrasonic bath for α-syn-PFFs, respectively.

Sonation Technique	Sonation Features		
	Cycles/Duration	Pulse (on/off)	Temperature
Probe	20	1 sec / 1 sec	Room temperature
		3 sec / 3 sec	Ice
		5 sec / 5 sec	Ice surrounded by dry ice
Ultrasonic Bath	1 hour		Water temperature, 10 °C

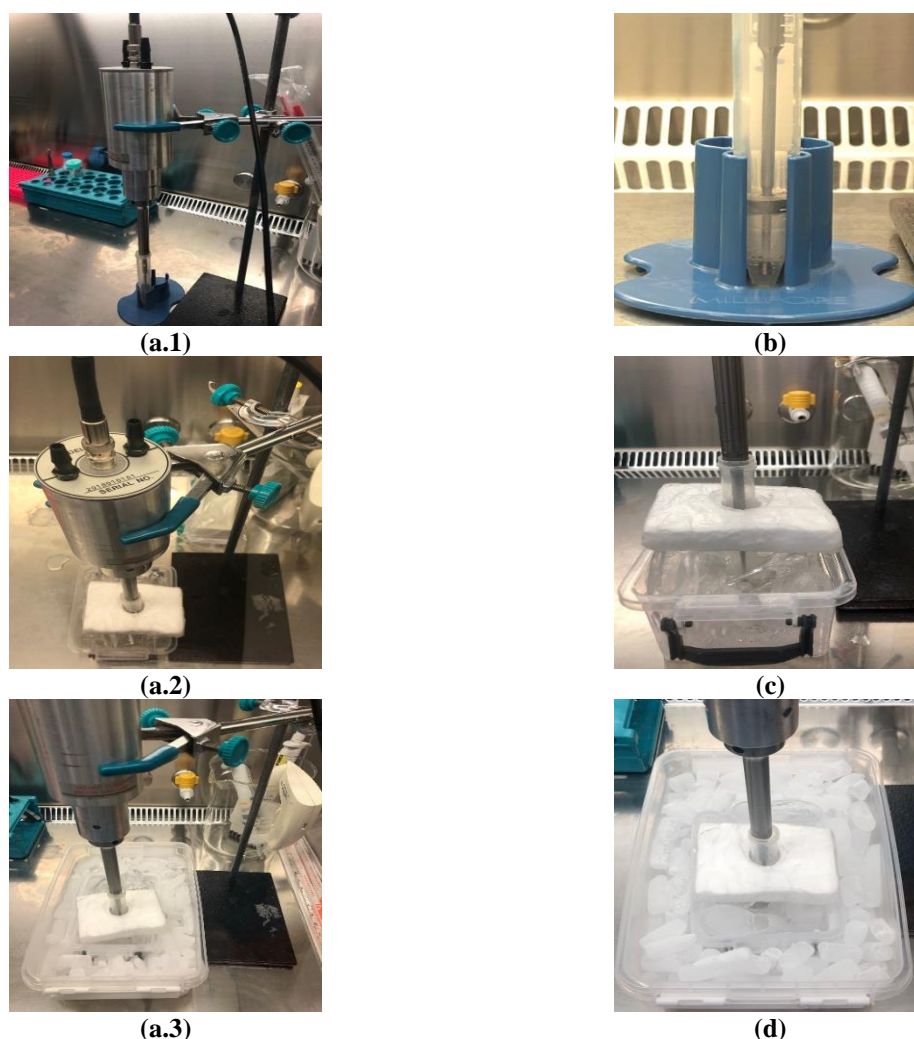


Figure 2. Images of probe sonication. a.1, a.2, a.3. A view of the probe fixation from various angles. **b.** Sonication at room temperature. **c.** Sonication in ice. **d.** Sonication in ice surrounded by dry ice. **b, c, d.** For each protocol, a black stopper wrapped in parafilm prevents the aerosolized fibrils from evaporation. **c and d.** A white stabilizer prevents the 15 ml centrifuge tube from slipping.

2.2.2. Determination of Hydrodynamic Diameter/Size of Sonicated Fibrils

To measure the particle size in relation to the hydrodynamic diameter of the fibrils, dynamic light scattering (DLS) was performed at 25°C using a Malvern Instruments Zetasizer Nano-ZS (Malvern Instruments, Malvern, UK). After sonication, 1000 µl of sonicated fibrils in deionized water are transferred to a quartz cuvette for DLS measurements. For each sample, the measurement is repeated three times. As a result of the homogeneity of the sample, the device automatically determines the number of repetitions in measurement. A scattering angle of 90° is used for the measurement. The results of the measurement are displayed graphically in terms of the percentage density versus the hydrodynamic diameter (nanometer, nm) of the particles [29, 32].

2.2.3. TEM Imaging of Sonicated and Unsonicated Fibrils

The bench is covered with parafilm to prepare a clean-hydrophobic work surface then the sample, and the controls were dropped on where the grids would be immersed sequentially. 4 drops of 200 µL sterile-filtered distilled water (ddH₂O) dropped on parafilm. The entire volume of samples prepared for TEM was added as one drop; two drops of 200 µl 2% uranyl acetate were added. Formvar/carbon coated

copper grids were held with fine tip lockable forceps. The dark side of the grid (formvar/carbon coating) was placed on the first drop of ddH₂O. Once the grid has been removed after one minute, ddH₂O is removed from the edge of the grid using a filter paper and the same procedure was repeated. Grids were placed on sonicated or unsonicated fibril drops for three minutes and excess fluids were removed with filter paper. After exposing the grids to the first drop of uranyl acetate for one-minute, excess uranyl acetate was removed with filter paper, and the process was repeated. Uranyl acetate process was carried out in the dark. Grids were kept in the third and fourth drops of ddH₂O for one minute each, and the ddH₂O was removed using filter paper on the grid edge (Figure 3). The grids were stored at room temperature in a grid box until imaging was performed [24]. The TEM imaging (FEI Tecnai™ G2 Spirit BioTwin model) was carried out by the TEM laboratory at Middle East Technical University, Central Laboratory. Fibrils and oligomers were imaged using magnifications of 13000 and 68000, respectively. The length of fibrils and diameter of oligomers, particles were measured three times using Image J 1.53k. Measurements were averaged from at least three scores.

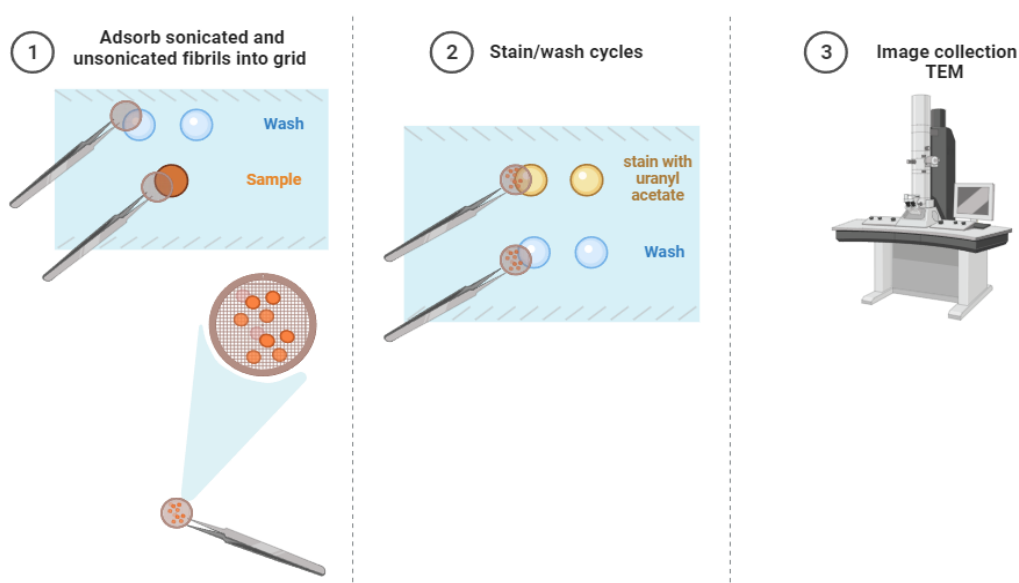


Figure 3. An illustration of the staining protocol for TEM. Grids were coated with formvar/carbon on their dark sides. 1) All drops were placed on parafilm. For one minute, the grid was floated in the first drop of ddH₂O with the dark side touching the drop, and the excess was wiped off using filter paper. Application repeats for one minute with the second drop of ddH₂O, three minutes with one drop of sonicated or unsonicated fibrils, 2) for one minute with two drops of uranyl acetate, and for one minute with two drops of ddH₂O. 3) Grids were stored in the grid box until they were displayed (designed with BioRender) [24].

2.2.4. Statistical Analysis

Results were presented as mean \pm standard error. The Student's t test was used to compare two groups, and a one-way analysis of variance (ANOVA) followed by a *posthoc* Tukey's multiple comparison test was used to compare more than two groups. $p < 0.05$ was considered statistically significant. The statistical analyses were conducted using GraphPad Prism 7 (GraphPad Software, Inc., San Diego, CA, USA).

3. RESULTS

3.1. Effects of Room Temperature on Sonication

The smallest particles were obtained with 5 sec on/off pulse by comparing other pulse durations with hydrodynamic diameters/particle sizes measured with DLS (Table 3). The size distribution of the

particles is shown in Figure 4. Since the measurement principle of the DLS device is optimized for spherical particles, the results obtained for fibrils and oligomers were considered as an indicator of the length alterations [33].

Table 3: Particle sizes obtained using probe sonication at room temperature (n = 3).

20 cycles and at room temperature			
Pulse (on/off)	1 sec on / 1 sec off	3 sec on / 3 sec off	5 sec on / 5 sec off
Average Particle Size (diameter, nm)	2959 ± 1355	817,6 ± 75,61	290,4 ± 25,09

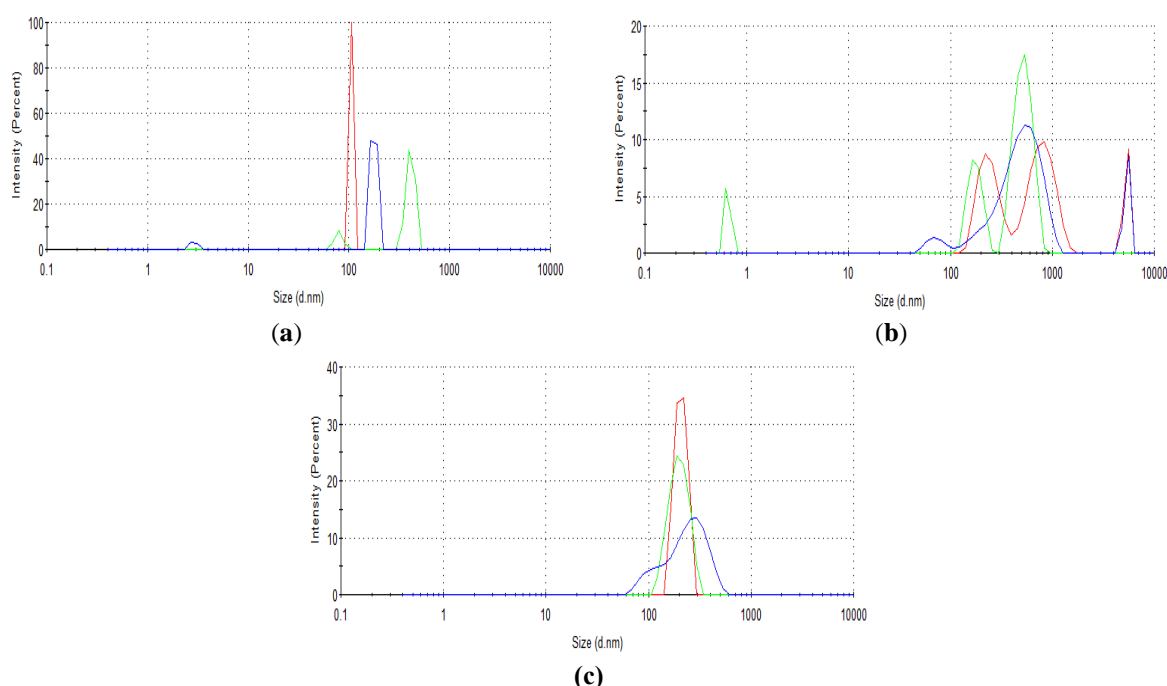


Figure 4. Particle size distribution obtained after sonication at room temperature. (a) 1 sec on/off, (b) 3 sec on/off, (c) 5 sec on/off (n = 3). The results of the measurement are displayed graphically in terms of the percentage density versus the hydrodynamic diameter (nm) of the particles.

As a result of TEM analysis, the average oligomer length (nm) was evaluated, and no significant differences were found in the 1 sec on/off or the 3 sec on/off group compared to the control. In the 5 sec on/off group, oligomer lengths were shorter on average than in the control or other pulse groups. ($p < 0.0001$ 5 s on/off vs control, $p = 0.0002$ 5 s on/off vs 1 s on/off, $p < 0.0001$ 5 s on/off vs 3 s on/off, Figure 5.1). Although fibril length decreased in the pulse groups compared to the control group, significance was not reached (Figure 5.2).

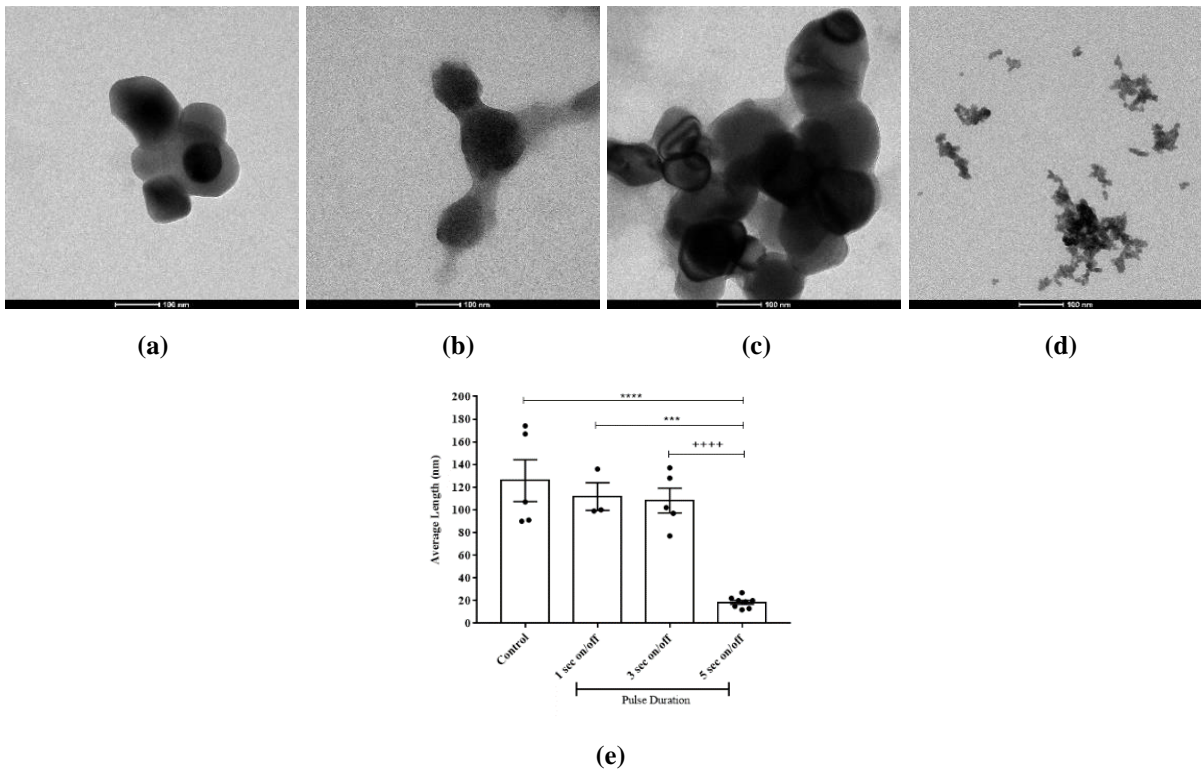


Figure 5.1. Oligomer lengths after probe sonication at room temperature. (a) Control, (b) 1 sec on/off, (c) 3 sec on/off, (d) 5 sec on/off. (e) Data are expressed as mean \pm standard error. One-way ANOVA followed by post hoc Tukey's multiple comparison tests were applied (**** p <0.0001 5 s on/off vs control, *** p =0.0002 5 s on/off vs 1 s on/off, ++++ p <0.0001 5 s on/off vs 3 s on/off). Scale bar: 100 nm.

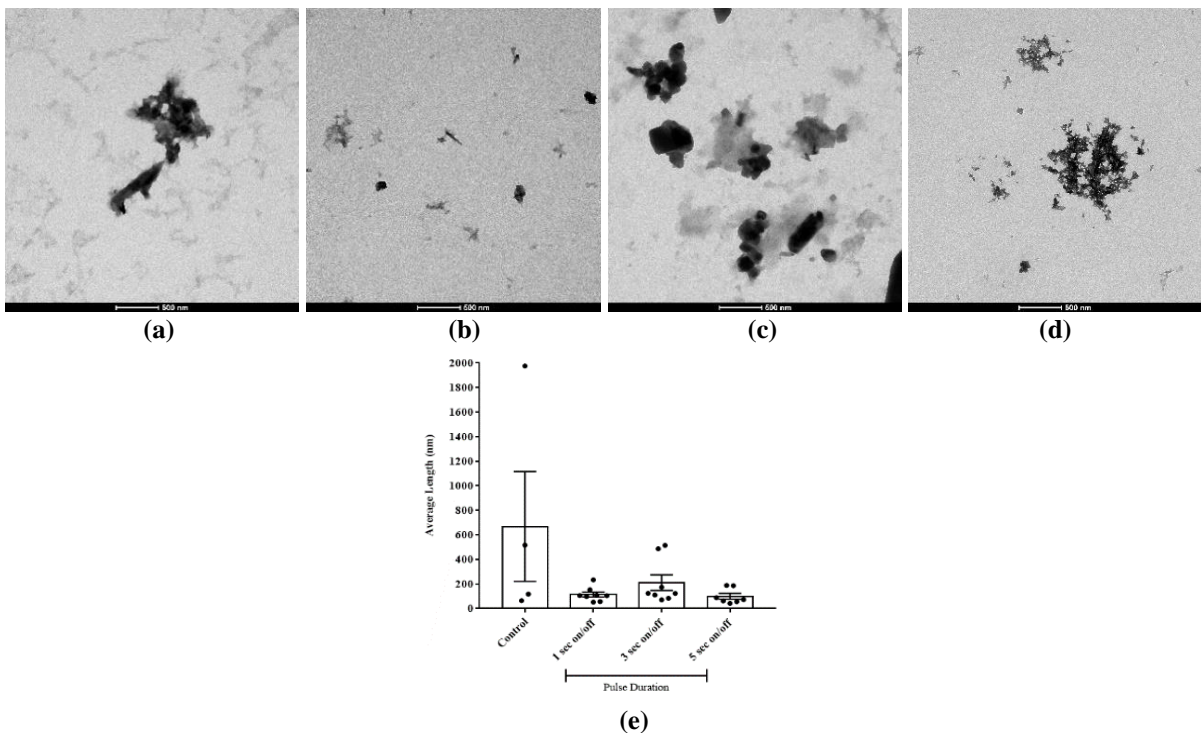


Figure 5.2. Fibril lengths after probe sonication at room temperature. (a) Control, (b) 1 sec on/off, (c) 3 sec on/off, (d) 5 sec on/off. (e) Data are expressed as mean \pm standard error. One-way ANOVA followed by post hoc Tukey's multiple comparison tests were applied. Scale bar: 500 nm.

3.2. Effects of Ice on Sonication

Based on measurements of average hydrodynamic diameter/particle sizes with DLS, smaller particles were obtained in an ice compared to room temperature at 1 sec on/off and 3 sec on/off pulse durations. At the same time, the particles are smaller in size due to the longer pulse duration of 3 sec on/off as opposed to 1 sec on/off. In contrast, particle size increased at a 5 sec on/off pulse duration in ice as compared to room temperature (Table 4). The size distribution of the particles is shown in Figure 6. Since the measurement principle of the DLS device is optimized for spherical particles, the results obtained for fibrils and oligomers were considered as an indicator of the length alteration [33].

Table 4: Particle sizes obtained using probe sonication in ice (n = 3).

20 cycles and in ice			
Pulse (on/off)	1 sec on / 1 sec off	3 sec on / 3 sec off	5 sec on / 5 sec off
Average Particle Size (diameter, nm)	1443 ± 1108	494,1 ± 69,21	613,3 ± 105,9

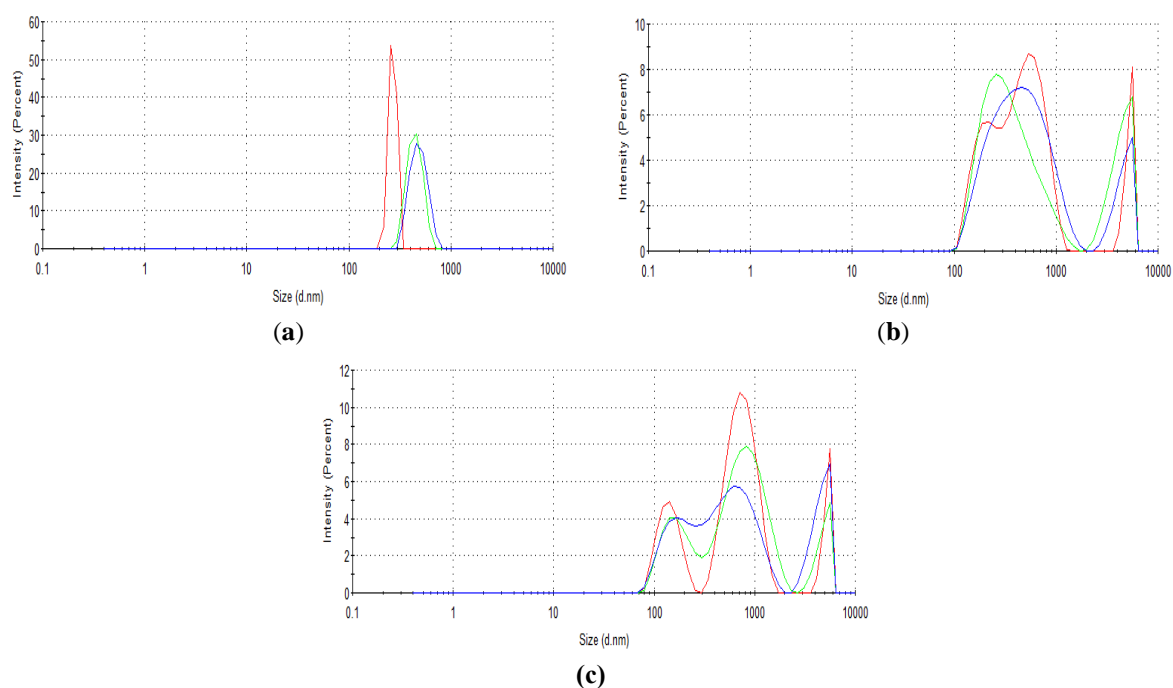


Figure 6. Particle size distribution obtained after sonication in ice. (a) 1 sec on/off, (b) 3 sec on/off, (c) 5 sec on/off (n = 3). The results of the measurement are displayed graphically in terms of the percentage density versus the hydrodynamic diameter (nm) of the particles.

Based on the TEM results, no difference was observed between the 1 sec on/off and the control, however, the average oligomer length of the 3 sec and 5 sec on/off groups was shorter than both the control and the 1 sec on/off group ($p=0.0001$ 3 s on/off vs control, $p=0.0002$ 3 s on/off vs 1 s on/off, $p<0.0001$ 5 s on/off vs control, $p<0.0001$ 5 s on/off vs 1 sec on/off, Figure 7.1). Although a decrease was observed in fibril length in the pulse groups compared to the control group, significance was not reached (Figure 7.2).

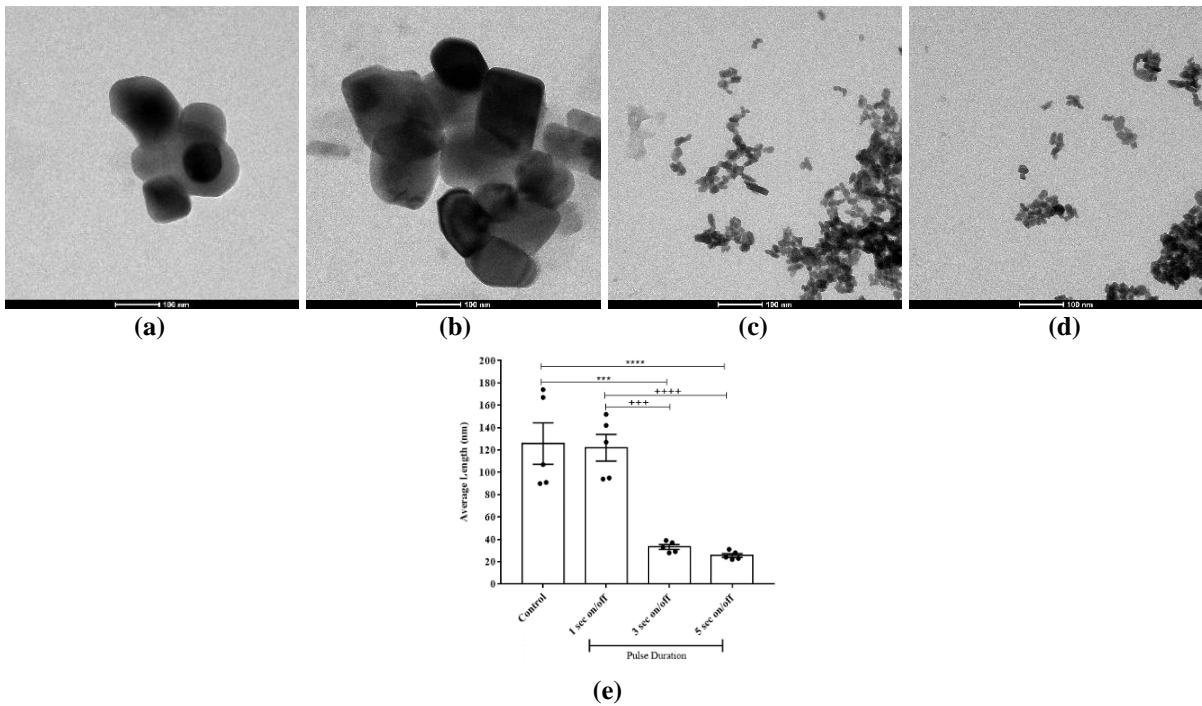


Figure 7.1. Oligomer lengths after probe sonication in ice. (a) Control, (b) 1 sec on/off, (c) 3 sec on/off, (d) 5 sec on/off. (e) Data are expressed as mean \pm standard error. One-way ANOVA followed by post hoc Tukey's multiple comparison tests were applied (** $p=0.0001$ 3 s on/off vs control, +++ $p=0.0002$ 3 s on/off vs 1 s on/off, **** $p<0.0001$ 5 s on/off vs control, +++++ $p<0.0001$ 5 s on/off vs 1 sec on/off). Scale bar: 100 nm.

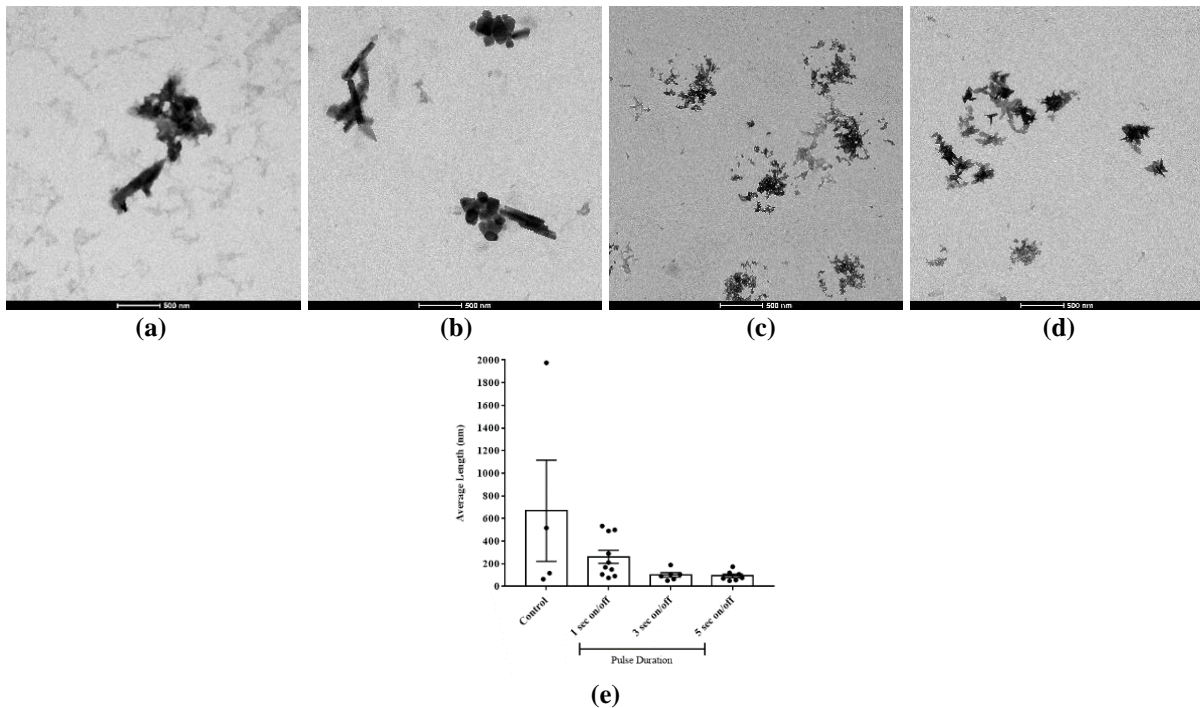


Figure 7.2. Fibril lengths after probe sonication in ice. (a) Control, (b) 1 sec on/off, (c) 3 sec on/off, (d) 5 sec on/off. (e) Data are expressed as mean \pm standard error. One-way ANOVA followed by post hoc Tukey's multiple comparison tests were applied. Scale bar: 500 nm.

3.3. Effects of Ice Surrounded by Dry Ice on Sonication

Measurements of hydrodynamic diameter/particle size with DLS in ice surrounded by dry ice indicated smaller particles were obtained at a 1 sec on/off pulse than at other temperatures. In addition, 5 sec on/off pulse duration has the smallest particle size compared to other pulse durations. On the other hand, particle size increased at both 3 sec on/off and 5 sec on/off pulse durations as compared to other temperatures (Table 5). The size distribution of the particles is shown in Figure 8. Since the measurement principle of the DLS device is optimized for spherical particles, the results obtained for fibrils and oligomers were considered as an indicator of the length alteration [33].

Table 5: Particle sizes obtained using sonication in ice surrounded by dry ice (n = 3).

20 cycles and in ice surrounded by dry ice			
Pulse (on/off)	1 sec on / 1 sec off	3 sec on / 3 sec off	5 sec on / 5 sec off
Average Particle Size (diameter, nm)	1105 ± 786,8	840 ± 189,7	719 ± 262,4

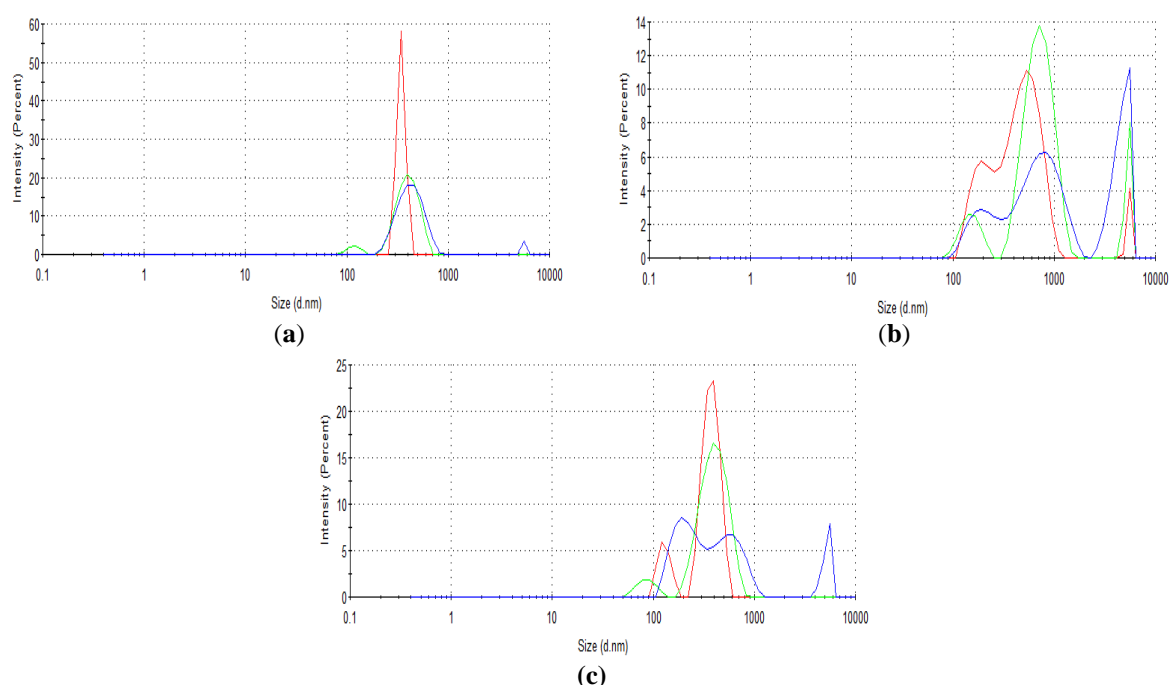


Figure 8. Particle size distribution obtained after sonication in ice surrounded by dry ice. (a) 1 sec on/off, (b) 3 sec on/off, (c) 5 sec on/off (n = 3). The results of the measurement are displayed graphically in terms of the percentage density versus the hydrodynamic diameter (nm) of the particles.

Based on the TEM results, there was no significant difference in the average oligomer length between the 3 sec on/off group and the control, but the average oligomer length was shorter in the 1 sec and 5 sec on/off groups than in the control ($p=0.0011$ 1 sec on/off vs control, $p=0.0007$ 5 sec on/off vs control). Furthermore, the average oligomer length was longer in the 3 sec on/off group than in the other pulse groups ($p=0.0115$ 3 sec on/off vs 1 sec on/off, $p=0.0091$ 3 sec on/off vs 5 sec on/off, Figure 9.1). Although fibril length was smaller in the pulse groups compared to the control, the difference was not statistically significant (Figure 9.2).

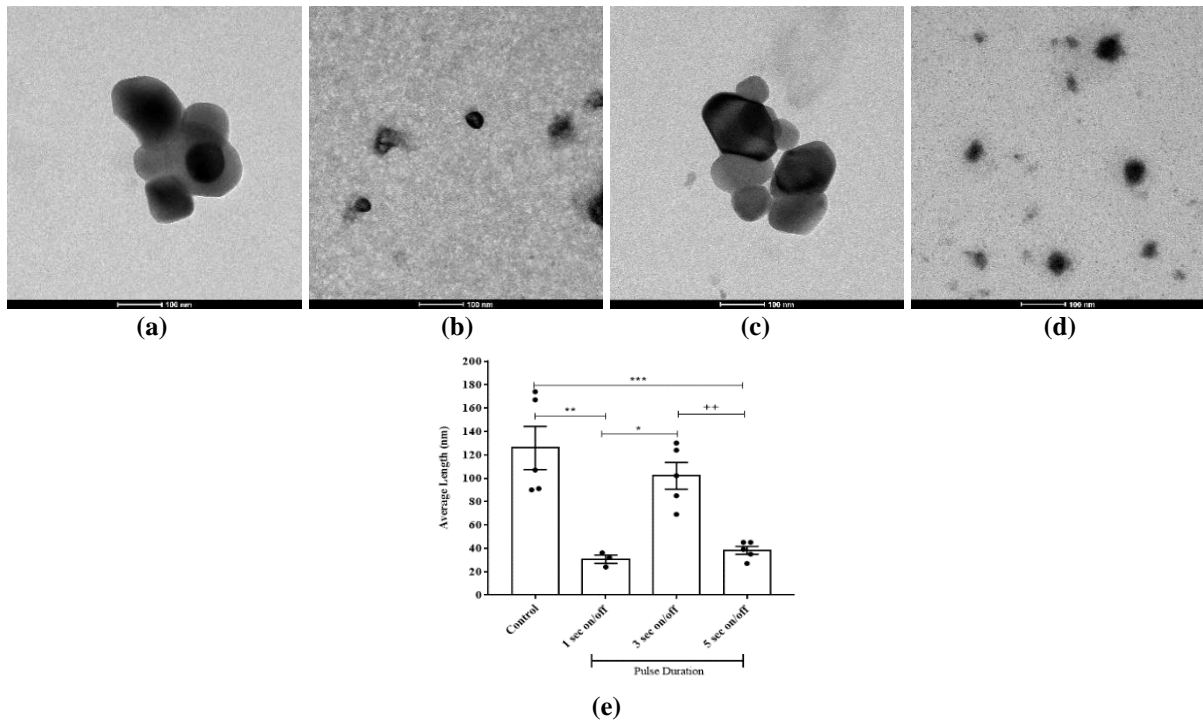


Figure 9.1. Oligomer lengths after probe sonication in ice surrounded by dry ice. (a) Control, (b) 1 sec on/off, (c) 3 sec on/off, (d) 5 sec on/off. (e) Data are expressed as mean \pm standard error. One-way ANOVA followed by post hoc Tukey's multiple comparison tests were applied ($p=0.0011$ 1 sec on/off vs control, *** $p=0.0007$ 5 sec on/off vs control, * $p=0.0115$ 3 sec on/off vs 1 sec on/off, ++ $p=0.0091$ 3 sec on/off vs 5 sec on/off). Scale bar: 100 nm.**

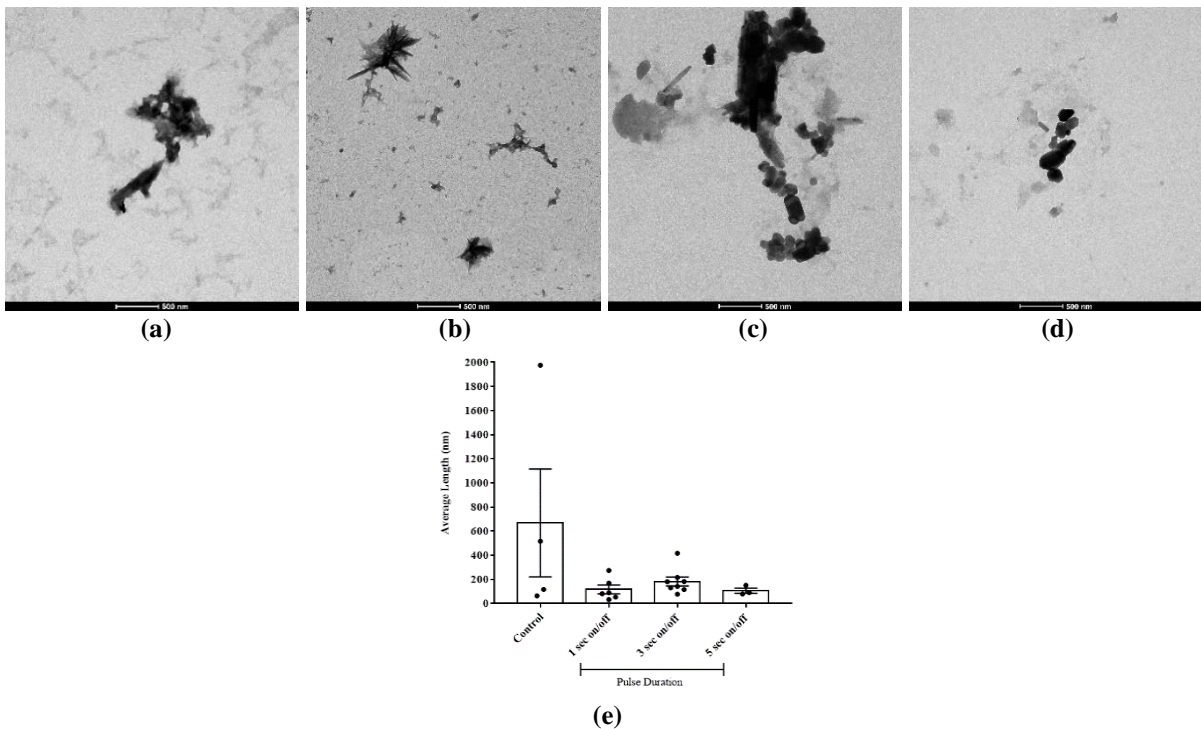


Figure 9.2. Fibril lengths after probe sonication in ice surrounded by dry ice. (a) Control, (b) 1 sec on/off, (c) 3 sec on/off, (d) 5 sec on/off. (e) Data are expressed as mean \pm standard error. One-way ANOVA followed by post hoc Tukey's multiple comparison tests were applied. Scale bar: 500 nm.

3.4. Effects of Ultrasonic Bath on Sonication

A DLS measurement of the average hydrodynamic diameter/particle size revealed that the particle sizes were similar to those obtained by probe sonication (Table 6). The size distribution of the particles is shown in Figure 10. Since the measurement principle of the DLS device is optimized for spherical particles, the results obtained for fibrils and oligomers were considered as an indicator of the length alteration [33].

Table 6: Particle sizes obtained using ultrasonic bath sonication (n = 3).

	1 hour and 10 °C water temperature
Average Particle Size (diameter,nm)	1017 ± 116,4

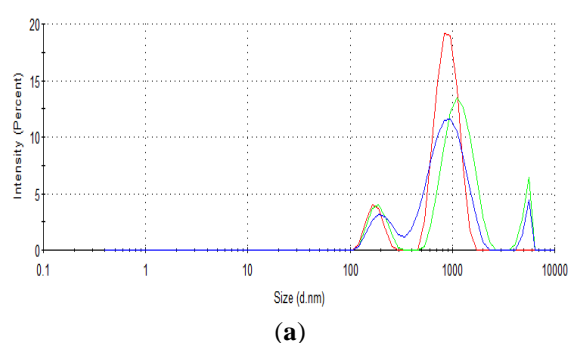


Figure 10. Particle size distribution obtained after ultrasonic bath sonication (n = 3). The results of the measurement are displayed graphically in terms of the percentage density versus the hydrodynamic diameter (nm) of the particles.

According to the TEM results, the oligomer lengths in the ultrasonic bath group were shorter than the control ($p=0.0012$ ultrasonic bath vs control, Figure 11.1). The length of fibrils was reduced in the ultrasonic bath group, but this difference was not statistically significant (Figure 11.2).

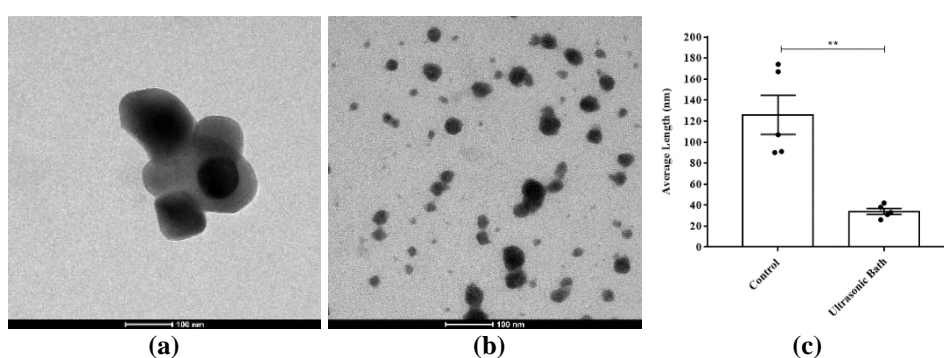


Figure 11.1. Oligomer lengths after ultrasonic bath sonication. (a) Control, (b) ultrasonic bath. (c) Data are expressed as mean ± standard error. Student’s t test was applied (** $p=0.0012$ ultrasonic bath vs control). Scale bar: 100 nm.

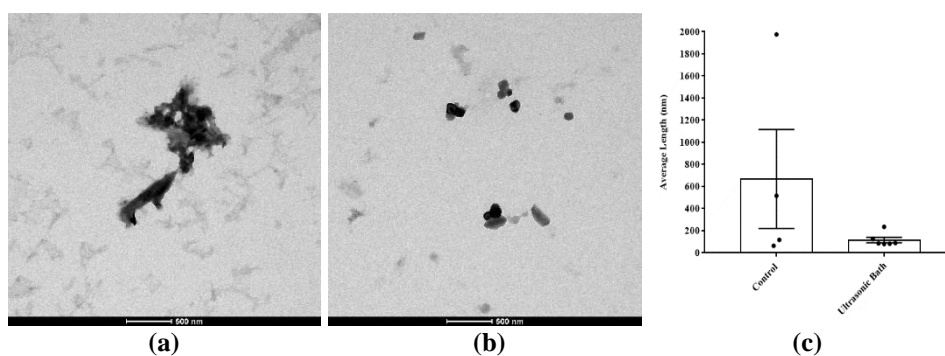


Figure 11.2. Fibril lengths after ultrasonic bath sonication. (a) Control, (b) ultrasonic bath. (c) Data are expressed as mean \pm standard error. Student's t test was applied. Scale bar: 500 nm.

4. DISCUSSION

The α -syn-PFFs model provides the opportunity to elucidate the role of α -syn in PD pathogenesis and investigate therapeutic approaches. In order to investigate the pathology of α -syn, long fibrils were broken by sonication into short fibrils with an average length of 50-100 nm [26,28,34,35]. It has been demonstrated that the presence of fibrils ranging in length from 50-100 nm has a crucial role in the development of pathology following the uptake of α -syn into the cell [25, 36]. In fact, fibrils smaller than 50 nm resulted in more protein aggregation in both cultured cells and mouse brains [28].

Sonication protocols vary based on the type of sonicator (probe or bath sonicator), and the ambient temperature, pulse duration, and number of repetitions in probe sonication. Following sonication of fibrils, it is induced misfolding and aggregate formation of endogenous α -syn. However, ensuring the formation and reproducibility of α -syn pathology is a challenging process because of variations in the sonication protocol [26, 28]. Consequently, standard sonication protocols are required to break fibrils to the appropriate size and, hence, form pathology [24, 25].

Our study examined the effect of pulse durations at three different temperatures on fibrils breaking and found that shorter oligomers were obtained by increasing the pulse duration at room temperature after probe sonication. At room temperature, the oligomers were shorter than 50 nm when only a 5 sec on/5 sec off pulse was applied. The reduction in ambient temperature was found to decrease the oligomer size in pulse applications of 1 sec on/1 sec off (in ice surrounded by dry ice) and 3 sec on/3 sec off (in ice), whereas it increased the size in pulse application of 5 sec on/5 sec off. These results indicate that in order to break the fibrils, the ambient temperature should be reduced in accordance with the decreasing frequency of the pulse. Further, an increase in oligomer length was observed in ice surrounded by dry ice after a 3 sec on/3 sec off pulse, suggesting that monomers released during sonication may re-oligomerize even at sufficiently low temperatures [37]. At all temperature, however, the oligomers of 50 nm or shorter length were obtained by sonicating for a 5 sec on/5 sec off pulse. According to these results, fibrils were more effectively broken by consecutive pulse applications.

Besides probe sonication, ultrasonic bath sonication is also used as a sonication method [25,29,31]. In our study, the oligomers were 50 nm and shorter after ultrasonic bath sonication, consistent with prior study [31]. In ultrasonic bath sonication, fibrils do not aerosolize, thereby preventing fibril volume loss. In addition, the stopper used in our study reduced fibril volume loss during probe sonication. Using a stopper is an addition that contributes to the method in our study.

Although the fibril lengths were reduced following sonication with both the probe and ultrasonic bath, some fibrils were not broken. There may be a need to increase the number of sonication repetitions in order to break all fibrils, as has been observed in previous studies [28,38]. It is also recommended that

a waiting period was allowed between each sonication repetition during probe sonication in order to prevent the sample from overheating and to increase the success of the sonication process [39], as used in our study.

5. CONCLUSION

In conclusion, different sonication methods changed the sizes of the oligomers in our study. The results indicate that different sonication methods may be used to obtain oligomers of 50 nm and shorter lengths. It is also necessary to lower the ambient temperature in accordance with the decreasing pulse frequency. Additionally, there are some fibril structures that cannot be broken regardless of the method. Therefore, in future studies, the method should be improved by an increase in the number of sonication repetitions. In this way, identifying optimized/standard sonication protocols will contribute to the formation of α -syn pathology by using α -syn-PFFs model in PD studies.

ACKNOWLEDGEMENT

We would like to thank Assoc. Prof. Urartu Özgür Şafak ŞEKER, for providing the opportunity to work at Bilkent University, National Nanotechnology Research Center (UNAM), Şeker Lab, to carry out the sonication experiments, and PhD student Cemile Elif ÖZÇELİK for her help in the laboratory.

CONFLICT OF INTEREST

The authors stated that there are no conflicts of interest regarding the publication of this article.

CRedit AUTHOR STATEMENT

Hilal Akyel: Conceptualization, investigation, formal analysis, visualization, writing – original draft. **Elham Bahador Zırh:** Conceptualization, investigation, resources, visualization, writing – review & editing. **Selim Zırh:** Conceptualization, investigation, visualization, writing – review & editing. **Banu Cahide Tel:** Conceptualization, resources, writing – review & editing, supervision.

REFERENCES

- [1] Poewe W, Seppi K, Tanner CM, Halliday GM, Brundin P, Volkman J, Schrag AE, Lang, AE. Parkinson disease. *Nat Rev Dis Primers* 2017; 3: 1–21.
- [2] Kalia LV, Lang AE. Parkinson's disease. *The Lancet* 2015; 386(9996): 896–912.
- [3] Spillantini MG, Schmidt ML, Lee VMY, Trojanowski JQ, Jakes R, Goedert M. α -Synuclein in Lewy bodies. *Nature* 1997; 388: 839–840.
- [4] Lashuel HA, Overk CR, Oueslati A, Masliah E. The many faces of α -synuclein: From structure and toxicity to therapeutic target. *Nat Rev Neurosci* 2013; 14(1): 38–48.
- [5] Sulzer D, Edwards. RH. The Physiological Role of α -Synuclein and Its Relationship to Parkinson's Disease. *J Neurochem* 2019; 150(5): 475–486.
- [6] Bartels T, Choi JG, Selkoe DJ. α -Synuclein occurs physiologically as a helically folded tetramer that resists aggregation. *Nature* 2011; 477(7362): 107–111.
- [7] Burré J, Sharma M, Südhof TC. α -Synuclein assembles into higher-order multimers upon membrane binding to promote SNARE complex formation. *PNAS* 2014; 111(40): 4274–4283.

- [8] Rocha EM, De Miranda B, Sanders LH. Alpha-synuclein: Pathology, mitochondrial dysfunction and neuroinflammation in Parkinson's disease. *Neurobiology of Disease* 2018; 109: 249–257.
- [9] Goedert M, Jakes R, Spillantini MG. The Synucleinopathies: Twenty Years on. *J Parkinsons Dis* 2017; 7: 53–71.
- [10] Miraglia F, Ricci A, Rota L, Colla E. Subcellular localization of alpha-synuclein aggregates and their interaction with membranes. *Neural Regen Res* 2018; 13(7): 1136–1144.
- [11] Tuttle MD, Comellas G, Nieuwkoop AJ, Covell DJ, Berthold DA, Kloepper KD, Courtney JM, Kim JK, Barclay AM, Kendall A, et al. Solid-state NMR structure of a pathogenic fibril of full-length human α -synuclein. *Nat Struc Mol Biol* 2016; 23(5): 405–417.
- [12] Brás IC, Outeiro TF. Alpha-synuclein: Mechanisms of release and pathology progression in synucleinopathies. *Cells* 2021; 10(2): 1–19.
- [13] Mao X, Ou MT, Karuppagounder SS, Kam TI, Yin X, Xiong Y, Ge P, Umanah GE, Brahmachari S, Shin JH, et al. Pathological α -synuclein transmission initiated by binding lymphocyte-activation gene 3. *Science* 2016; 353(6307).
- [14] Masaracchia C, Hnida M, Gerhardt E, Lopes da Fonseca T, Villar-Pique A, Branco T, Stahlberg MA, Dean C, Fernández CO, Milosevic I, et al. Membrane binding, internalization, and sorting of alpha-synuclein in the cell. *Acta Neuropathol Commun* 2018; 6(1): 79.
- [15] Luk KC, Song C, O'Brien P, Stieber A, Branch JR, Brunden KR, Trojanowski JQ, Lee VMY. Exogenous α -synuclein fibrils seed the formation of Lewy body-like intracellular inclusions in cultured cells. *PNAS* 2009; 106(47): 20051–20056.
- [16] Luk KC, Kehm VM, Zhang B, O'Brien P, Trojanowski JQ, Lee VMY. Intracerebral inoculation of pathological α -synuclein initiates a rapidly progressive neurodegenerative α -synucleinopathy in mice. *J Exp Med* 2012; 209(5): 975–988.
- [17] Volpicelli-Daley LA, Luk KC, Patel TP, Tanik SA, Dawn M, Stieber A, Meany DF, Trojanowski JQ, Lee VM. Exogenous α -Synuclein fibrils induce Lewy body pathology leading to synaptic dysfunction and neuron death. *Neuron* 2011; 72(1): 57–71.
- [18] Volpicelli-Daley LA, Luk KC, Lee VMY. Addition of exogenous α -synuclein preformed fibrils to primary neuronal cultures to seed recruitment of endogenous α -synuclein to Lewy body and Lewy neurite-like aggregates. *Nat Protoc* 2014; 9(9): 2135–2146.
- [19] Thakur P, Breger LS, Lundblad M, Wan OW, Mattsson B, Luk KC, Lee VMY, Trojanowski JQ, Björklund A. Modeling Parkinson's disease pathology by combination of fibril seeds and α -synuclein overexpression in the rat brain. *PNAS* 2017; 114(39): 8284–8293.
- [20] Gegg ME, Verona G, Schapira AHV. Glucocerebrosidase deficiency promotes release of α -synuclein fibrils from cultured neurons. *Hum Mol Genet* 2020; 29(10): 1716–1728.
- [21] Ueda J, Uemura N, Sawamura M, Taguchi T, Ikuno M, Kaji S, Taruno Y, Matsuzawa S, Yamakado H, Takahashi R. Perampanel Inhibits α -Synuclein Transmission in Parkinson's Disease Models. *Mov Disord* 2021; 36(7): 1554–1564.

- [22] Carta AR, Boi L, Pisanu A, Palmas MF, Carboni E, De Simone A. Advances in modelling alpha-synuclein-induced Parkinson's diseases in rodents: Virus-based models versus inoculation of exogenous preformed toxic species. *J Neurosci Methods* 2020; 338: 108685.
- [23] Karpowicz RJ, Trojanowski JQ, Lee VMY. Transmission of α -synuclein seeds in neurodegenerative disease: recent developments. *Lab Invest* 2019; 99(7): 971–981.
- [24] Patterson JR, Polinski NK, Duffy MF, Kemp CJ, Luk KC, Volpicelli-Daley LA, Kanaan NM, Sortwell CE. Generation of alpha-synuclein preformed fibrils from monomers and use in vivo. *J Vis Exp* 2019; 2(148): 1–10.
- [25] Polinski NK, Volpicelli-Daley LA, Sortwell CE, Luk KC, Cremades N, Gottler LM, Froula J, Duffy MF, Lee VMY, Martinez TN, et al. Best practices for generating and using alpha-synuclein pre-formed fibrils to model Parkinson's disease in rodents. *J Parkinsons Dis* 2018; 8(2): 303–322.
- [26] Kumar ST, Donzelli S, Chiki A, Syed MMK, Lashuel HA. A simple, versatile and robust centrifugation-based filtration protocol for the isolation and quantification of α -synuclein monomers, oligomers and fibrils: Towards improving experimental reproducibility in α -synuclein research. *J Neurochem* 2020; 153(1): 103–119.
- [27] Pieri L, Chafey P, Le Gall M, Clary G, Melki R, Redeker V. Cellular response of human neuroblastoma cells to α -synuclein fibrils, the main constituent of Lewy bodies. *Biochim Biophys Acta* 2016; 1860(1): 8–19.
- [28] Tarutani A, Suzuki G, Shimozawa A, Nonaka T, Akiyama H, Hisanaga SI, Hasegawa M. The effect of fragmented pathogenic α -synuclein seeds on prion-like propagation. *J Biol Chem* 2016; 291(36): 18675–18688.
- [29] Singh V, Castellana-Cruz M, Cremades N, Volpicelli-Daley LA. Generation and sonication of α -synuclein fibrils. *Protocols.io* 2020; 1–13.
- [30] Ryan T, Bamm V V, Stykel MG, Coackley CL, Humphries KM, Jamieson-Williams R, Ambasudhan R, Mosser DD, Lipton SA, Harauz G, et al. Cardiolipin exposure on the outer mitochondrial membrane modulates α -synuclein. *Nature Communications* 2018; 9(1): 1–17.
- [31] Creed RB, Memon AA, Komaragiri SP, Barodia SK, Goldberg MS. Analysis of hemisphere-dependent effects of unilateral intrastriatal injection of α -synuclein pre-formed fibrils on mitochondrial protein levels, dynamics, and function. *Acta Neuropathol Commun* 2022; 10(1): 1–19.
- [32] Afitska K, Fucikova A, Shvadchak VV, Yushchenko DA. α -Synuclein aggregation at low concentrations. *Biochim Biophys Acta Proteins Proteom* 2019; 1867(7–8): 701–709.
- [33] Kaplan M, Öztürk K, Öztürk SC, Tavukçuoğlu E, Esendağlı G, Calis S. Effects of particle geometry for PLGA-based nanoparticles: preparation and in vitro/in vivo evaluation. *Pharmaceutics* 2023; 15(1): 175.
- [34] Mahul-Mellier AL, Vercautere F, Maco B, Ait-Bouziad N, De Roo M, Muller D, Lashuel HA. Fibril growth and seeding capacity play key roles in α -synuclein-mediated apoptotic cell death. *Cell Death and Differentiation* 2015; 22(12): 2107–2122.
- [35] Mahul-Mellier AL, Burtscher J, Maharjan N, Weerens L, Croisier M, Kuttler F, Leleu M, Knott

- GW, Lashuel HA. The process of Lewy body formation, rather than simply α -synuclein fibrillization, is one of the major drivers of neurodegeneration. *PNAS* 2020; 117(9): 4971–4982.
- [36] Xue WF, Hellewell AL, Gosal WS, Homans SW, Hewitt EW, Radford SE. Fibril fragmentation enhances amyloid cytotoxicity. *J Biol Chem* 2009; 284(49): 34272–34282.
- [37] Shvadchak VV, Claessens MMAE, Subramaniam V. Fibril breaking accelerates α -synuclein fibrillization. *J. Phys. Chem. B* 2015; 119(5): 1912–1918.
- [38] Redmann M, Wani WY, Volpicelli-Daley L, Darley-Usmar V, Zhang J. Trehalose does not improve neuronal survival on exposure to alpha-synuclein pre-formed fibrils. *Redox Biology* 2017; 11: 429–437.
- [39] Abdelmotilib H, Maltbie T, Delic V, Liu Z, Hu X, Fraser KB, Moehle MS, Stoyka L, Anabtawi N, Krendelchtchikova V, Volpicelli-Daley LA, West A. Alpha-synuclein fibril-induced inclusion spread in rats and mice correlates with dopaminergic neurodegeneration. *Neurobiol Dis* 2017; 105: 84-98.



RESEARCH ARTICLE

ALLEVIATING SALT STRESS IN TOMATO PLANTS THROUGH HYDROGEN PEROXIDE PRIMING: DIFFERENTIATIONS OF ANTIOXIDANT ENZYME ACTIVITIES AND GENE EXPRESSION PATTERNS

Musa KAR^{1,*}, Gökhan GÖKPINAR², Özlem DOĞAN³

¹ Department of Molecular Biology and Genetics, Science & Art Faculty, Nevşehir Hacı Bektas Veli University, 50300 Nevşehir, Turkey

musa.kar@nevsehir.edu.tr - [0000-0001-7983-4814](https://orcid.org/0000-0001-7983-4814)

² Department of Molecular Biology and Genetics, Science Institute, Nevşehir Hacı Bektas Veli University, 50300 Nevşehir, Turkey

gokhan.gokpinar@gmail.com - [0000-0002-3079-1486](https://orcid.org/0000-0002-3079-1486)

³ Department of Molecular Biology and Genetics, Science Institute, Nevşehir Hacı Bektas Veli University, 50300 Nevşehir, Turkey

ozlmdgn4@gmail.com - [0000-0002-8606-6216](https://orcid.org/0000-0002-8606-6216)

Abstract

Plants, being sessile organisms, rely on their antioxidant systems to respond to the stress factors induced by both abiotic and biotic stresses in their environment. Among abiotic stress factors, salinity and alkalinity pose the most significant challenges to plant growth. To counteract these stresses, plants activate various signalling pathways to enhance their stress tolerance. While a wide range of pesticides, including insecticides and herbicides, are employed to protect agricultural crops from biotic agents, there exists no established practice for fortifying their defence mechanisms against abiotic stresses. This study delves into the effect of H₂O₂ pre-treatment on mitigating salt stress in tomato seedlings. Four experimental groups were established: control, H₂O₂, Salt, and Salt+H₂O₂. The study evaluated changes in chlorophyll content, malondialdehyde (MDA) accumulation, superoxide dismutase (SOD), catalase (CAT), and ascorbate peroxidase (APX) enzyme activities and expressions. The results revealed that priming treatment led to increased chlorophyll levels and reduced MDA accumulation compared to the group only exposed to salt stress. Additionally, the activation of stress-related enzymes was significantly higher in the priming group compared to the group only exposed to salt stress. Expression levels exhibited a statistically significant increase compared to the control group; however, CAT and APX expression levels were found to be lower than those in the the group only exposed to salt stress. These findings suggest that H₂O₂ priming can enhance plant stress tolerance. Priming can serve as a highly effective tool to alleviate stress in plants; however, the type, concentration, and exposure time of the priming agent are crucial factors in regulating the priming effect.

Keywords

Abiotic Stress,
Hydrogen Peroxide Priming,
Antioxidant Enzymes, Stress
Tolerance,
Chlorophyll Content

Time Scale of Article

Received :28 November 2023
Accepted : 26 February 2024
Online date :30 July 2024

1. INTRODUCTION

Within the realm of agricultural production, the arsenal of preventative and lethal chemical agents employed for combating biotic stressors has achieved an advanced stage of development. Nevertheless, recent years have borne witness to an escalated research focus on enhancing plant resilience to abiotic stressors, encompassing conditions such as drought, heat, cold, and salinity [1, 2]. In this context, the

*Corresponding Author: musa.kar@nevsehir.edu.tr

concept of priming has emerged as a more intricate and efficacious modality for fortifying plant response mechanisms vis-à-vis environmental challenges, transcending traditional paradigms. Priming, particularly when executed through the application of diverse compounds during the seed or seedling stages, elicits a controlled and mild stress response within the plant. This subtle stress imprint, when subsequently confronted with both biotic and abiotic adversities, engenders a heightened state of tolerance and adaptability [3]. The ensuing adaptive responses encompass an augmentation of the plant's antioxidant capacity, fine-tuning of enzymatic antioxidant expression levels, regulation of cellular turgor, synthesis of osmoprotectants, and the meticulous control of stomatal dynamics [4, 5]. It is noteworthy that various priming methodologies, including hydropriming, osmopriming, hormone-priming, and redox-priming, engender analogous mechanisms, which are effectively harnessed in combatting an array of distinct stressors encountered by the plant [6].

In sum, the contemporary scientific exploration into priming strategies has unveiled a promising avenue for the augmentation of plant stress resilience, showcasing the potential to revolutionize the agricultural landscape by equipping crops with a heightened capacity to navigate the multifarious challenges posed by abiotic stress conditions.

The uncontrolled drilling of wells for irrigation purposes depletes underground freshwater resources, increases the salt content of irrigation water, and indirectly causes plants to be exposed to excessive salt. In later stages, it causes a loss of productive agricultural land due to excessive soil salinization. In addition, irregularities in rainfall regimes due to global climate change are another important factor affecting soil salinization. Because many economically critical agricultural plants do not have salinity tolerance, plant growth and crop yield are also negatively affected [7].

In the context of plants subjected to various abiotic stressors, encompassing salinity, drought, cold, heat, and heavy metal exposure, a conspicuous escalation in the levels of reactive oxygen species (ROS) becomes a pivotal event, precipitating redox disequilibrium and oxidative stress. The deleterious consequences of elevated ROS concentrations are profound, inducing extensive damage to essential cellular components, including proteins, DNA, and lipids, thereby instigating a cascade of events leading to metabolic dysfunction and, ultimately, the demise of the plant organism [8].

To address these challenges, extensive research has been conducted to elucidate plant responses to abiotic stressors, with a particular focus on alterations in the activities of antioxidant enzymes. Notably, Duman and Öztürk (2010) subjected *Mentha aquatica* to varying concentrations and durations of nickel exposure, observing a pronounced enhancement in the activities of crucial antioxidant enzymes, including SOD, CAT, and APX [9]. Furthermore, Soydam-Aydın and colleagues (2015) conducted experiments involving the imposition of copper and zinc stress on tomato and aubergine plants, revealing a significant upregulation in the expression levels of CAT and APX enzymes, further underscoring the pivotal role of antioxidant enzymes in the plant's response to abiotic stressors [10].

Over the course of several years, reactive oxygen species (ROS) have been traditionally perceived as deleterious byproducts of cellular metabolism. However, contemporary perspectives on these molecular entities have undergone a profound shift, wherein ROS are now recognized as pivotal molecules that facilitate plant adaptation to diverse environmental conditions. Among the ROS, the " H_2O_2 " radical has garnered substantial scientific attention due to its distinctive attributes, including reduced intrinsic toxicity in comparison to other oxygen radicals, facile cellular membrane permeability on account of its molecular dimensions, and an extended half-life of approximately 1 millisecond [11, 12]. The multifaceted roles of H_2O_2 are manifold, spanning participation in protein, carbohydrate, and lipid metabolism, mediation of signal transduction, orchestration of transcriptional regulation for responsive genes, and central involvement in various other metabolic activities, thereby underscoring the complexity of its functional significance [13].

H₂O₂ priming is capable of engendering a controlled oxidative stress response, thereby activating a redox-dependent signalling network. This stress-induced priming effect culminates in the production of latent defensive proteins, including enzymes and transcription factors, which serve to quench reactive oxygen species, consequently catalysing an amplified stress response in the primed plant [14].

Notably, salt stress instigates oxidative bursts within plants, and the application of low concentrations of H₂O₂ as a priming agent has been demonstrated to augment salt tolerance by serving as a signalling molecule capable of governing the expression of stress-responsive genes. Wahid et al. (2007) conducted a study that revealed wheat seedlings derived from seeds subjected to H₂O₂ priming and subsequently exposed to salt stress exhibited significantly lower levels of H₂O₂ production compared to seedlings from non-primed seeds exposed to salt stress [15]. Furthermore, Ashraf and colleagues (2015) investigated the advantageous effects of exogenous H₂O₂ on drought stress tolerance in maize. Maize seedlings were pretreated with varying concentrations of H₂O₂ and subsequently cultivated under drought stress conditions, wherein seeds primed with 140 mM H₂O₂ exhibited heightened germination percentages. Drought-induced alterations included a marked decrease in photosynthetic pigments, accompanied by elevated levels of endogenous H₂O₂, lipid peroxidation, as well as augmented activities of CAT, SOD, and peroxidase (POX), underscoring the role of H₂O₂ in mitigating the consequences of drought stress [16].

The principal aim of the present study is to delineate alterations in total chlorophyll content, MDA accumulation, as well as the activities of antioxidant enzymes SOD, CAT, and APX, alongside the examination of gene expression levels in tomato seedling leaves primed with H₂O₂ and subsequently subjected to salt stress. This inquiry endeavours to elucidate the role of H₂O₂ priming in bolstering abiotic stress tolerance, contributing to our comprehension of the intricate mechanisms underpinning plant resilience in challenging environmental conditions.

2. MATERIALS AND METHODS

2.1. Plant Material and Experimental Conditions

The experimental study was conducted within the growth chamber of the Stress Biology Laboratory at Nevsehir Haci Bektas Veli University, Department of Molecular Biology and Genetics. The controlled environmental conditions encompassed a temperature of 28°C, relative humidity maintained at 58%, and a photoperiod of 16 hours of light followed by 8 hours of darkness (16/8 h).

Tomato seeds underwent sterilization through immersion in a 0.7% sodium hypochlorite solution, followed by germination in a perlite-soil mixture. Germinated seedlings were subsequently transplanted into a hydroponic medium comprised of Hoagland's solution and were continuously aerated to ensure optimal growth conditions.

After eight days in hydroponic medium, seedlings were subjected to two distinct treatments: either distilled water (control) or a 10 mM H₂O₂ solution containing 0.025% Tween 20 detergent (to reduce surface tension and facilitate penetration). Application was administered via foliar spraying, with each plant receiving 15 ml of either H₂O₂ or distilled water. The initial treatment was conducted at 6:30 a.m, followed by a second application after 24 hours. Subsequently, after 48 hours from the initial spraying, the seedlings were subjected to salt stress, administered as an 80 mM NaCl treatment. To mitigate the risk of osmotic shock, the salt concentration was incrementally increased by 40 mM per day.

The experimental treatments were categorized as follows: Distilled water spray without salt stress (water/control), H₂O₂ solution spray without salt stress (H₂O₂/control), Distilled water spray under salt stress (water/salt-stressed) H₂O₂ solution spraying with salt stress (H₂O₂/salt-stressed).

To evaluate the effects of these treatments, samples were systematically collected at three distinct time points: 24 hours, 72 hours, and 120 hours following the induction of saline stress. Collected samples were promptly stored in a refrigeration unit at -80°C to preserve their integrity until further analysis. All measurements and analyses were performed with a minimum of three biological replicates to ensure robust statistical assessment.

2.2. Determination of Total Chlorophyll and Lipid Peroxidation

Plant samples (0.1 g) were crushed in 100 ml of 80% acetone. The filtrate was passed through filter paper and the total chlorotic content was calculated according to Witham et al. [17].
 $\text{mg chl.a/g tissue} = [12.7 (D630) - 2.69 (D450)] \cdot (V/1000.A)$

MDA was measured using thiobarbituric acid reactive substances (TBARS), according to the method described by Heath and Packer [18]. The concentrations of lipid peroxides were calculated using an extinction coefficient of $155 \text{ mM}^{-1} \text{ cm}^{-1}$ and were expressed as $\text{nmol TBARS g}^{-1} \text{ protein}$.

2.3. Measurements Antioxidant Enzyme Activities

Enzyme activities were measured according to Chen and Zhang [19].

2.4. Crude Protein/Enzyme Extract

0.5 g of tomato seedling leaves were pulverized with liquid nitrogen in a mortar and pestle. Then 100 mM 6 ml PBS buffer was added and homogenised. The homogenate was distributed into four different 1.5 ml centrifuge tubes and centrifuged at 10000 g for 20 min at +4°C.

The protein concentration of the resulting solution is determined by the Warburg-Christian formula: $(\text{protein}) (\text{mg/ml}) = 1.55 \times A_{280} - 0.76 \times A_{260}$. For the reliability of further studies, this value should be below 2. In case of excess, dilution with PBS buffer will be performed. The supernatant is taken and stored in a -80 °C degree freezer for further analysis.

2.5. Determination of Superoxide Dismutase (SOD) Activity

A reaction solution containing 100 mM PBS (pH 7.8), 1 mM EDTA-2Na, 130 mM Methionine, 750 μM NBT, and 20 μM Riboflovin was prepared. Then 50 μl of crude protein extract was added to each 1 ml of reaction solution. In addition, 2 control tubes with PBS instead of 50 μl of crude enzyme solution are prepared. The samples are to be analysed and one of the control tubes is exposed to 4000 lux light for 10-15 minutes. The other control tube is kept in the dark without exposure to light. At 560 nm, the tube kept in the dark is taken as a reference.

$\text{SOD total activity (unit: u/mg protein)} = [(A_{\text{ck}} - A_{\text{s}}) \times V] / (0.5 \times A_{\text{ck}} \times V_{\text{t}}) / C_{\text{p}}$

A_{ck} absorbance of the control tube kept in the light, as absorbance of the tube with sample, V : total volume of crude protein, V_{t} . Volume of crude protein used in the test tube, C_{p} : concentration of crude protein extraction (mg/ml)

2.6. Determination of Catalase (CAT) Activity

Add 77.5 μl of 30% H_2O_2 into 50 ml of 10 mM PBS buffer to obtain the reaction solution. Then 50 μl of crude protein extract was added to the cuvette and 1 ml of reaction solution was added. Measurements at 240 nm are taken every 15 seconds. Instead of the enzyme extract, 50 μl of 100 ml PBS buffer is used as a reference reading.

CAT activity (unit: u/mg protein) = $\Delta A_{240} \times (V/Vt) / (0.1 \times t) / Cp$

ΔA_{240} : absorbance change at 240 nm every 15 s, V: total crude protein extraction volume, Vt: volume of crude enzyme used in the test tube, t: reaction time (min), Cp: crude protein concentration (mg/ml).

2.7. Determination of Ascorbate Peroxidase Activity

A reaction mixture containing 50 mM potassium phosphate buffer (pH 7), 0.5 mM ascorbate, 0.5 mM H₂O₂, and 10 μ l of crude protein was prepared in a cold medium. The prepared mixture was read at 290 nm wavelength for 3 minutes using a quartz quartet. The extinction coefficient of 2.8 mM⁻¹ cm⁻¹ for reduced ascorbate will be used to calculate the enzyme activity.

2.8. RNA Isolation cDNA Synthesis and qRt-PCR Analysis

Transgenbiotech EasyPure® plant RNA kit was used for RNA isolation from leaves. The amounts of RNA obtained from all samples were determined by nanodrop. Then, the total RNA amount of the samples to be used in cDNA synthesis was adjusted to 40 ng. EasyScript First strand cDNA synthesis kit was used to synthesize cDNA. Bioneer AccuPower® RT-PCR PreMix was used for real-time reactions. The DNA fragment was amplified for 35 cycles using the following thermal conditions: denaturing the DNA template at 94 °C for 30 s, primer annealing at 5 °C below primer T_m for 15 s, and DNA synthesis at 72 °C for 1 min. The primer sequence was taken from SolGenomik Network. The primer list is given in Table 1. The data obtained from Real-Time PCR were analysed using the 2^{- $\Delta\Delta C_T$} method [20]

Table 1. Primer pairs used in real-time PCR

Name	Accession Number	Forward	Reverse
Actin7	Solyc03g078400	GGGATGGAGAAGTTTGGTGGTGG	CTTCGACCAAGGGATGGTGTAGC
Cu/Zn-SOD	Solyc11g066390	TCACCACAACCAGCACTACCA	AGTGACAACCCCTCAACATTAG
CAT1	Solyc12g094620	CGCATAACGACACCCCTTTC	CGGAGAAAATCAGCACAAGTAAG
APX	Solyc06g005160	TCTGAATTGGGATTTGCTGA	CGTCTAACGTAGCTGCCAAA

2.9. Statistical Analysis

One-way ANOVA and post hoc Tukey tests were performed to determine the differences between the groups and the significance level of the difference (p<0.05). All calculations were performed with the SPSS 22.0 software package.

3. RESULTS

In this study, tomato plants were divided into four different groups: control (C), H₂O₂ (H), salt (S), and H₂O₂+salt (HS), and collected at various sampling times. The changes in total chlorophyll content, lipid peroxidation, SOD, CAT, APX enzyme activity, and gene expression levels in plant leaves were studied. When the change in total chlorophyll content was analysed, it was found that there was no significant difference between the C and H groups. However, there was a significant difference between the S and HS groups. The amount of chlorophyll in the HS group was higher than that in the S group was (Figure 1. A).

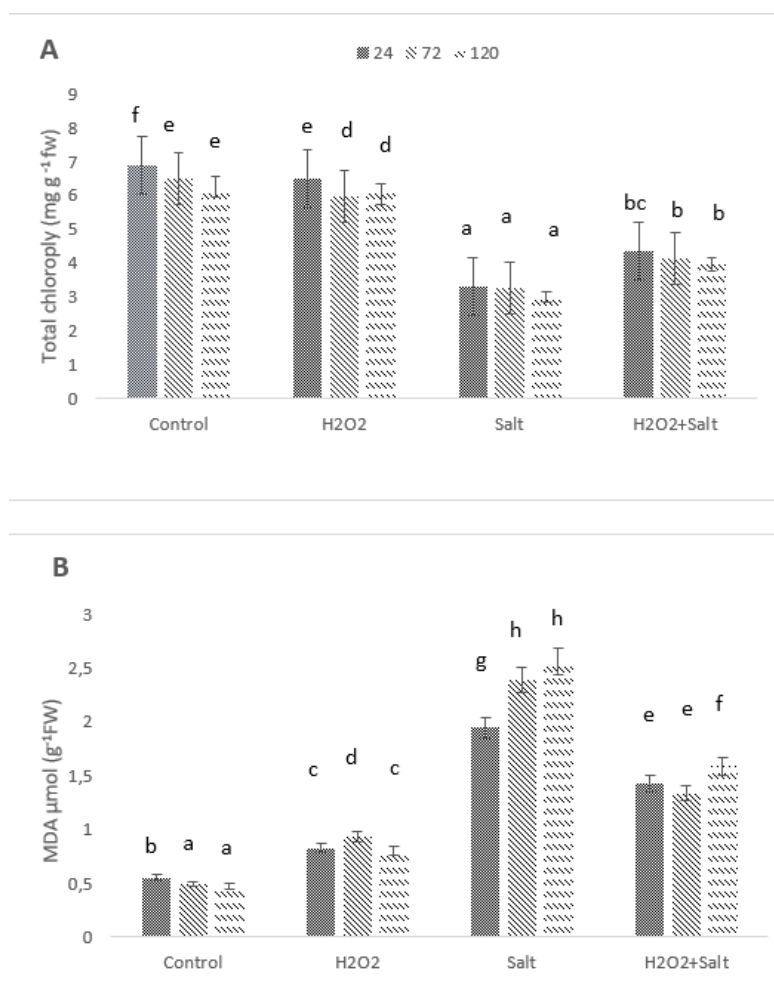


Figure 1. Effect of H₂O₂ pretreatment on total chlorophyll and MDA concentrations in tomato seedlings exposed to salt stress for different periods. (A) Total chlorophyll and (B) MDA levels. Bars indicate a standard error; different letters indicate statistical difference (p<0.05)

The first target of stress-induced reactive oxygen species is lipid peroxidation of the cell membrane. MDA produced as a result of peroxidation provides an idea of the stress status of the plant. In this study, the H group was statistically different from the C group, and the highest MDA accumulation occurred in the S group at 72 and 120 h. In addition, MDA accumulation in all HS groups was lower than that in the S group (Figure 1 B).

When antioxidant enzyme activities were examined, upward changes occurred in enzyme activities depending on the application time and group, compared to the control. SOD enzyme activity reached the highest value at 72 h and 120 h of H₂O₂+ salt treatment. Compared to the control, a statistically significant increase was observed in all treatment groups (Figure 2 A).

The highest CAT activity was detected after 120 h of salt stress. CAT activity was found to be significantly higher than the control group in the H₂O₂+Salt treated groups at different time points, but lower than that in the salt-only treated group (p<0.05) (Figure 2 B).

When APX enzyme activity was analysed, the highest activity was detected after 120 and 72 h of H₂O₂+ salt treatment. Although the activity was higher than that of the control at the concentration where only salt was applied, it was lower than that of the H₂O₂+salt treatment (Figure 2. C).

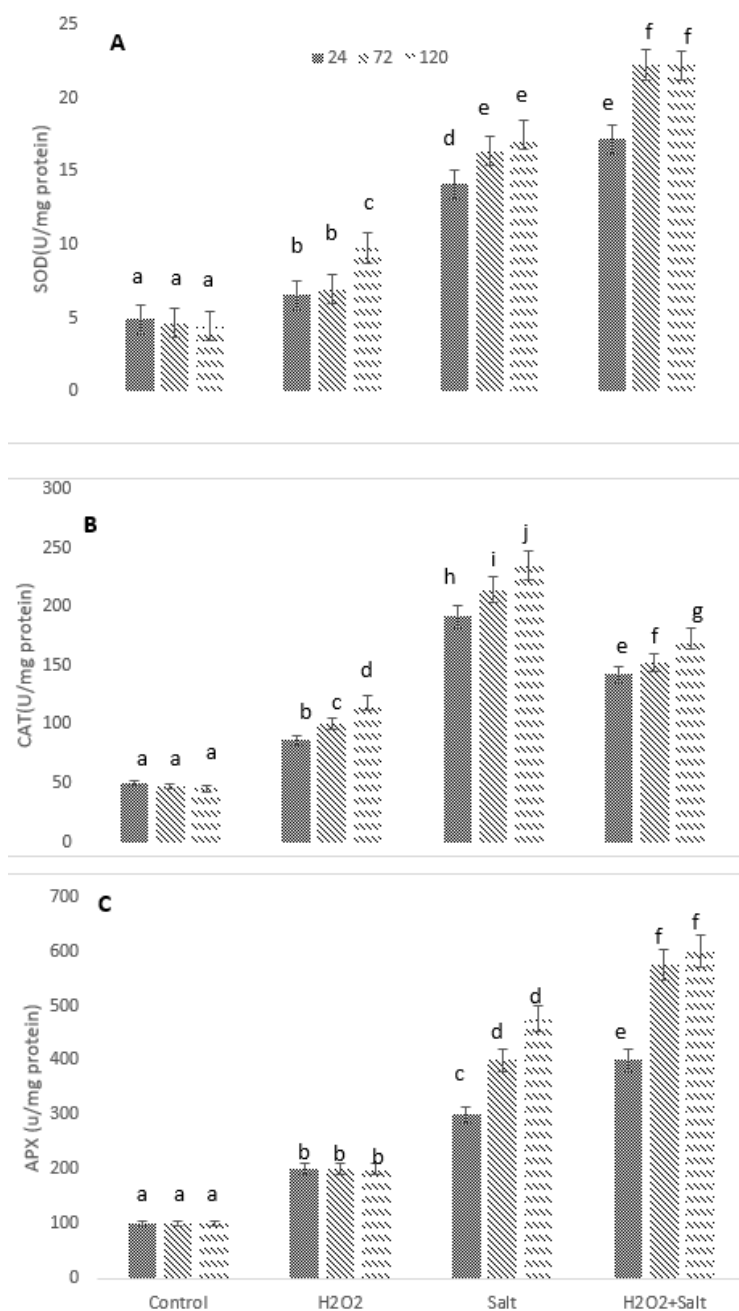


Figure 2. Effect of H₂O₂ pretreatment on antioxidant enzyme activities in tomato seedlings exposed to salt stress for different periods. A. SOD, B. CAT, and C. APX. Bars indicate a standard error; different letters indicate statistical difference (p<0.05).

Changes in antioxidant gene expression were evaluated according to the expression of the actin7 gene used as a housekeeping gene.

When SOD expression was analysed, the highest expression level was found at 72 h and 120 h H₂O₂+salt concentrations, which were 4 fold higher than that of the control group. In addition, it was determined that the expression level was statistically different from that of the control group under other application conditions (Figure 3A).

There was a statistically significant increase in CAT gene expression in the group treated with H₂O₂ alone compared to the control. The highest CAT expression was detected after 120 h of salt application, which was 3 fold higher than that in the control. Expression levels in the H₂O₂+salt application group were higher than those in the control and H₂O₂ groups but lower than those in the salt-only group (p<0.05) (Figure 3-B).

When APX gene expression was analysed, similar to CAT, the highest expression levels were observed only in the salt treatment group, whereas the expression level in the H₂O₂+salt treatment group was statistically lower than that in the salt treatment group and higher than that in the control group (P<0.05) (Figure 3-C).

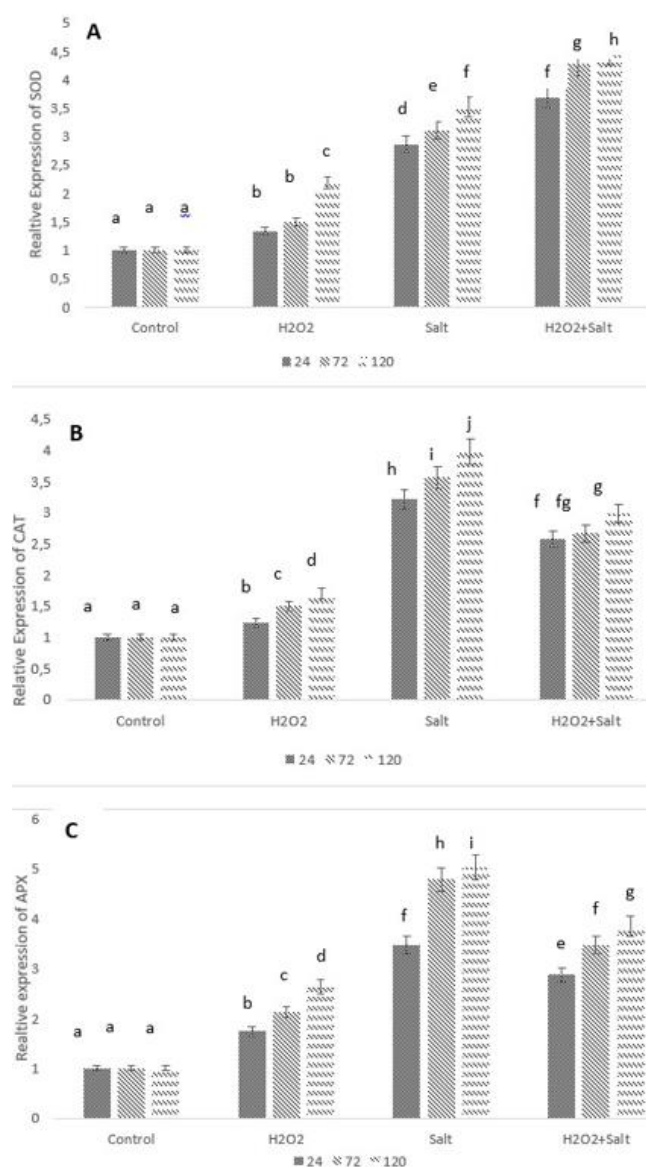


Figure 3. Effect of H₂O₂ pre-treatments on antioxidant enzyme expression in tomato seedlings exposed to salt stress for different periods. A. SOD, B. CAT, and C. APX. Bars indicate a standard error; different letters indicate statistical difference (p<0.05)

4. DISCUSSION

Salinity represents a significant environmental factor that poses challenges for plants. The strategies developed to mitigate the effects of salinity stress are pivotal for enhancing plant tolerance and crop productivity. In the current study, tomato seedlings were subjected to a pre-treatment with H₂O₂ prior to exposure to salt stress, revealing the establishment of a more effective defence mechanism against this form of stress.

The quantification of changes in chlorophyll concentration is recognized as a reliable indicator for evaluating stress tolerance in plants. In this investigation, the concentration of chlorophyll observed in the HS treatment group exceeded that in the salt treatment group. Salt stress, by its nature, leads to chlorophyll damage due to increased sodium content, consistent with findings from other studies [21]. Notably, similar studies on various plant species have also reported a significant reduction in chlorophyll content under salt stress, aligning with the observations in the current study [22, 23]. In related research, Yao et al. explored the exogenous application of H₂O₂ to mitigate salt stress in buckwheat seedlings and noted that 5 mM H₂O₂ pre-treatments resulted in higher total chlorophyll content than the stress group, with no significant difference between the 10 mM H₂O₂ pre-treatments and the stress group. In accordance with Yao et al. in this study we figure out that; the HS stress group exhibited higher chlorophyll content, with the specific H₂O₂ concentration critical for improvement depending on plant species and concentration. In this study, a significant improvement in chlorophyll levels was observed with 10 mM H₂O₂ [24]. Furthermore, Asgher et al. investigated the effects of H₂O₂ pre-treatments in response to arsenic stress in rice and found that chlorophyll content decreased by 14.8% upon arsenic exposure compared to the control. Notably, H₂O₂ treatment resulted in a 29.6% increase in total chlorophyll content compared to that in the control group, aligning with findings similar to the current study [25]. These findings underscore the potential of H₂O₂ pre-treatment as an effective strategy to enhance stress tolerance in plants, particularly in the context of salinity stress, and emphasize the importance of species-specific responses and optimal H₂O₂ concentrations in achieving these benefits.

Reactive oxygen species (ROS) serve as initiators of stress responses in plant cells, where their first interaction occurs with the cell membrane, causing lipid peroxidation. MDA, a product of lipid peroxidation, is a primary indicator of stress in plants. In this study, a notable increase in MDA concentration in leaves was observed solely in response to salt exposure. Intriguingly, a decrease in MDA concentration was detected in the HS stress group, suggesting that the addition of H₂O₂ induces a protective mechanism against oxidative damage, aligning with findings from Bagheri et al. (2019).

Priming treatments using various organic and inorganic compounds have proven effective in reducing MDA concentration in response to stress. For instance, Jiang et al. found that the exogenous application of salicylic acid reduced MDA levels in response to arsenic stress in rice plants [26]. Similarly, certain plant extracts, such as Cupressus, have been employed as priming agents to enhance stress tolerance, leading to decreased MDA concentrations compared to stress-only treatments [27]. Consistent with these studies, our findings demonstrated a decrease in MDA levels in the pre-treated group, further emphasizing the efficacy of priming in mitigating oxidative damage.

Moreover, studies like that of Silva et al. (2021) have indicated that H₂O₂ pretreatment can lead to a reduction in MDA levels in plants exposed to salt stress, suggesting that H₂O₂ may prevent MDA accumulation by activating the antioxidant system early through its signalling effect. These results coincide with this study, which found that exogenous H₂O₂ application reduced lipid peroxidation and preserved leaf chloroplast structure, as evidenced by both changes in chlorophyll content and MDA accumulation [28]

Priming, especially during the early stages of seed or seedling development, has garnered significant interest for enhancing plant tolerance to abiotic stresses. [27, 29].

Among the array of priming agents, H₂O₂ stands out as a particularly intriguing choice due to its dual nature [30]. Despite its classification as a potentially toxic molecule, H₂O₂ has gained recognition in recent years as a key signalling molecule in oxidative stress responses due to its high permeability and relatively long half-life in cellular membranes [31]. SOD activity is vital in determining a plant's response to stress, as it represents the front line of defence against oxidative stress. This study demonstrated an increase in SOD activity in the H₂O₂-treated salt stress group compared to the control group, with the highest activity observed in the group subjected to combined H₂O₂ and salt application. Similar findings were reported by Gomez et al, who noted an increase in SOD enzyme activity under salinity stress [32]. In another study, the effects of H₂O₂ priming against temperature stress were explored, revealing that SOD activity increased independently of the stress factor. This suggests that H₂O₂ pre-treatments can mitigate lipid peroxidation by modulating the relative levels of superoxide radicals (O₂⁻) and H₂O₂ via SOD under stress conditions [33]. These results are in line with the current study, which also suggests that H₂O₂ priming can enhance SOD activity and reduce lipid peroxidation.

Additionally, Asgher et al. reported that SOD and APX activity increased primarily in the H₂O₂ treatment group, with the highest increase occurring when H₂O₂ and arsenic were applied together, underscoring the potential of H₂O₂ application at low concentrations to enhance plant tolerance to subsequent arsenic stress [25].

In plant cells exposed to abiotic stress, the glutathione-ascorbate cycle plays a crucial role in detoxifying H₂O₂, primarily by converting it to H₂O through APX isoenzymes. APX is pivotal in plant tolerance to salinity and alkaline stress, as well as in inhibiting reactive oxygen species (ROS). The regulation of H₂O₂ detoxification through ascorbic acid (AsA) homeostasis in different cellular components contributes to intercellular ROS regulation. Notably, H₂O₂ priming can act as a signalling molecule, triggering the up-regulation of antioxidant defence systems in plants, including the activation of enzymes like APX, responsible for H₂O₂ detoxification [34]. Consistent with this study, that APX activity was higher in the priming group than in other groups.

CAT and APX activities play a crucial role in mitigating the detrimental effects of H₂O₂ to counteract metabolic damage. Elevated CAT activity is closely associated with an enhanced ability to withstand salinity stress, as it facilitates the detoxification of H₂O₂. Notably, Afrin et al. conducted a study in which they explored the impact of H₂O₂ priming on rice plants subjected to freezing stress, reporting a notable increase in CAT activity following the application of H₂O₂ [35]. In this study, the highest levels of CAT activity were detected in the group exposed to salt-induced stress. It is important to acknowledge that variations in CAT activity are contingent upon a myriad of factors, including the developmental stage of the plant, its metabolic status, as well as the duration and intensity of the stress. Furthermore, the work by Yao et al. is relevant, where they noted that the application of 5 nmol of H₂O₂ combined with salt during priming resulted in the highest CAT activity, while 10 nmol of H₂O₂ applied with salt led to a decrease in activity, aligning it with the levels observed in the group subjected to salt stress alone [24]. These dynamics in enzyme activities observed in our study may indeed be correlated with the findings of Yao and colleagues.

Antioxidant enzyme activation and expression represent distinct aspects of the antioxidant defence system in plants. Enzyme activation pertains to the conversion of an enzyme from an inactive form to its active state, while enzyme expression levels refer to the amount of mRNA or protein produced by a gene encoding an antioxidant enzyme. Both aspects are vital for maintaining ROS balance in plant cells and enhancing plant tolerance to abiotic stress conditions, and post-transcriptional processing can contribute to the divergence between enzyme activation and expression [24]. The variations in activity observed in our study may be attributed to factors like the specific concentration of H₂O₂ applied for priming and the salt concentration and duration.

This study focused on the multifaceted role of H₂O₂ in inducing stress-related genes and stress responses in plants. Studies like the one by Yao et al. have shown that exogenous application of H₂O₂ can significantly increase the expression of stress-related genes and related enzyme genes, with these changes in gene expression paralleling other physiological and biochemical alterations [24]. Moreover, numerous research findings have indicated that priming applications can indeed enhance the expression of stress-related genes [36, 37].

However, it's interesting to note that, while stress-related gene expression levels increased as a result of priming compared to the control group, this increase did not necessarily follow the same pattern as the activation of antioxidant enzymes. Specifically, when examining CAT activity and CAT and APX expression levels, the expression levels did not reach the highest levels of activity and expression, contrasting with what's commonly reported in the literature.

It's important to recognize that the effectiveness and outcomes of priming treatments can vary depending on a multitude of factors, including the specific concentration of H₂O₂ applied, the type of stress (in this case, salt concentration and exposure duration), and the timing of the applications. The discrepancies between our study and some of the literature may indeed be attributed to these variations.

Although an increase in the expression level was detected in our study compared to the control group, it did not show a pattern such as enzyme activation. When CAT activity and CAT and APX expression levels were considered, the expression levels did not reach the highest levels of activity and expression, unlike in the literature. Si et al. examined the effect of H₂O₂ pre-treatment on freezing tolerance caused by mechanical injury and found that there was no significant effect, unlike other studies on freezing stress. This situation was associated with the temperature in the experimental setup that they set up for the cold stress. [38] Similarly, the reason why our study differs from the literature may be the amount of H₂O₂ applied for priming and the salt concentration and durations.

Antioxidant enzyme activation and expression are two different aspects of the antioxidant defense system in plants. Antioxidant enzyme activation refers to the process of converting the inactive form of an enzyme into its active form, whereas antioxidant enzyme expression levels refer to the amount of mRNA or protein produced by a gene encoding an antioxidant enzyme. Both are important for maintaining the balance of ROS in plant cells and enhancing the tolerance of plants to abiotic stress conditions. This may be because of post-transcriptional processing after expression [39, 40].

5. CONCLUSIONS

In conclusion, this comprehensive study provides valuable insights into the potential of H₂O₂ priming as a powerful tool for enhancing stress tolerance in tomato seedlings, offering a promising avenue for addressing the challenges posed by abiotic stressors, particularly salinity.

The evaluation of chlorophyll content revealed that H₂O₂ priming, particularly at a 10 mM concentration, significantly improved stress tolerance. This enhancement may result from the ability of H₂O₂ to activate a protective mechanism against oxidative stress, as evidenced by the decreased accumulation of MDA, a marker of oxidative damage, in the H₂O₂+salt group. Antioxidant enzyme activities, including SOD, CAT, and APX, exhibited dynamic responses to the treatments. SOD activity peaked at 72 and 120 hours in the H₂O₂+salt group, while CAT activity was highest in the salt-stressed group. APX activity was significantly enhanced in the H₂O₂+salt treatment. These findings underscore the role of H₂O₂ priming in regulating antioxidant enzyme activities for enhanced stress tolerance. Moreover, gene expression analyses illuminated the complex interplay between H₂O₂ priming and stress responses. Stress-related gene expression levels increased due to priming, although not always in tandem with enzyme activities, highlighting the intricate nature of plant stress responses. This study emphasizes the multifaceted dynamics of plant adaptation to environmental stressors, influenced by factors such as

priming agent concentration, type, and timing, as well as the specific stress conditions. These findings open up new possibilities for advancing agricultural strategies to bolster crop resilience against abiotic stresses. In the face of increasing environmental challenges, our research underscores the importance of developing innovative approaches to enhance plant stress tolerance, offering a promising path to improve crop yields and sustainability in agriculture. Further investigation into the nuances of priming conditions and their interaction with specific stress factors is warranted to unlock the full potential of this promising technique.

CONFLICT OF INTEREST

The authors stated that there are no conflicts of interest regarding the publication of this article.

CRedit AUTHOR STATEMENT

Musa Kar: Conceptualization, Project administration, Investigation, Writing, and editing—original draft
Gökhan Gökpinar: Investigation, Writing – review & editing, **Özlem Doğan** Investigation, Writing – review & editing

REFERENCES

- [1] El-Badri AM, Batool M, Wang C, Hashem AM, Tabl KM, Nishawy E, Kuai J, Zhou G, Wang B. Selenium and zinc oxide nanoparticles modulate the molecular and morpho-physiological processes during seed germination of Brassica napus under salt stress. *Ecotoxicol. Environ. Saf.* 2021; 225: 112695.
- [2] Ellouzi H, Oueslati S, Hessini K, Rabhi M, Abdely C. Seed-priming with H₂O₂ alleviates subsequent salt stress by preventing ROS production and amplifying antioxidant defense in cauliflower seeds and seedlings. *Sci. Hortic. (Amsterdam)*. 2021; 288: 110360.
- [3] Savvides A, Ali S, Tester M, Fotopoulos V. Chemical Priming of Plants Against Multiple Abiotic Stresses: Mission Possible? *Trends Plant Sci.* 2016; 21: 329–340.
- [4] Ishibashi Y, Yamaguchi H, Yuasa T, Iwaya-Inoue M, Arima S, Zheng SH. Hydrogen peroxide spraying alleviates drought stress in soybean plants. *J. Plant Physiol.* 2011; 168: 1562–1567.
- [5] Uchida A, Jagendorf AT, Hibino T, Takabe T, Takabe T. Effects of hydrogen peroxide and nitric oxide on both salt and heat stress tolerance in rice. *Plant Sci.* 2002; 163: 515–523.
- [6] Antoniou C, Savvides A, Christou A, Fotopoulos V. Unravelling chemical priming machinery in plants: the role of reactive oxygen–nitrogen–sulfur species in abiotic stress tolerance enhancement. *Curr. Opin. Plant Biol.* 2016; 33: 101–107.
- [7] Machado RMA, Serralheiro RP. Soil Salinity: Effect on Vegetable Crop Growth. Management Practices to Prevent and Mitigate Soil Salinization. *Horticulturae*. 2017; 3(2):30..
- [8] Anjum NA, Sofu A, Scopa A, Roychoudhury A, Gill SS, Iqbal M, Lukatkin AS, Pereira E, Duarte AC, Ahmad I. Lipids and proteins—major targets of oxidative modifications in abiotic stressed plants. *Environ. Sci. Pollut. Res.* 2015; 22(6):4099-121

- [9] Duman F, Ozturk F. Nickel accumulation and its effect on biomass, protein content and antioxidative enzymes in roots and leaves of watercress (*Nasturtium officinale* R Br). *J. Environ. Sci.* 2010; 22: 526–532.
- [10] Soydam-Aydin S, Buyuk I, Cansaran-Duman D, Aras S. Roles of catalase (CAT) and ascorbate peroxidase (APX) genes in stress response of eggplant (*Solanum melongena* L) against Cu(+2) and Zn(+2) heavy metal stresses. *Environ. Monit. Assess.* 2015; 187: 726.
- [11] Maruta T, Noshi M, Tanouchi A, Tamoi M, Yabuta Y, Yoshimura K, Ishikawa T, Shigeoka S. H₂O₂-triggered retrograde signaling from chloroplasts to nucleus plays specific role in response to stress. *J. Biol. Chem.* 2012; 287(15):11717-29
- [12] Foyer CH, Noctor G. Oxidant and antioxidant signalling in plants: A re-evaluation of the concept of oxidative stress in a physiological context. *Plant, Cell Environ.* 2005; 28: 1056–1071.
- [13] Li JT, Qiu ZB, Zhang XW, Wang LS. Exogenous hydrogen peroxide can enhance tolerance of wheat seedlings to salt stress. *Acta Physiol. Plant.* 2011;
- [14] Hossain MA, Bhattacharjee S, Armin S-M, Qian P, Xin W, Li H-Y, Burritt DJ, Fujita M, Tran L-SP. Hydrogen peroxide priming modulates abiotic oxidative stress tolerance: insights from ROS detoxification and scavenging. *Front. Plant Sci.* 2015; 6: 1–19.
- [15] Wahid A, Perveen M, Gelani S, Basra SMA. Pretreatment of seed with H₂O₂ improves salt tolerance of wheat seedlings by alleviation of oxidative damage and expression of stress proteins. *J. Plant Physiol.* 2007; 164(3):283-94
- [16] Ashraf MA, Rasheed R, Hussain I, Iqbal M, Haider MZ, Parveen S, Sajid MA. Hydrogen peroxide modulates antioxidant system and nutrient relation in maize (*Zea mays* L) under water-deficit conditions. *Arch. Agron. Soil Sci.* 2015; 61(4), 507–523.
- [17] Witham FH, Blaydes DF, Devlin RM. *Experiments in plant physiology*, New York,
- [18] Heath RL, Packer L. Photoperoxidation in isolated chloroplasts I Kinetics and stoichiometry of fatty acid peroxidation. *Arch. Biochem. Biophys.* 1968; 125: 189–198.
- [19] Chen T, Zhang B. Measurements of Proline and Malondialdehyde Content and Antioxidant Enzyme Activities in Leaves of Drought Stressed Cotton. *Bio-Protocol* 2016; 6: 1–14.
- [20] Livak KJ, Schmittgen TD. Analysis of relative gene expression data using real-time quantitative PCR and the 2⁻($\Delta\Delta C_T$) Method. *Methods* 2001; 25 : 402–8.
- [21] Aazami MA, Rasouli F, Ebrahimzadeh A. Oxidative damage, antioxidant mechanism and gene expression in tomato responding to salinity stress under in vitro conditions and application of iron and zinc oxide nanoparticles on callus induction and plant regeneration. *BMC Plant Biol.* 2021; 21: 1–23.
- [22] Meloni DA, Oliva MA, Martinez CA, Cambraia J. Photosynthesis and activity of superoxide dismutase, peroxidase and glutathione reductase in cotton under salt stress. *Environ. Exp. Bot.* 2003; 49: 69–76.
- [23] Sevengor S, Yasar F, Kusvuran S, Ellialtıođlu S. The effect of salt stress on growth, chlorophyll content, lipid peroxidation and antioxidative enzymes of pumpkin seedling, . 2011, 6.21: 4920-

4924

- [24] Yao X, Zhou M, Ruan J, Peng Y, Ma C, Wu W, Gao A, Weng W, Cheng J. Physiological and Biochemical Regulation Mechanism of Exogenous Hydrogen Peroxide in Alleviating NaCl Stress Toxicity in Tartary Buckwheat (*Fagopyrum tataricum* (L) Gaertn). *Int. J. Mol. Sci.* 2022 14;23(18):10698.
- [25] Asgher M, Ahmed S, Sehar Z, Gautam H, Gandhi S, Khan NA. Hydrogen peroxide modulates activity and expression of antioxidant enzymes and protects photosynthetic activity from arsenic damage in rice (*Oryza sativa* L). *J. Hazard. Mater.* 2021; 401: 123365.
- [26] Jiang Y, Gao Z, Zhang X, Nikolic M, Liang Y. Effects of exogenous salicylic acid on alleviation of arsenic-induced oxidative damages in rice. *J. Plant Nutr.* 2022; 46: 2811–2826.
- [27] ElSayed AI, Rafudeen MS, Ganie SA, Hossain MS, Gomaa AM. Seed priming with cypress leaf extract enhances photosynthesis and antioxidative defense in zucchini seedlings under salt stress. *Sci. Hortic. (Amsterdam)*. 2022; 293: 110707.
- [28] Gao Y, Guo YK, Lin S-H, Fang Y-Y, Bai J-GG, Li SH, Fangg YY, Bai J-GG, Lin S-H, Fang Y-Y, Bai J-GG. Hydrogen peroxide pretreatment alters the activity of antioxidant enzymes and protects chloroplast ultrastructure in heat-stressed cucumber leaves. *Sci. Hortic. (Amsterdam)*. 2010; 126: 20–26.
- [29] Zulfiqar F, Nafees M, Chen J, Darras A, Ferrante A, Hancock JT, Ashraf M, Zaid A, Latif N, Corpas FJ, Altaf MA, Siddique KHM. Chemical priming enhances plant tolerance to salt stress. *Front. Plant Sci.* 2022; 13: 1–22.
- [30] Cuypers A, Hendrix S, Amaral dos Reis R, De Smet S, Deckers J, Gielen H, Jozefczak M, Loix C, Vercamp H, Vangronsveld J, Keunen E. Hydrogen Peroxide, Signaling in Disguise during Metal Phytotoxicity. *Front. Plant Sci.* 2016; 25;7:470
- [31] Nazir F, Fariduddin Q, Khan TA. Hydrogen peroxide as a signalling molecule in plants and its crosstalk with other plant growth regulators under heavy metal stress. *Chemosphere* 2020; 252: 126486.
- [32] Gomez JM, Jimenez A, Olmos E, Sevilla F. Location and effects of long-term NaCl stress on superoxide dismutase and ascorbate peroxidase isoenzymes of pea (*Pisum sativum* cv Puget) chloroplasts. *J. Exp. Bot.* 2004; 55: 119–130.
- [33] Gao Y, Guo Y-K, Lin S-H, Fang Y-Y, Bai J-G. Hydrogen peroxide pretreatment alters the activity of antioxidant enzymes and protects chloroplast ultrastructure in heat-stressed cucumber leaves. *Sci. Hortic. (Amsterdam)*. 2010; 126: 20–26.
- [34] Wang G, Xiao Y, Deng X, Zhang H, Li T, Chen H. Exogenous Hydrogen Peroxide Contributes to Heme Oxygenase-1 Delaying Programmed Cell Death in Isolated Aleurone Layers of Rice Subjected to Drought Stress in a cGMP-Dependent Manner. *Front. Plant Sci.* 2018; 9: 84.
- [35] Afrin S, TahjibArif M, Sakil M, Sohag A, Polash M, Hossain M. Hydrogen peroxide priming alleviates chilling stress in rice (*Oryza sativa* L) by enhancing oxidant scavenging capacity. *Fundam. Appl. Agric.* 2018; 4: 1.
- [36] Ma N, Hu C, Wan L, Hu Q, Xiong J, Zhang C, Strigolactones improve plant growth,

photosynthesis, and alleviate oxidative stress under salinity in rapeseed (*Brassica napus* L) by regulating gene expression. *Front. Plant Sci.* 2017; 8:

- [37] Zhao P, Wang Y, Lin Z, Zhou J, Chai H, He Q, Li Y, Wang J, The alleviative effect of exogenous phytohormones on the growth, physiology and gene expression of *Tetraselmis cordiformis* under high ammonia-nitrogen stress. *Bioresour. Technol.* 2019; 282: 339–347.
- [38] Si T, Wang X, Zhao C, Huang M, Cai J, Zhou Q, Dai T, Jiang D, The role of hydrogen peroxide in mediating the mechanical wounding-induced freezing tolerance in wheat. *Front. Plant Sci.* 2018; 9: 1–15.
- [39] Rossatto T, do Amaral MN, Benitez LC, Vighi IL, Braga EJB, de Magalhaes Junior AM, Maia MAC, da Silva Pinto L, Gene expression and activity of antioxidant enzymes in rice plants, cv BRS AG, under saline stress. *Physiol. Mol. Biol. Plants* 2017; 23: 865–875.
- [40] Bagheri M, Gholami M, Baninasab B, Hydrogen peroxide-induced salt tolerance in relation to antioxidant systems in pistachio seedlings. *Sci. Hortic. (Amsterdam)*. 2019; 243: 207–213.



BIOCHAR-SUPPORTED IN VITRO CULTURES OF *Lavandula officinalis* L.

Pınar NARTOP ^{1,*}, Sena ÖZDİL ŞENER ², Seray Begüm GÖK ³

¹ Department of Biomedical Engineering, Faculty of Engineering, Tekirdağ Namık Kemal University, Çorlu, Tekirdağ, Turkey
pnartop@nku.edu.tr - [0000-0003-2765-6133](https://orcid.org/0000-0003-2765-6133)

² Department of Biomedical Engineering, Faculty of Engineering, Tekirdağ Namık Kemal University, Çorlu, Tekirdağ, Turkey
senaozdil@gmail.com - [0000-0002-0156-7629](https://orcid.org/0000-0002-0156-7629)

³ Department of Biomedical Engineering, Faculty of Engineering, Tekirdağ Namık Kemal University, Çorlu, Tekirdağ, Turkey
begum.gok22@gmail.com - [0000-0001-6979-2737](https://orcid.org/0000-0001-6979-2737)

Abstract

Plants are the sources of valuable biomass that are being currently used in many areas. It is important to produce high biomass for efficient commercial production. Amongst the many factors that affect *in vitro* propagation of plants, changing or enriching the media composition is one of the commonly used techniques in micropropagation of plants. Biochar is a solid product obtained from organic wastes and because of its rich composition, it has many beneficial effects on plants. In our study, *Lavandula officinalis* plantlets were subjected to two types of biochars (Geocharged biochar and Biorfe biochar) at 0.5 and 2 g/L concentrations and their effects were investigated by means of plant growth, biomass accumulation and biochemical composition. The results showed that 0.5 g/L concentration of biochar had better effects than 2 g/L concentration and except for biochemical composition, biochar type had no significant effect on plant growth and biomass accumulation. Mean root dry weights and multiple shoot formations/explant enhanced up to 3.7 and 4.17 times higher than the control at 0.5 g/L concentration. Explant browning was also detected lower in biochar-applied media. The differences between biochemical accumulations of different media were also found statistically significant. The total concentrations of phenolics and flavonoids and radical scavenging activities were detected lower when biochars were applied. The total antioxidant concentration was higher in the control group. These findings showed that biochars lowered the negative effects of the culture conditions for *L. officinalis* plantlets.

Keywords

Lavandula officinalis,
Micropropagation,
Biochar,
Biomass and biochemical
accumulations

Time Scale of Article

Received :13 December 2023
Accepted : 08 July 2024
Online date : 30 July 2024

1. INTRODUCTION

Plant tissue cultures offer different options for the higher production of plant biomass. It is possible to trigger the regeneration of shoots and roots with the addition of different materials to culture media. Generally, cytokinins and auxins have been used for the induction of biomass accumulations. These growth regulators are effective as a result of their physiological effects [1-3]. However, they are expensive and push up the cost of commercial productions. Therefore, alternative products have been tested to increase the growth parameters of *in vitro*-grown plantlets.

Biochar is the solid by-product of biomass (plant, manure, organic wastes, animal bones, etc.) pyrolysis performed under high temperatures (200-900°C) and in the absence of oxygen. Its positive effects on soil quality and crop improvement have been known since ancient times. Its use in agriculture is beneficial because of the improved physicochemical and biological properties of soil and enhanced

*Corresponding Author: pnartop@nku.edu.tr

sequestration of atmospheric carbon. It is also known that biochar is effective in disease suppression of pathogens and very enduring because of its resistance to microbial degradation caused by its wide C-to-N ratio [4-7]. Chang et al. [8] reported that root length, number of root forks and crossings of *Vitis rotundifolia* were improved by adding 20% pinewood-based biochar into pure sandy soil. Biochar addition also enhanced the fine root and total mass of *Phragmites australis* [9] and shoot biomass of tomato seedlings [10]. It was also reported that biochar can balance and alleviate endogenous phytohormone concentration under stress conditions [11].

Lavandula officinalis L. is a valuable medicinal plant that is native to the Mediterranean region and has multiple pharmacological effects. Its essential oils, primarily composed of monoterpenes and sesquiterpenes, are frequently used in the perfume and cosmetic industry. Because of its wide range of uses, the large-scale production of this medicinal plant is important. In order to enhance production, it is not a preferable option to use agrochemicals due to their possible adverse effects on humans and the environment [12, 13]. Therefore, it is important to apply an appropriate biomass enhancer, especially environment-friendly organic-based products.

Biochar, obtained from different organic sources, is used in agronomic studies as stated above. However, only a few *in vitro* studies were conducted about the utilization of biochar in plant tissue cultures. Because of their rich organic content, biochar may be an alternative for highly-prized plant growth regulators and can be used to obtain high-quality plantlets in *in vitro* conditions. In this perspective, in this study, we used two biochars, Geocharged biochar and Biorfe biochar, at 0.5 and 2 g/L concentrations to trigger higher biomass production and better growth in *in vitro* cultures of *L. officinalis*.

2. MATERIALS AND METHODS

Geocharged biochar (T) and Biorfe biochar (P) were used in this study. Nodal explants of *L. officinalis*, grown in Woody Plant Medium (WPM) containing 6 g/L agar and 30 g/L [14] were used as explant sources. The subcultures of the cultures were done with intervals of four weeks and the explant was incised from the *L. officinalis* plantlets grown in these conditions.

The nodal segments (0.5-1 cm long) were incised and put into semi-solid WPM supplemented with 0.5 and 2 g/L of biochar. Basal WPM was determined as the control group. The media were coded as T0, T5 and T20 for Geocharged biochar and P0, P5 and P20 for Biorfe biochar. The pH of all the media used in this study was set to 5.8. All the media were sterilized for 15 minutes at 121°C and 1.2 kg/cm³ pressure in an autoclave. The cultivation duration of the nodal explants was determined as four weeks, they were cultured at 4000 lux and 6 h photoperiod. The temperature was kept constant at 23±1°C. The roots and bottom parts were washed carefully with distilled water and the excess water was moved with the help of a napkin.

Root, node and shoot numbers/explant were calculated by dividing the total number of plant parts (shoots, nodes and roots) by the total number of explants. Their fresh weights (shoots – SFW, roots - RFW) were also determined and recorded. The biomass was dried overnight in an oven (50°C) in order to specify their dry weights. Their growth parameters were stated as; average shoot length (SL) (cm), node (NN), root (RN), shoot (SN) numbers, internode length (IL) (cm), multiple shoot numbers (MSN), explant browning (EB) percentage (%). Biomass accumulations were also specified (shoot fresh weights – SFW (g), shoot dry weights - SDW (g), root fresh weights – RFW (g), root dry weights - RDW (g)).

Shoot and root samples (0.025 g) were mixed with 5 mL ethanol and the mixture was sonicated and heated (50°C) for 1h (Bandelin Sonorex) with a frequency of 35 kHz. The extracts were centrifugated (5000 rpm) for 15 min and the supernatants were distinguished from precipitate. The determinations of total phenolic concentrations (TPC) were performed according to Stoica et al [15] method. 250 µL extract, 9 mL distilled water and 250 µL of Folin&Ciocalteu's phenol reagent were put together and

agitated. 2.5 mL 7% Na₂CO₃ was added after 5 mins and agitated again. 1.25 mL double distilled water was added and mixed once again. After 90 mins, the absorbance of each sample was read in a spectrophotometer at 750 nm (Shimadzu UV-1201 V). As the standard, Gallic acid (GA) was employed and TPCs were given as mg gallic acid equivalents (mg GAE/g). DPPH scavenging activity were performed according to Desta and Cherie [16] method. 4 ml of ethanolic solution of DPPH (0.004%) was mixed with 2 mL of extract. They were agitated for 10 s and kept for 30 min in dark conditions. The absorbances of the samples were measured at 517 nm. The radical scavenging activities (RSA) (%) of the samples were decided using the equation given below: (A₀ = Absorbance of the control, A₁ = Absorbance of the sample)

$$\% \text{ RSA} = [(A_0 - A_1) / A_0] \times 100$$

The determinations of total flavonoid concentrations (TFC) were performed according to Aluminum chloride assay [17]. 4 ml of 2% AlCl₃ and 4 mL of the extracts were mixed. After 10 mins, the absorbances of these mixtures were measured at 415 nm. As the standard, quercetin was employed and TFCs were given as mg quercetin equivalents (mg QE/g). The determination of total antioxidant capacity (TAC) was performed according to Phosphomolybdate method [17,18]. Phosphomolybdate reagent was prepared by mixing 50 milliliters of 0.6 M H₂SO₄, 28 mM Na₃PO₄ and 4 mM (NH₄)₆Mo₇O₂₄. 0.3 mL of this reagent and the extracts were mixed and incubated for 90 min at 95°C. The absorbances of the samples were determined at 695 nm. As the standard, ascorbic acid was employed and TACs were expressed as ascorbic acid equivalents (mg AAE/g).

All experiments were performed in three replications. In each replication, 15 explants were cultivated. Experiments were set to a factorial randomized plots design. All the data were analyzed with ANOVA and for posthoc tests, Tukey tests ($p < 0.05$) were deployed.

3. RESULTS

Biomass accumulation of shoots and roots of *L. officinalis* plantlets were not statistically affected by biochar applications, except mean RDW values ($p < 0.05$). SFW values varied between 0.5 g (T20) and 1.02 g (P5) (**Table 1a**). The values showed an increase in T5 and P5 media when compared to control media. In T20 and P20, the values detected were lower than control media. These results were also verified by mean SFW values. The highest mean SFW was detected in 0.5 g/L biochar-containing media (0.87 g) and this increase was 32% higher than the control (0.66 g) (**Table 1b**). The total SFW of T (0.75 g) was 21% higher than P (0.62 g) (**Table 1c**). In SDW values, increasing biochar concentrations decreased biomass accumulations gradually (**Table 1a**). The total SDW values were found almost the same (0.11 g for T and 0.10 g for P) (**Table 1c**). RFW values were in accordance with SFW values. The values varied between 0.025 g (P20) and 0.105 g (P5), and showed an increase in T5 (0.071 g) and P5 (0.105 g) which were 1.97 and 2.92 times higher than the control (0.036 g), respectively (**Table 1a**). The highest mean RFW was detected in 0.5 g biochar concentration (0.09 g) and T had a higher biomass accumulation than P concerning total RFW (**Table 1b and 1c**). Mean RDW values were significantly affected by biochar concentrations (**Table 1b**); 0.5 g biochar was in the first group (A group) with 0.015 g biomass accumulation and a sharp decrease was observed in 2 g biochar concentration (AB group). However, both concentrations had higher biomass accumulations than the control group (B group).

In the growth parameters of *L. officinalis* plantlets, only mean MSN values were significantly affected by biochar concentrations. All the other parameters were found statistically insignificant ($p > 0.05$). Lengths of shoots varied between 2.44 cm (T0 and P0) and 4.36 cm (P5) (**Table 2a**). The highest SLs were detected in T5 and P5, but as the biochar concentrations enhanced to 2 g/L, SL values decreased. However, all the values of biochar applications were higher than the control group. The mean SL value was higher at 0.5 g/L biochar concentration (**Table 2b**) and P (3.59 cm) had higher SL than T (2.86 cm) (**Table 2c**). NNs varied between 5.24 (T20) and 7.31 (P5) and the highest values were obtained in 0.5 g/L biochar concentration (T5 and P5) (**Table 2a**). This result was also verified by the mean NN values;

the highest mean NN was detected at 0.5 g/L biochar concentration (**Table 2b**). Total NN of P (6.30) was detected higher than T (6.00) (**Table 2c**). The lengths of internodes were higher in biochar-applied plantlets than in the control groups (**Table 2a**). In 2 g/L biochar-containing media, the plantlets had the highest mean IL (0.59 cm) (**Table 2b**). Total IL of P (0.57 cm) was higher than T (0.49 cm) (**Table 2c**). The number of roots per explant decreased in media supplemented with biochar (**Table 2a**). Similar to the other growth parameters, the total RN of P (1.23) was also found higher than T (1.04) (**Table 2c**).

Table 1. (a) Shoot fresh (SFW) and dry (SDW) weights and root fresh (RFW) and dry (RDW) weights of *L. officinalis* plantlets, and their mean and total weights with regard to (b) biochar concentrations and (c) biochar types.

Table 1a				
Media	SFW (g)	RFW (g)	SDW (g)	RDW (g)
T0	0.656 ± 0.150	0.036 ± 0.009	0.120 ± 0.027	0.004 ± 0.001
T5	0.703 ± 0.179	0.071 ± 0.008	0.103 ± 0.020	0.013 ± 0.003
T20	0.500 ± 0.075	0.041 ± 0.025	0.085 ± 0.014	0.009 ± 0.005
P0	0.656 ± 0.150	0.036 ± 0.009	0.120 ± 0.027	0.004 ± 0.001
P5	1.020 ± 0.308	0.105 ± 0.046	0.113 ± 0.028	0.017 ± 0.008
P20	0.562 ± 0.078	0.025 ± 0.002	0.094 ± 0.019	0.004 ± 0.001

Table 1b				
Conc.(g/L)	Mean SFW (g)	Mean RFW (g)	Mean SDW (g)	Mean RDW (g)
0	0.66	0.04	0.12	0.004 B
0.5	0.87	0.09	0.11	0.015 A
2.0	0.54	0.03	0.09	0.006 AB

Table 1c				
Biochar Type	Total SFW (g)	Total RFW (g)	Total SDW (g)	Total RDW (g)
T	0.75	0.06	0.11	0.008
P	0.62	0.05	0.10	0.008

(The values with different letters are statistically significant according to Tukey test)

Table 2. (a) Shoot lengths (SL), node numbers (NN), internode lengths (IL) and root numbers (RN) of *L. officinalis* plantlets, and their mean and total values with regard to (b) biochar concentrations and (c) biochar types.

Table 2a				
Media	SL (cm)	NN	IL (cm)	RN
T0	2.44 ± 0.73	5.42 ± 1.47	0.44 ± 0.02	1.36 ± 0.55
T5	3.45 ± 0.60	7.29 ± 2.03	0.51 ± 0.11	0.84 ± 0.24
T20	2.68 ± 0.32	5.24 ± 0.45	0.52 ± 0.08	0.93 ± 0.07
P0	2.44 ± 0.73	5.42 ± 1.47	0.44 ± 0.02	1.36 ± 0.55
P5	4.36 ± 0.38	7.31 ± 0.95	0.63 ± 0.12	1.31 ± 0.12
P20	3.97 ± 0.41	6.16 ± 1.04	0.66 ± 0.04	1.02 ± 0.09

Table 2b				
Conc. (g/L)	Mean SL (cm)	Mean NN	Mean IL (cm)	Mean RN
0	2.44	5.42	0.44	1.36
0.5	3.90	7.30	0.57	1.08
2.0	3.33	5.70	0.59	0.98

Table 2c				
Biochar Type	Total SL (cm)	Total NN	Total IL (cm)	Total RN
T	2.86	6.00	0.49	1.04
P	3.59	6.30	0.57	1.23

SNs of *L. officinalis* were affected by the addition of biochar, however, except for mean MSN values, they were not found statistically significant ($p > 0.05$). SNs varied between 1.78 (control – T0 and P0) and 2.31 (T5). In T5 and T20, as the result of the ascending biochar concentration, SN showed a decrease. However, both SN values were higher than T0 (**Table 3a**). In mean SNs, it was detected that 0.5 g/L and 2 g/L biochar applications had 1.25 and 1.13 times higher values than the control (**Table 3b**). The total SN of P was higher than T (**Table 3c**). In MSN values, remarkable results were observed. The values ranged between 0.47 (control) and 2.11 (P20). The addition of 0.5 g/L and 2 g/L T into the media, MSN values enhanced 4.34 and 3.49 times, respectively. The addition of P at 0.5 g/L and 2 g/L concentrations also enhanced MSN values approximately by 4 and 4.5 times, respectively (**Table 3a**). Mean MSN values were found statistically significant ($p < 0.05$); 0.5 g/L concentration of biochar had the highest MSN (1.96) and in the same statistical group with 2 g/L biochar application (1.88). These MSN values were 4.17 and 4 times higher than the control (0.47) (group B) (**Table 3b**). Total MSN values were 1.39 and 1.48 in T and P, respectively (**Table 3c**). Browning percentages of the node explants were all found lower in biochar-added media than in the control (26.67%), as expected. The lowest browning was observed in P20 (2.22%) (**Table 3a**). EB decreased gradually as the concentration of biochar increased (**Table 3b**). Total EB of P was detected as 17.77%, whereas 22.22% was observed in T (**Table 3c**).

Table 3. (a) Shoot number (SN), multiple shoot number (MSN) and explant browning (EB) percentages of *L. officinalis* plantlets and their mean and total values with regard to (b) biochar concentrations and (c) biochar types.

Table 3a			
Media	SN	MSN	EB (%)
T0	1.78 ± 0.53	0.47 ± 0.10	26.67 ± 9.11
T5	2.31 ± 0.35	2.04 ± 0.36	17.78 ± 5.89
T20	1.80 ± 0.10	1.64 ± 0.11	22.22 ± 2.22
P0	1.78 ± 0.53	0.47 ± 0.10	26.67 ± 9.11
P5	2.13 ± 0.10	1.87 ± 0.10	24.44 ± 5.89
P20	2.22 ± 0.30	2.11 ± 0.26	2.22 ± 2.22

Table 3b			
Conc. (g/L)	Mean SN	Mean MSN	Mean EB (%)
0	1.78	0.47 B	26.67
0.5	2.23	1.96 A	21.11
2.0	2.02	1.88 A	12.22

Table 3c			
Biochar Type	Total SN	Total MSN	Total EB (%)
T	1.78	1.39	22.22
P	2.02	1.48	17.77

(The values with different letters are statistically significant according to Tukey test)

TPC values of the shoot and root parts of *L. officinalis* were observed in the range of 38.35-83.35 mg GAE/g (**Table 4a**). The effect of biochar concentrations, plant parts, interactions between biochar types*biochar concentrations and biochar concentrations*explant types were found statistically significant ($p < 0.05$). Mean TPCs decreased contrary to enhancing biochar concentrations (**Table 4b**). Biochar type did not have a distinct effect on TPCs (**Table 4c**). Shoot parts had higher TPCs than root parts of the plantlets (**Table 4d**). TACs were detected in the range of 45.55-114.69 mg AAE/g. The interaction between biochar types*biochar concentrations*plant parts was found statistically significant ($p < 0.05$). Shoot parts were detected superior to root parts (**Table 4d**); the highest TACs were in P20 and P5 (Group A), and T5, T20, T0 and P0 followed (Group B). The lowest TAC was detected in root parts obtained from T20 (**Table 4a**). Mean TACs were increased in parallel with biochar concentrations (**Table 4b**) and P was found superior to T (**Table 4c**). TFC values ranged between 5.70-13.80 mg QE/g

in shoot parts and 1.41-2.12 mg QE/g in root parts (**Table 4a**). The interaction between biochar types*biochar concentrations*plant parts was found statistically significant ($p<0.05$). The highest TFCs were obtained from the control group and the addition of biochars lessened TFC values (**Table 4b**). P was detected superior to T (7.19 mg QE/g and 5.54 mg QE/g, respectively) and shoot parts had higher TFCs than roots, distinctly (**Table 4c and 4d**). RSA percentages were observed between 91.73-92.53% in shoot parts and 68.87-85.63% in root parts of *L. officinalis* (**Table 4a**). The interaction between biochar types*biochar concentrations*plant parts was also found statistically significant in RSA percentages ($p<0.05$). Similar to TFC values, mean RSA percentages decreased when biochars were applied (**Table 4b**). Biochar type was found effective on mean RSA percentages and P was more effective than T (84.92% and 81.08%, respectively) (**Table 4c**). Similar to TPC, TAC and TFC results, total RSA percentages were found higher in shoot parts (92.06%) than in root parts (73.95%) (**Table 4d**).

Table 4. (a) Total phenolic (TPC), antioxidant capacity (TAC), flavonoid (TFC) and radical scavenging activity (RSA) of *L. officinalis* plantlet in response to biochar concentrations **(b)** Mean TPC, TAC, TFA and RSA in response to biochar concentrations **(c)** Mean TPC, TAC, TFA and RSA in response to biochar type **(d)** Mean TPC, TAC, TFA and RSA in response to plant parts.

Table 4a					
Plant Part	Media	TPC (mg GAE/g)	TAC (mg AAE/g)	TFC (mg QE /g)	RSA (%)
Shoot	T0	83.35± 5.77	90.46±6.00 B	13.80±0.16 A	91.87± 0.00
	T5	64.85±10.97	94.31±0.67 B	5.70±0.02 E	91.80±1.02
	T20	38.85±2.45	93.92±0.44 B	8.72±0.20 D	91.87±0.19
	P0	83.35± 5.77	90.46±6.00 B	13.80±0.16 A	91.87± 0.00
	P5	69.10±2.31	113.15±0.89 A	10.86±0.04 C	92.53±0.34
	P20	49.85±2.74	114.69±1.33 A	12.53±0.17 B	91.73±0.19
Root	T0	45.73±1.52	49.69±0.22 CD	2.12±0.01 F	78.81±1.26
	T5	54.85±0.00	49.69±0.22 CD	1.41±0.01 G	70.54±3.77
	T20	38.35±2.89	45.85±0.67 D	1.49±0.13 G	61.03±2.05
	P0	45.73±1.52	49.69±0.22 CD	2.12±0.01 F	78.81±1.26
	P5	47.85±2.31	49.31±0.89 CD	1.70±0.01 FG	68.87±0.54
	P20	54.23±0.22	59.69±0.67 C	2.12±0.11 F	85.63±0.25

Table 4b				
Conc. (g/L)	Mean TPC (mg GAE/g)	Mean TAC (mg AAE/g)	Mean TFC (mg QE /g)	Mean RSA (%)
0	64.54 A	70.01 B	7.96 A	85.34 A
0.5	59.16 A	76.62 A	4.92 C	81.10 B
2.0	45.32 B	78.54 A	6.22 B	82.57 B

Table 4c				
Biochar Type	Mean TPC (mg GAE/g)	Mean TAC (mg AAE/g)	Mean TFC (mg QE /g)	Mean RSA (%)
T	58.35	70.66 B	5.54 B	81.08 B
P	54.33	79.50 A	7.19 A	84.92 A

Table 4d				
Plant Part	Total TPC (mg GAE/g)	Total TAC (mg AAE/g)	Total TFC (mg QE /g)	Total RSA (%)
Shoot	64.90 A	99.50 A	10.90 A	92.06 A
Root	47.79 B	50.65 B	1.83 B	73.95 B

(The values with different letters are statistically significant according to Tukey test)

4. DISCUSSION

Biochar is an interesting and cost-effective product to be used as a plant growth promotor agent, because of its ethylene-inhibiting and growth hormones-promoting effects on plant tissues [11,19]. Biochar was also investigated for its effects on soil biota [20,21]. Despite its beneficial effects, most studies were conducted in this field but only a few *in vitro* studies were reported.

In our study on *in vitro*-grown *L. officinalis* plantlets, fresh weights of shoots and roots, and dry weights of shoots were not statistically affected by the biochar addition to media. SFWs, RDWs and RDWs showed an increase at 0.5 g/L concentrations but decreased under the control at 2 g/L concentration (**Table 1**). In SDW, both concentrations lowered the dry weight when compared to the control. The only significant effect was detected in mean RDW; 0.5 g/L concentration of biochars enhanced the dry weight 3.74 times more than control. Root growth-promoting effects of biochars were previously reported. **Di Lonardo et al.** [19] studied the effects of biochars on *Populus alba* L. clones and reported that dry biomass of roots and root numbers/shoots increased at 0.5 and 1.5 g/L biochar applications. **Hammer et al.** [21] reported that total plant biomass and root biomass were enhanced when *Lactuca sativa* plants were exposed to biochar application. Shoot and root biomass of *L. officinalis* plants grown in greenhouse conditions were detected higher [22]. **Miclea et al. (2020)** [13] reported that shoots of *L. angustifolia* grew taller when activated charcoal was added to the plant growth medium.

SL, NN, IL and RN were also not significantly affected by biochar applications at 0.5 and 2 g/L concentrations. However, at both concentrations, SL, NN and IL values were detected higher than the control. SL and NN values were enhanced higher by 0.5 g/L concentration than 2 g/L concentration. RN values were lower than the control at both concentrations for both biochar types (**Table 2**). **Di Lonardo et al.** [19] reported a higher elongation rate in *Populus alba* L. clones when biochar was used and this effect was attributed to the absorption of ethylene molecules by biochar.

Multiple shoot formation enhances not only shoot biomass but also plantlets' numbers in *in vitro* propagation. Therefore, it is an important parameter for micropropagation studies. In our study, in both concentrations of two biochars, SNs and MSNs were higher than the control (**Table 3a**). Biochar concentration was found statistically significant on mean MSN and 0.5 g/L concentration of biochars enhanced mean MSN by 4.17 times higher than the control (**Table 3b**). This result may be attributed to the ethylene inhibition and growth-promoting effects of biochars and indicate that biochar can be used instead of non-natural growth regulators to stimulate plant growth.

Prevention of explant from browning is a predictable effect of biochars because of their absorption capacity, similar to activated charcoal [23]. Di Lonardo et al. [19] used biochar instead of activated charcoal successfully. In our study, both concentrations inhibited explant browning. Although there was no statistical significance, rising concentrations of biochars decreased browning. The highest browning-preventing effect was detected in P20 (2.22%) which was approximately 12 times lower than the control (**Table 3a**).

Biochemical compositions of plant biomass change when different chemicals are applied to plant cells and tissues and secondary metabolites are the defense system of plants [24-25]. TPC, TAC, TFC and RSA values of *L. officinalis* plantlets were strongly affected by the utilized concentrations of biochars in this study. TPC, TFC and RSA values were detected as lower than the control in biochar-applied biomass, however, the control had higher TAC values (**Table 4c**). These results confirmed that phenolic and flavonoid contents of *in vitro*-grown *L. officinalis* plantlets were lowered by biochar applications. Similar to our findings, **Kul et al.** [26] reported biochar applications at 2.5% and 5% concentrations decreased the antioxidant activities and gave the bean plantlets strength towards stress conditions. Although the two main secondary metabolite groups (phenolics and flavonoids) productions were detected lower in biochar-supplemented media, antioxidant capacities were higher than in the control

group. Moreover, explant brownings were also lower when biochars were applied. These findings revealed that biochar applications can help plant tissues fight against the stress of *in vitro* conditions.

5. CONCLUSION

Biochar can be produced from different organic wastes and has beneficial effects on plant growth, biomass accumulation and biochemical content. It has also proved that different types of biochars may boost the *in vitro* production of plants. Consequently, biochars derived from different sources should be used and their utilization should be optimized. Therefore, in order to reveal their protective effects, more studies about biochar applications on different plant types and culture types should be conducted.

ACKNOWLEDGEMENTS

This research received no external funding.

CONFLICT OF INTEREST

The authors declare no conflict of interest.

CRedit AUTHOR STATEMENT

Pınar Nartop: Laboratory experiments, Data collection, Data Analysis, Investigation, Conceptualization, Writing – Original draft preparation, Supervision. **Sena Özdil Şener:** Laboratory experiments, Data collection. **Seray Begüm Gök:** Laboratory experiments, Data collection.

REFERENCES

- [1] Mathur J, Koncz C. Callus Culture and Regeneration. In: Martínez-Zapater JM, Salinas J, editors. *Methods in Molecular Biology™: Arabidopsis Protocols*, New Jersey: Humana Press, 1998. 82, pp. 31-35p.
- [2] Chawla HS. *Introduction to Plant Biotechnology*. Second edition, New Hampshire, United States of America, USA: Science Publishers Inc., 2002.
- [3] Nartop P. Engineering of Biomass Accumulation and Secondary Metabolite Production in Plant Cell and Tissue Cultures. In: Ahmad P, Ahanger MA, Singh VP, editors. *Plant Metabolites and Regulation Under Environmental Stress*, Chapter 9, Elsevier, 2018, pp. 169-194, ISBN: 978-0-12-812689-9.
- [4] Rawat J, Saxena J, Sanwal P. Biochar: A Sustainable Approach for Improving Plant Growth and Soil Properties, *Biochar - An Imperative Amendment for Soil and the Environment*, 2019. DOI: <http://dx.doi.org/10.5772/intechopen.82151>.
- [5] Bonanomi G, Ippolito F, Scala FA. Black Future For Plant Pathology? Biochar As A New Soil Amendment For Controlling Plant Diseases. *J Plant Pathol*. 2015; 97(2): 223-234.
- [6] Jha P, Biswas AK, Rao AS. Biochar in agriculture – Prospects and related implications. *Curr Sci* 2010; 99(9): 1218-1225.
- [7] Lehmann J, Gaunt J, Rondon M. Bio-char sequestration in terrestrial ecosystems – A review. *Mitig Adapt Strateg Glob Chang* 2006; 11: 403-427.

- [8] Chang Y, Rossi L, Zotarelli L, Gao B, Shahid MA, Sarkhosh A. Biochar improves soil physical characteristics and strengthens root architecture in Muscadine grape (*Vitis rotundifolia* L.). *Chem Biol Technol Agric* 2021; 8:7.
- [9] Liang JF, Li QW, Gao JQ, Feng JG, Zhang XY, Wu YQ, Yu FH. Biochar rhizosphere addition promoted *Phragmites australis* growth and changed soil properties in the Yellow River Delta. *Sci Total Environ* 2021; 761: 143291.
- [10] Guo LL, Borno ML, Niu WQ, Liu FL. Biochar amendment improves shoot biomass of tomato seedlings and sustains water relations and leaf gas exchange rates under different irrigation and nitrogen regimes. *Agric Water Manag* 2021; 106580.
- [11] Farhangi-Abriz S, Torabian S. Biochar Increased Plant Growth-Promoting Hormones and Helped to Alleviates Salt Stress in Common Bean Seedlings. *J Plant Growth Regul* 2015; 37: 591–601.
- [12] Giannoulisa KD, Evangelopoulos V, Gougoulis N, Wogiatzi E. Lavender organic cultivation yield and essential oil can be improved by using bio-stimulants. *Acta Agric Scand B Soil Plant Sci* 2020; 70(8): 648–656.
- [13] Miclea I, Suhani A, Zahan M, Bunea A. Effect of Jasmonic Acid and Salicylic Acid on Growth and Biochemical Composition of In-Vitro-Propagated *Lavandula angustifolia* Mill *Agron* 2020; 10: 1722.
- [14] Lloyd GB, McCown BH. Commercial-feasible micropropagation of mountain laurel-*Kalmia latifolia* by use of shoot-tip culture. *Proc Int Plant Prop Soc* 1980; 30: 421–427.
- [15] Stoica R, Velea S, Ilie L, Calugareanu M, Ghimis BS, Ion R-M. The influence of ethanol concentration on the total phenolics and antioxidant activity of *Scenedesmus opoliensis* algal biomass extracts. *Rev Chim (Bucharest)* 2013; 64(3): 304–306.
- [16] Desta ZY, Cherie DA. Determination of antioxidant and antimicrobial activities of the extracts of aerial parts of *Portulaca quadrifida*. *Chem Cent J* 2018; 12:146
- [17] İçli N. Total antioxidant capacity, total phenolic compounds and total flavonoid amounts of darak dalı and basil which are materials of tarhana soup of Kastamonu. *Sağlık Akademisi Kastamonu*. 2018; 3(3): 171–184.
- [18] Ahmed D, Fatima K, Saeed R. Analysis of phenolic and flavonoid contents, and the anti-oxidative potential and lipid peroxidation inhibitory activity of methanolic extract of *Carissa opaca* roots and its fractions in different solvents. *Antioxidants* 2014; 3: 671–683.
- [19] Di Lonardo, S., Vaccari, F.P., Baronti, S., Capuana M., Bacci L., Sabatini F., Lambardi M., Miglietta F. Biochar successfully replaces activated charcoal for in vitro culture of two white poplar clones reducing ethylene concentration. *Plant Growth Regul* 2013; 69: 43–50.
- [20] Lehmann J, Rillig MC, Thies J, Masiello CA, Hockaday WC, Crowley D. Biochar effects on soil biota – A review. *Soil Biol Biochem* 2011; 43(9): 1812-1836.
- [21] Hammer E.C., Forstreuter M., Rilliga M.C., Kohlera J. Biochar increases arbuscular mycorrhizal plant growth enhancement and ameliorates salinity stress. *Appl Soil Ecol* 2015; 96: 114-121.

- [22] Hashemi SB, Momayezi M, Talee D. Biochar Effect on Cadmium Accumulation and Phytoremediation Factors by Lavender (*Lavandula stoechas* L.). *Open J Ecol* 2017; 7:447-459.
- [23] Mohamed-Yasseen, Y. Application of charcoal in horticulture. *Trop Fruit News* 1994; 28:7.
- [24] Bennett RC, Wallsgrove RM. Secondary metabolites in plant defencemechanisms. *New Phytol* 1994; 127: 617-633.
- [25] Scott CD, Dougall DK. Plant cell tissue culture - A potential source of chemicals. Oak Ridge National Laboratory, Department of Botany, Tennessee, USA; 1987; pp 1-34.
- [26] Kul R, Ekinici M, Turan M, Yıldırım E. Impact of biochar on growth, physiology and antioxidant activity of common bean subjected to salinity stress. *Glob J Bot Sci* 2021; 9: 8-13.